INFORMATION TO USERS

This manuscript has been reproduced from the microfilm master. UMI films the text directly from the original or copy submitted. Thus, some thesis and dissertation copies are in typewriter face, while others may be from any type of computer printer.

The quality of this reproduction is dependent upon the quality of the copy submitted. Broken or indistinct print, colored or poor quality illustrations and photographs, print bleedthrough, substandard margins, and improper alignment can adversely affect reproduction.

In the unlikely event that the author did not send UMI a complete manuscript and there are missing pages, these will be noted. Also, if unauthorized copyright material had to be removed, a note will indicate the deletion.

Oversize materials (e.g., maps, drawings, charts) are reproduced by sectioning the original, beginning at the upper left-hand corner and continuing from left to right in equal sections with small overlaps.

Photographs included in the original manuscript have been reproduced xerographically in this copy. Higher quality 6" x 9" black and white photographic prints are available for any photographs or illustrations appearing in this copy for an additional charge. Contact UMI directly to order.

UMI®

Model Reference Adaptive Control System Using Frequency Domain Performance Specifications.

Bhagirath Patel ©

April 30, 1999

A THESIS SUBMITTED IN PARTIAL FULFILLMENT OF THE
REQUIREMENTS OF THE MSc Eng DEGREE
IN
CONTROL ENGINEERING
FACULTY OF ENGINEERING
LAKEHEAD UNIVERSITY
THUNDER BAY, ONTARIO.

The author has granted a non-exclusive licence allowing the National Library of Canada to reproduce, loan, distribute or sell copies of this thesis in microform, paper or electronic formats.

The author retains ownership of the copyright in this thesis. Neither the thesis nor substantial extracts from it may be printed or otherwise reproduced without the author's permission.

L'auteur a accordé une licence non exclusive permettant à la Bibliothèque nationale du Canada de reproduire, prêter, distribuer ou vendre des copies de cette thèse sous la forme de microfiche/film, de reproduction sur papier ou sur format électronique.

L'auteur conserve la propriété du droit d'auteur qui protège cette thèse. Ni la thèse ni des extraits substantiels de celle-ci ne doivent être imprimés ou autrement reproduits sans son autorisation.

Abstract

MRAS (Model Reference Adaptive System) to achieve frequency domain performance specifications with different transfer function identification techniques are experimentally studied. Standard open loop and closed loop recursive least squares (RLS) system identification techniques are implemented along with methods based on bandpass filters and steady-state Kalman filter. The behavior of the MRAS when combined with the different system identification techniques is discussed.

Based on experimental work performed on MRAS using open loop system identification, it was found that the system can achieve performance specifications in all process conditions. It was noticed that the DC bias changes in process input when process changes, delays the convergence of the system identification in open loop system identification. Closed loop system identification was found inadequate for use in MRAS. The system identification based on bandpass filter approach was found slow in convergence and so inefficient for use in MRAS. The use of Kalman filter for system identification resulted in noisy gains on adaptive PI controller. Based on the results obtained, it is concluded that MRAS to achieve frequency domain performance specifications is practical and capable of being used in industrial process control when coupled with open loop identification based on frequency domain concepts. The proposed approach provides a better method for maintaining performance robustness while guaranteeing stability margins in adaptive control than that obtained from time domain adaptive control.

Acknowledgements

I dedicate this work to my great mentors Dr. K. Natarajan and Dr. A.F. Gilbert for their help and support, and to my family who always stood by me.

i

Contents

ii

List of Figures

iv

v

vi

Chapter 1

An Overview of Adaptive Controller with an Application of Self-Tuning Adaptive Control System.

1.1 Introduction

Conventional controllers have fixed parameters. A conventional control system is designed upon assumptions that the plant and controller parameters are time-invariant and the plant is a linear dynamical process. Practically, the plant parameters often vary with time and it is not always possible to predict and correlate the variations to any measurable variable(s). Also most plants are nonlinear in nature. To construct a suitable open loop control system, one must select all the components of the open loop transfer function very carefully so that it responds accurately and variations in parameters can not be tolerated. The major advantage of the closed loop control system over open loop control system is that the components could be less accurate since the sensitivity to parameter variations in $G(s)C(s)$(open loop transfer function) is reduced by a factor of $1+G(s)C(s)$. The addition of the negative feedback loop also reduces the time constant. However the use of closed loop feedback system will increase the number of components of the system, which increases the complexity and also introduce the possibility of instability [9, 10, 16, 21].

In most feedback control systems, small deviations in plant parameter values from their design values will not cause problems in the normal operation of the system as appropriate stability margins are included in the design. But if plant parameters vary widely, then the control system may exhibit satisfactory response for conditions around designed values but may fail to provide required performance under all other conditions and may even cause instability. To demonstrate the effect of variations in plant parameters on the performance of a system with fixed controller parameters, a laboratory experiment on a temperature control apparatus (Appendix A) is considered here. The fixed parameter PI controller with P gain of 0.5 and I gain of 1.5 is used with the fan set at medium speed. A sampling rate

1
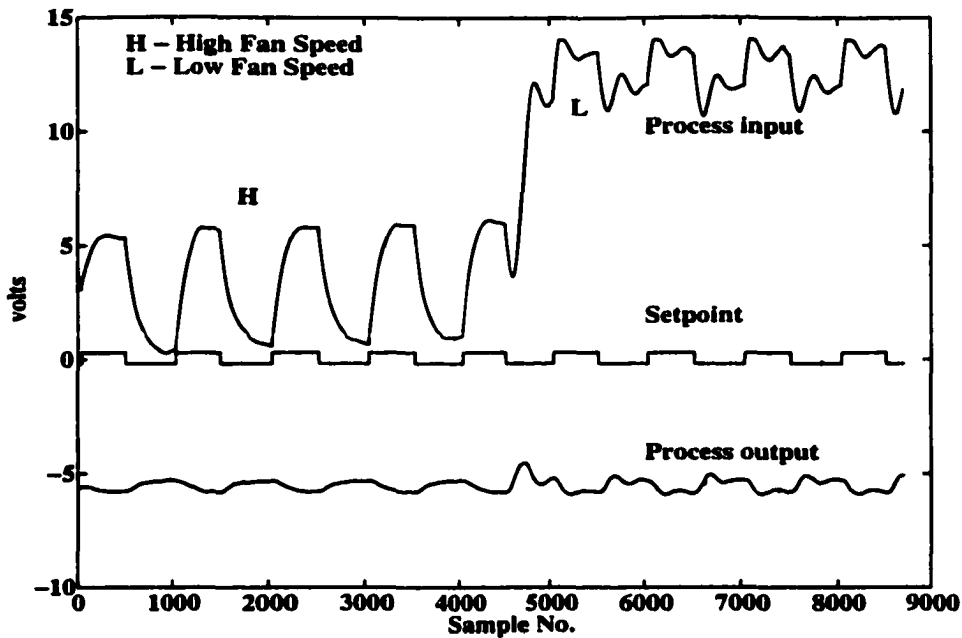
Figure 1.1: Effect of variations in plant parameters on control system performance.

of 0.05 s is used. The closed loop system behavior when fan speed is increased (low process gain condition) and fan speed is lowered (high process gain condition) with the same fixed parameter controller is as shown in Figure 1.1. The figure shows the process variables - setpoint, process input (manipulated variable) and process output. Process output is biased to show it clearly vis-a-vis setpoint for graphing purposes.

In Figure 1.1, the closed loop response of the system with high fan speed is over damped. The fan speed is changed to low speed at sample number 4500. The process parameters change resulting in higher gain for the process. The closed loop response of system is now under damped. The fixed parameter controller, which gives required response in one condition (medium fan speed) fails to meet response requirements in other conditions. In most processes, the variations in process parameters are unpredictable and many times cannot be correlated to any measurable variable. For e.g. the calcification on a heat exchanger wall changes the heat transfer rates of the vessel and thus the process dynamics. In a concentration control processes, the base constituent flow rate and concentration affects the gain, time constant and delay of the process and thus control system performance drastically. In industrial processes highly under damped behavior cannot be tolerated and may violate the safety of the plant. So it is a general practice that in such processes that fixed parameter controllers are tuned in high process gain condition to avoid any under damped behavior of the control system. But then the closed loop response of system in low gain condition will be very sluggish. This in most cases affects production rate. The underlying reasons for the variations are in most cases not fully understood. When

2

the physics of the process is reasonably well known, it is possible to determine suitable controller parameters for different operating conditions by linearizing the models and using some method for control design. Most industrial processes are very complex and not well understood. It is neither possible nor economical to make a sound investigation of the causes of the process variations. If controller parameters would change on recognition of process parameter changes, then better performance can be achieved, hence the need for adaptive control.

1.2 Adaptive Controllers

As seen in the experiment on the temperature control system with fixed parameter controller, the system performance changes with process dynamics. In practice there are many different sources of variations, and there is usually a mixture of different phenomena. The problem of maintaining system performance can be overcome if the plant transfer function or plant state equation can be identified continuously, and the changes in the transfer function or state equation of the plant are compensated by varying adjustable parameters of the controller. Thus adaptive control is required to guarantee system performance over wide variations of plant parameters [4]. An adaptive control system is one that continuously and automatically measures the closed loop dynamic characteristics of the control system, compares them with the desired closed loop dynamic characteristics, and uses the difference to vary adjustable system parameters (usually controllers characteristics) and generate an actuating signal so that the control system performance can be maintained regardless of the process changes. Alternatively, such a system may continuously measure its own performance according to a given performance index and modify its adjustable parameters so as to maintain performance regardless of the plant changes. There are also situations in which the key issue is variations in disturbance characteristics affecting the system. For e.g. in process control, the key issue is often to perform accurate regulation of quality variables against disturbances. In such cases, use of an adaptive controller as feedforward compensators have been found particularly beneficial. The reason for this is that feedforward control requires good models and feedforward model dynamics can change independently of the process dynamics, so in conventional implementation of feedforward controls, the feedforward model is always approximated [4]. Another reason is that it is always difficult and time consuming to tune feedforward loops because it is necessary to wait for a proper disturbance to occur.

An adaptive controller mainly involves identification of dynamic characteristics of the plant, decision making mechanism to achieve desired closed loop dynamics based on the identification of the plant and modification or actuation in controller parameters based on the decision made. Adaptive control techniques are classified in three major categories as gain scheduling adaptive control, model reference adaptive control and self-tuning adaptive control [4, 6].

Sometimes it is possible to find measurable variables that correlate well with changes in

3

process dynamics. Then these variables can be used to change the controller parameters. This approach is called gain scheduling as the scheme schedules the controller to compensate for changes in the process. A gain scheduling adaptive controller can be regarded as a mapping from process parameters to controller parameters using a measurable or estimatable variable(s). It can be implemented as a function or a lookup table. In process control the production rate can often be chosen as a scheduling variable, since time constants and time delays are often inversely proportional to production rate. In practice this scheme has limitation that there must be some measurable or estimatable variable(s) which can correlate changes in the process dynamics. This method also requires engineering efforts to determine the scheduling scheme. Gain scheduling requires that all operating conditions are covered in schedules and has limitations when the operating condition is due to unpredictable disturbances, which were not covered in schedules. It can only be applied to slowly varying processes.

In model reference adaptive system (MRAS), the performance specifications are given in terms of a reference model of the closed loop system. This reference model tells how the closed loop system should ideally responds to the setpoint signal. In the MRAS the output of the model and that of the plant are compared and the difference is used to generate the signals to change controller parameters. The key problem in MRAS is to determine the adjustment mechanism to bring the difference between reference model performance and actual closed loop model to zero. This adaptive scheme can be direct or indirect. In the direct scheme, the adjustment rules tell directly how the controller parameters should be updated based on error between model and actual current closed loop system performance. In the indirect scheme, first plant parameters are obtained, from which controller parameters are obtained using adjustment rules [4]. The applications of frequency domain MRAS to a temperature control system with different system identification methods are studied in Chapters 2, 3, 4 and 5 of this thesis.

In self-tuning adaptive system the estimates of the process parameters are updated and the controller parameters are obtained from the solution of the design problem using estimated parameters. The system may be viewed as an automation of the process modeling and design, in which the process model and the control design are updated at each sampling period. This adaptive scheme can also be direct or indirect. The controller in this scheme automatically tunes its parameters to obtain the desired properties of the closed loop system. This method is very flexible with respect to the choice of the underlying design and estimation methods. The detailed application of self-tuning adaptive scheme is studied in Section 1.4.

1.3 Process Model Estimation

On-line determination of process parameters is key element in adaptive control. A recursive parameter estimator appears as a component of self-tuning adaptive controllers and model reference adaptive controllers. It appears explicitly in indirect adaptive scheme and im-

4

plicitly in direct adaptive scheme. Dynamic processes evolve continuously in time and are nonlinear in nature. The most commonly used parametric models are linear in parameters and input-output variables. This eases the problems of estimation and controller design, which are to be performed on-line in adaptive systems [22, 23].

Three configurations of system identification are possible: closed loop, open loop and true open loop. In closed loop identification, changes from the set point to the closed loop process output are used to identify the closed loop system from which the known controller dynamics are factored out to obtain process information. In open loop identification, with the controller in automatic mode, the changes in the manipulated variable and process output are used to identify the process dynamics. In this case the loop is still closed and set point changes are applies to effect changes in manipulated variable and process response. In true open loop identification, the controller is put on manual and changes are applied directly to the manipulated variable and process response is used to identify the dynamics of the process. Many different approaches have been suggested and studied for system identification in [2, 6, 4, 8]. The true open loop identification as well as non-parametric approaches such as frequency response schemes are often batch type identification schemes rather than on-line recursive schemes. From the point of use of the identification results in adaptive control, it is often desirable to have on-line recursive identification schemes. In adaptive control, the parameter estimation scheme should be iterative, allowing the estimated model of the system to be updated at each sampling interval as new data become available. The recursive identification procedures involve a parametric transfer function in the z-domain of known order whose parameters are estimated recursively using least-squares. The recursive form allows significant savings in computation. Instead of recalculating the least-squares estimate in its entirety, requiring the storage of all previous data, it is both efficient and elegant to merely store the 'old' estimate calculated up to current time, and to obtain the new estimates by an updating step involving the new observation only. The details of the recursive least-squares (RLS) methods can be found in [4, 6, 19, 23, 22].

To allow for changes in plant parameters standard RLS is modified as follows: In the case that plant parameters change abruptly but infrequently, the covariance matrix can be reset to large number. This implies that the gain matrix in the estimator becomes large and the estimate can be updated with a large step. In the case that plant parameters are slowly time-varying, a relatively simple exponential weighting of old data can be carried out. The most recent data is given unit weight, but data that is n time units old is weighted by λ^n, where λ is an exponential forgetting factor ($0 < \lambda \leq 1$). A disadvantage of exponential forgetting is that old data is discounted even if recent process output or input does not contain any new information about the parameters.

The order of the transfer function has to be known a priori requiring preliminary identification for applying standard RLS. If the model is under parameterized then the system cannot be completely identified. One can assume an over parameterized model of the process. But these will result in computational overhead. Thus one has to assume the reasonable model of the system and this model should be able to capture the required dy-

namics of the system. The system delay in discrete time can be calculated from knowledge of the continuous time delay and sampling interval. The knowledge of the delay can be incorporated in RLS estimation. For RLS used in estimation of z-domain transfer function, it is usually assumed that the controller is a sampled-data controller with a zero-order hold at its output and that the identification experiment is carried out at the same rate, in synchrony with the control loop. In industrial process control, the controller is usually implemented in a distributed control system (DCS), where control calculations take place at much higher rate. The facility to add real-time identification code into a particular controller is often limited. Data logged into a database by a central DCS processor is usually at a slower rate then that of the control rate. If this logged data is used for the identification, then the zero-order hold assumption is invalid. If the identification is carried out on a separate computer different from the control computer, synchronization to the control computer is impossible and again the true identification will not be possible. If facility is available to add the identification code into the control processor, then due to the high sampling rate of this processor and the variable dead-time of the process, the order of the parameterized transfer function will be high, leading to a high dimensional, memory demanding and time consuming RLS algorithm. Some form of averaging of inputs and outputs is necessary to reduce the order of the transfer function [8]. It is normally the case in the identification of system that the data used are corrupted by the noise. The noise affects the results. Also the RLS system identification requires persistent input excitation condition. The input signal should have sufficient magnitude to cause the excitation of system dynamics and should be persistent. The requirement for persistent excitation can be met by adding 'dither' in the loop. In all experiments reported in this thesis the square wave is used for excitation of the setpoint. RLS requires an initial value of parameters and covariance matrix as a starting point for the recursion. The choices of these values will also influence the RLS estimate's convergence. The performance of the RLS depends upon the noise in the system. If the noise is low, then RLS will converge quickly. This is because in low noise condition, the RLS is solving a set of (mostly) linear deterministic equations for unknown parameters [4, 6]. It is a requirement for RLS that the data used (i.e. process input and output in open loop system identification, and setpoint and process output in closed loop system identification) should be free of DC bias. The reason for this requirement is as follows: Linearized models that are being identified are valid for small perturbations around an operating point which in most industrial systems is set by the DC bias applied to process input. The setpoint perturbation applied to the closed loop system are usually considered as inducing small changes in both directions on this DC bias of the input without changing the DC bias and the linearized (transfer function) model seeks to find and explain only the behavior due to these changes. Also the effect of load disturbance on system identification can be neglected by removing DC bias developed due to integral action of the controller from process variables before feeding to RLS. The DC bias estimation can be implemented using a filter or taking mean of set of data. In case of the temperature control system used in experiments in this thesis, the system is noisy and

6

the parameters and DC bias estimation take many samples to converge.

1.4 Experimental Application of Self-Tuning Adaptive Control System

When implementing an adaptive controller, the system identification procedure has to be carried out on-line. When the system identification converges, then the adaptive controller can design the controller parameters using design specification for implementation on the plant. While the system identification is under way for the first calculation of adaptive controller parameters, the system should be run on a conventional controller. Thus there is a definite need to know that the system identification has converged before adaptive control can be switched on. A sufficient number of samples has to be taken to ensure system identification has converged before carrying out actual adaptive controller implementation. Also the switchover mechanism from conventional to adaptive controller has to be designed in such a way as to avoid unnecessary bumps to the process. The bumps are normally caused due to different levels of the control effort computed by existing conventional controller and the adaptive controller at the switchover sampling instant. This can be avoided if the integrator state of the conventional controller is taken into account when switching over to the adaptive controller. This bumpless switchover mechanism [15] is applied in the experiment performed here while switching over from conventional controller to adaptive controller and also when changing adaptive controller parameters in successive sampling instants to avoid unnecessary bumps in control effort. For purpose of estimation of process parameters in standard z-domain transfer function model, standard RLS with exponential forgetting factor is used in the experiment performed below.

A self-tuning adaptive controller is implemented in the laboratory experimental set up (Appendix A) of a temperature control system as shown in Figure 1.2. The adaptive scheme is designed in the state space after the system is augmented with an integrator to ensure steady state tracking of step inputs and disturbance rejection [6, 25, 24]. The process delay estimated from the time domain response of the identification experiment performed for process in low, medium and high fan speed was negligible. The process can be modeled as a first order process in continuous time domain. The z-domain transfer function of the process given by Equation (1.1) is assumed reasonably parameterized to capture the required dynamics of the process at a sampling period of 400 ms.

$$G(z) = \frac{b_0 z^{-1} + b_1 z^{-2}}{1 + a_1 z^{-1} + a_2 z^{-2}} \tag{1.1}$$

The state space model of the system with an augmented integrator state α_k is given by Equation (1.2).

$$\begin{bmatrix} x_{k+1} \\ x_{k+2} \\ \alpha_{k+1} \end{bmatrix} = \begin{bmatrix} 0 & 1 & 0 \\ -a_2 & -a_1 & 0 \\ -b_1 & -b_0 & 1 \end{bmatrix} * \begin{bmatrix} x_k \\ x_{k+1} \\ \alpha_k \end{bmatrix} + \begin{bmatrix} 0 \\ 1 \\ 0 \end{bmatrix} * \begin{bmatrix} u_k \end{bmatrix} + \begin{bmatrix} 0 \\ 0 \\ 1 \end{bmatrix} * SP_k$$

7
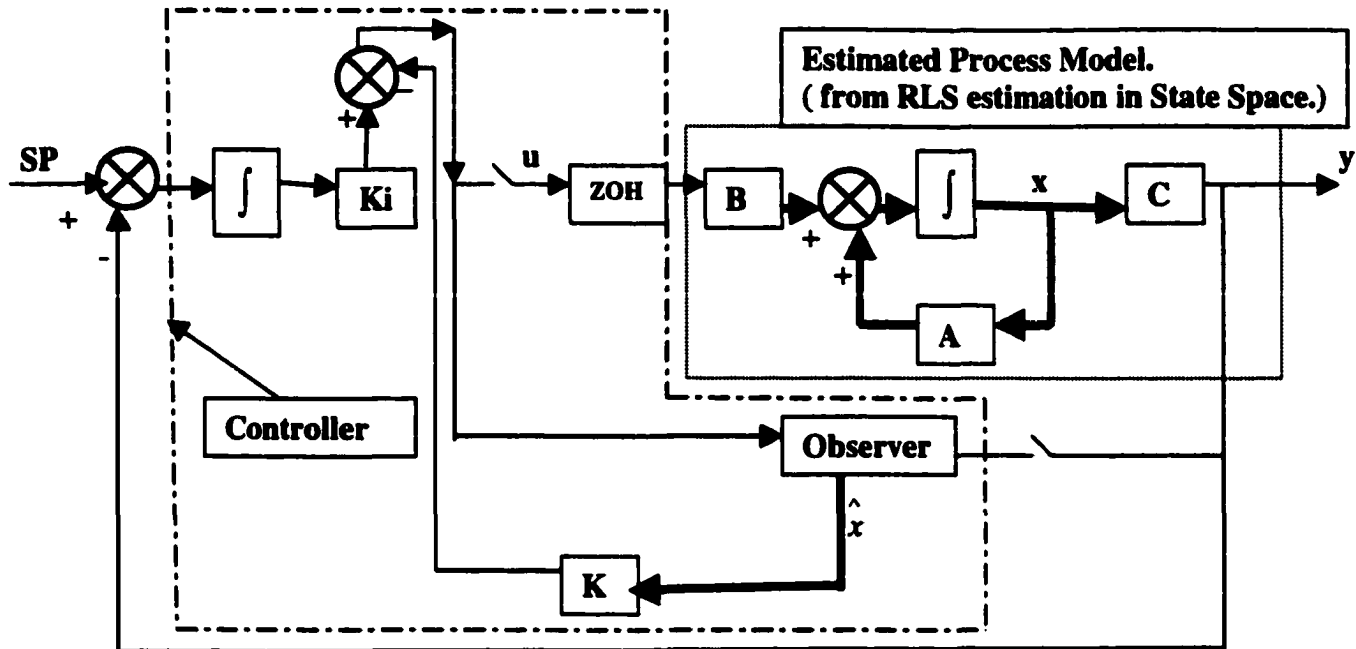
Figure 1.2: Block diagram of self-tuning adaptive control scheme.

$$(1.2)$$

$$y_k = \begin{bmatrix} b_1 & b_0 & 0 \end{bmatrix} * \begin{bmatrix} x_k \\ x_{k+1} \\ \alpha_k \end{bmatrix}$$

The adaptive controller design specifications were based on the quadratic performance criterion given in Equation (1.3). The control input u_k for the system is determined at each sample, which minimizes the performance index given by Equation (1.3).

$$\mathcal{J} = \sum_0^\infty x_k^T Q x_k + u_k^T R u_k \qquad (1.3)$$

where Q is positive-definite (or positive-semidefinite) symmetric matrix and R is positive-definite symmetric matrix. The matrices Q and R determine the relative importance of the error and the expenditure of control (effort) energy [25, 24, 26, 27]. The discrete Riccati equation was solved for to determine the optimal control vector gain matrix K (Figure 1.2) with $Q = $ diag $[0.2,0,1]$ and $R = 5$. An observer is needed to estimate the two states of the process (Equation (1.1)) to implement the controller. The observer gain matrix L was designed using the duality approach by solving the corresponding Riccati equation with $Q = $ diag $[0,0]$ and $R = 8$ [9, 10, 4, 24]. The observer is always designed to be

8
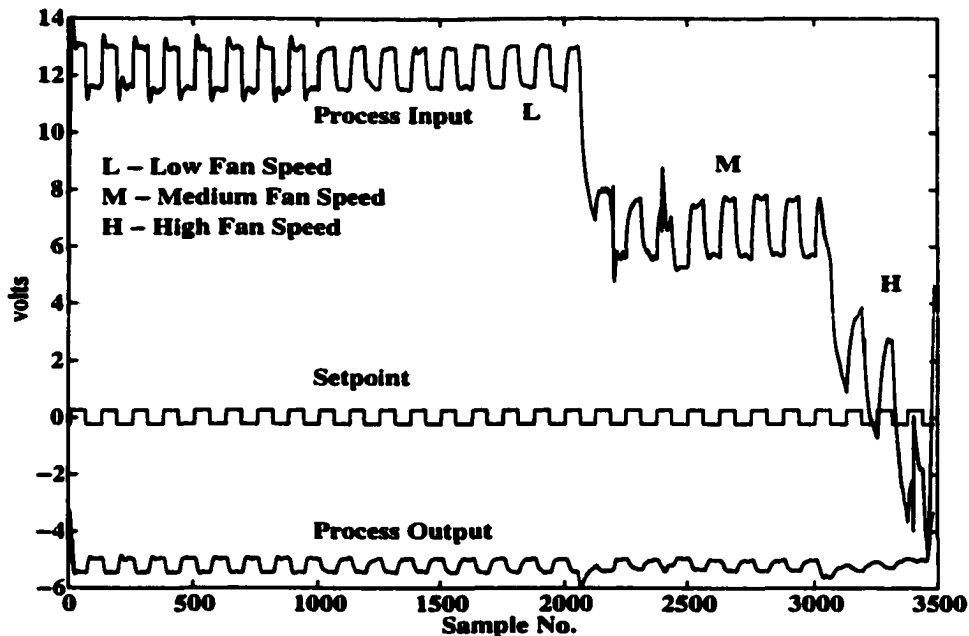
Figure 1.3: Process variables - setpoint, process input (manipulated variable) and process output under self-tuning adaptive control.

faster than the controller. The run time optimized C language code was generated using symbolic processing (Maple) software [14]. Open loop system identification method using standard RLS with exponential forgetting factor is used for process model estimation. The process input and process output are fed to RLS after removal of DC bias. The DC bias is estimated every 200 samples, by taking the mean of previous 200 data samples. The initial values for covariance matrix in RLS is 100 on each element, and all process transfer function parameters were initialized to value 0. A forgetting factor of 0.999 is used. A sampling time of 400 ms is used in the experiment. The results of the self-tuning adaptive controller applied to the temperature control system, based on the quadratic performance index minimization are shown in Figure 1.3.

Initially with fan in low speed and a conventional PI controller is used with P gain of 2 and I gain of 1 up to sample number 1000. During this time RLS is used to identify the system. There after the adaptive controller is designed on each sampling instant and gains of the observer and controller are applied. Variation in process parameters is induced by varying the fan speed to medium speed at sample number 2055 and again to high speed at sample number 3000. Figure 1.3 shows setpoint, process input (manipulated variable) and process output. Note that the difference in the setpoint and output is due to bias on input amplifier as detailed in Appendix A.

Several conclusions can be drawn out of this experiment on self-tuning adaptive control and about system identification:

9
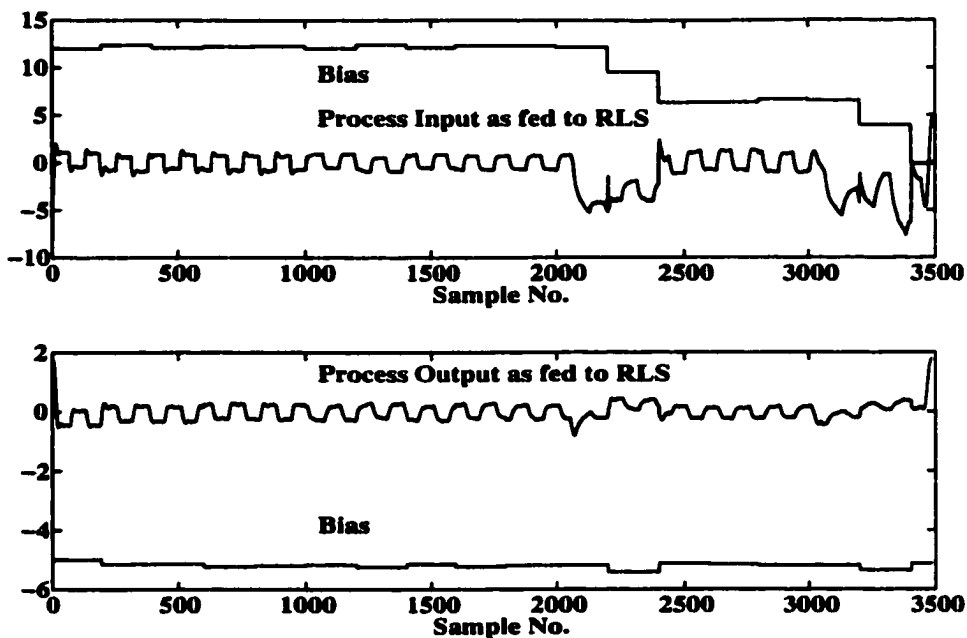
Figure 1.4: Estimated DC bias in process input and input as fed to RLS, and DC bias in process output and output as fed to RLS.

1. The system designed on the quadratic performance index results in stable system as can be seen after switchover to adaptive control at sample number 1000.

2. The resulting system is also less aggressive in applying control effort than PI control (up to sample number 1000) due to the choice of Q and R.

3. The characteristics of an optimal control law based on quadratic performance index is that it is a linear function of the state variables, which implies that one need to feedback all the state variables. This requires the state observer to estimate the unmeasurable states. This puts a lot of computational overhead.

4. The optimal control based on performance index designed here has the drawback that the transient response characteristics can not be met as required, over all process conditions. As a general rule, increase in Q and decrease in R values, results in fast transient response but the response is difficult to obtain in all process conditions using one value of Q and R (i.e. Q and R have to be adaptively changed to meet transient response specifications).

5. The variations in process dynamics introduced by varying fan speed at sample number 2055, resulted in the change in process input (control effort) level due to the change in process parameters, particularly process gain as can be seen in Figure 1.3. The DC bias value in control effort has changed too, but it is difficult to sense this situation

10

and estimate DC bias instantaneously. The estimation of DC bias requires sufficient number of samples. The estimated DC bias and process variables after removal of DC bias are then fed to RLS are shown in Figure 1.4. The wrong DC bias estimate used just after process condition has changed, results in poor data fed to RLS as can be seen in input and output fed to RLS in Figure 1.4. The RLS estimates resulting from these data are incorrect. The controller designed on these estimates deteriorates the performance of the system. This is a vulnerable situation for all adaptive controllers. While many schemes are available for DC bias estimation, they all take some time to estimate the bias. Consequently, adaptive control design must have a higher margin of stability against periods of poor parameter estimation.

6. The situation is usually aggravated as RLS estimates require some samples to converge to the correct process model after a process change. The convergence rate can be increased by resetting the covariance matrix, but it is difficult to implement, as it is difficult to sense the process variations.

7. It is worth noting that once the process input or process output went into saturation (attaining maximum or minimum limit), true identification of process can not be done. The saturation limit for the experimental set up is due to maximum output limit of output amplifier and minimum is due to heater circuit behavior. The minimum saturation limit for process input is 0 volt and maximum saturation limit for process input is 14.3 volt. The process input applied outside minimum and maximum limit has no effect on process output. As shown in Figure 1.3, the process input went into such saturation at high speed at about sample number 3250 and onward. Even though the persistent exciting signal is provided at setpoint, it has no effect on process output as process input is in saturation. For practical implementation of any adaptive controller, one has to make sure that 'persistent excitation' condition is maintained while carrying out system identification at RLS input and output.

1.5 Conclusion

Adaptive controller is required for maintaining system performance in processes which vary considerably. The self-tuning adaptive control system designed in this chapter did not meet the requirements. Even though it gives a dominantly stable system, it is difficult to guarantee the system performance with a single set of Q and R values. There is a need for adaptation of Q and R i.e. performance specifications must be met by a secondary adaptive control loop. The change in control effort level when the process dynamics changes has severe effect on system identification. The effect is again worsened by slow response of the control system due to poor choice of values of Q and R for this new condition of the process. With self-tuning adaptive control, it is difficult to guarantee system performance over all process conditions unless secondary adaptive performance control loops are provided. Other methods have to be tried which guarantee the system performance (besides stability).

11

Model reference adaptive system (MRAS) using frequency domain performance specifications is studied in Chapter 2, 3, 4 and 5 of this thesis. The importance of designing adaptive control using frequency domain performance specifications are discussed and the experimental results of such MRAS using open loop system identification is provided in Chapter 2.

Chapter 3 discusses the importance of closed loop system identification over open loop system identification. The experimental results and analysis of results showing associated problems in performing closed loop identification are detailed.

Chapter 4 emphasis the importance of non-parametric system identification methods. The application of MRAS using bandpass filters approach (non-parametric method) for system identification is provided.

An alternative approach to system identification is tried in Chapter 5 using steady-state Kalman filters. Use of Kalman filters for DC bias estimation is demonstrated and compared with conventional methods. The advantages and disadvantages of performing system identification using Kalman filters over bandpass filters are discussed.

12

Chapter 2

Model Reference Adaptive Control System Using Frequency Domain Performance Specifications And Open Loop System Identification.

2.1 Introduction

In model reference adaptive system (MRAS), the desired performance is expressed in terms of a reference model. As already seen, self-tuning adaptive system has difficulty in meeting required performance specification for all process conditions. In this previously designed self-tuning adaptive system, the position of the closed loop poles depends on the identified plant model and specified values of Q and R. In MRAS, the controller parameters are obtained in such a way that resulting closed loop system matches a specified reference model in input output properties. In all adaptive systems, there is always ambiguity in system identification due to model under or over parameterization, convergence of RLS or variations in plant delay at different conditions etc. An accurate adaptive controller can be designed if the process can be identified truly. Also many adaptive control systems "invert" the plant in some sense [4] and the cancellation of process zeros often creates problems in industrial systems. The reason is that, unstable zeros (outside the unit circle) are frequently created by choice of sampling rate vis-a-vis time delay of process. This leads in many cases to unstable control behavior [11, 4].

13

2.2 MRAS Based on Frequency Domain Performance Specifications

In this approach to MRAS, controller parameters are obtained in such a way as to minimize difference between closed loop frequency response of reference model and resulting closed loop system with the identified plant [18, 28]. The main justification for this approach is provided by the observation (Figure 2.2 of this thesis) that the open loop frequency response of the identified plant exhibits faster convergence for a given process condition even though the coefficients of over or under parameterized model identified by RLS varies and has not converged. This observation is justified by comparing frequency responses of the estimated model of a plant at different instances (for same plant operating condition) in the following experiment.

The process input (manipulated variable) and process output data from the temperature control system (Appendix A) operating under PI control with P gain of 2 and I gain of 1, sampling period of 400 ms and fan at high speed is used in an off-line identification. First the DC bias is removed from the whole set of data by subtracting the mean of the data from each datum value. Then bias removed input and output are fed to RLS. The open loop process model assumed is a second order model as given by Equation (1.1). The variations in coefficients a_1, a_2, b_0 and b_1 of the identified process model at each sampling instant are shown in Figure 2.1. The open loop frequency response plots of identified plant model at sample numbers - 20, 340, 360, 850 and 1024 are shown in Figure 2.2. The open loop frequency responses at different samples are practically the same in the lower frequencies up to the bandwidth of the closed loop system. The bandwidth of the closed loop system using the identified process model is about 0.25 rad/s. The differences in the frequency responses at much higher frequencies than bandwidth are due to noise corrupting the identification and possible convergence. It is important to note that even though the coefficient a_1 and a_2 in Figure 2.1 changes drastically between sample number 340 and sample number 360, the frequency response at those sampling instants remains unchanged for given process condition. The change in coefficients is caused due to the nature of RLS scheme. Such variations in coefficients may cause variations in controller coefficients in adaptive control, if designed directly on estimated process coefficients. These variations are however irrelevant as the process frequency response (and impulse response) are invariant to these coefficient values.

Advantages of frequency response based design in adaptive control system can be summarized as:

1. The frequency response is unique for the process condition, even if the coefficients of the identified process model through RLS changes. The adaptive controller designed based on the frequency response will also be unique, irrespective of changes in coefficients of the identified process model.

2. RLS is said to have converged when coefficients attain steady values for given process

14
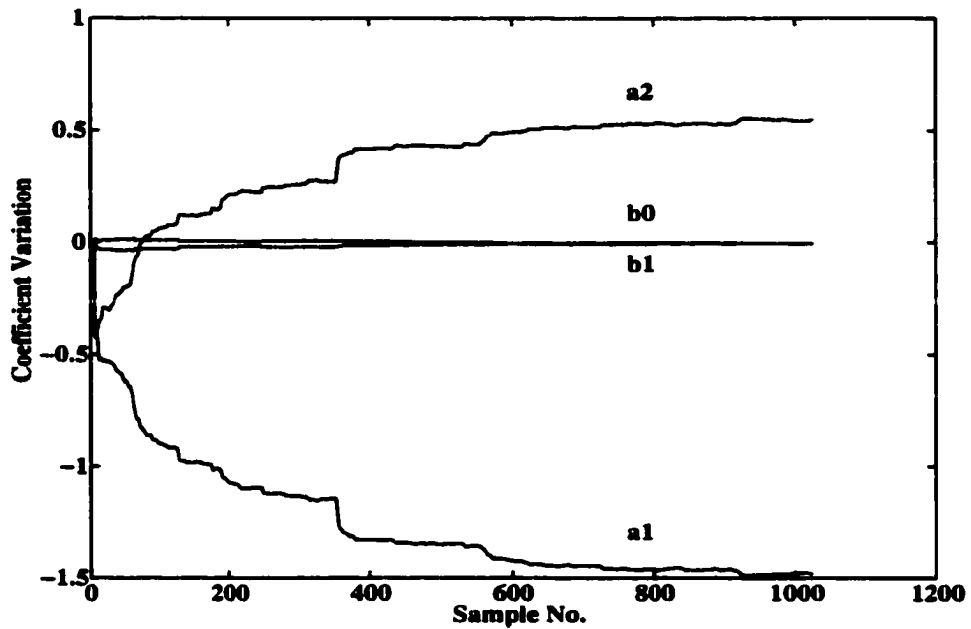
Figure 2.1: Variations in coefficients of estimated process model at each sample.
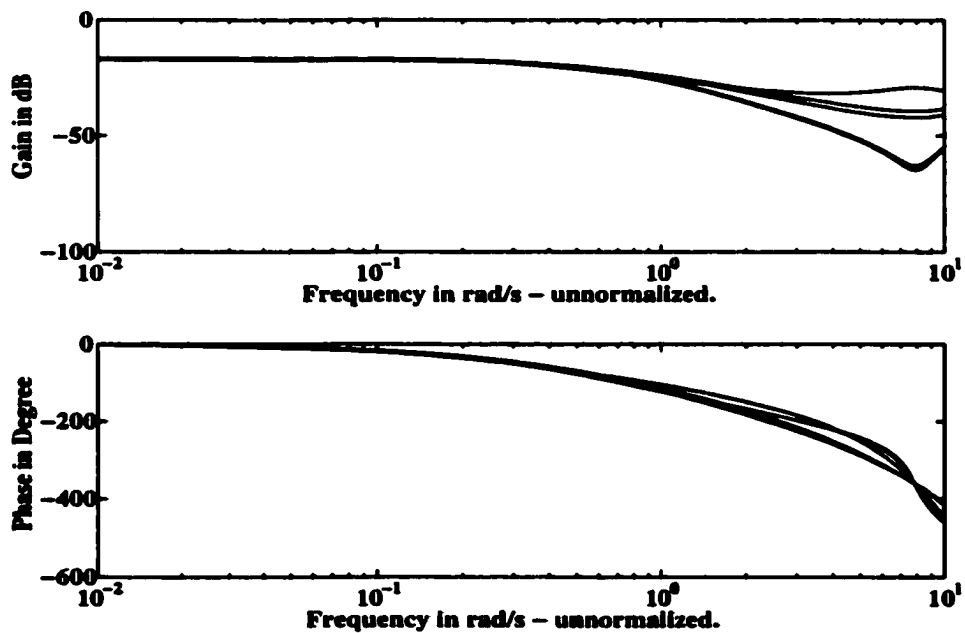
Figure 2.2: Frequency responses of estimated process model at sample numbers - 20, 340, 360, 850 and 1024.

15

condition [6]. From Figure 2.1, RLS convergence takes about 800 samples. The RLS convergence however requires just 20 samples to identify reasonably the frequency response of the process as is evident in Figure 2.2. The faster convergence of RLS in terms of frequency response will be of great benefit when the process dynamics change and there is a need to update adaptive controller as soon as possible to meet required performance of the control system.

3. The well proven different approaches of robust frequency domain design can be applied easily [9, 10].

4. The closed loop performance model can easily be formulated in accordance with the required specification in terms of the natural frequency, damping factor and time delay as a second order model with time delay. For a second order system, the correlation is well established between the transient response and frequency response. This knowledge can be incorporated easily in specifying the closed loop performance model in frequency domain.

5. The stability robustness of the closed loop system can be guaranteed by specification on the phase margin and gain margin.

6. Plants with uncertainties can be handled well by the frequency response method [3]. Most of the problems arising in the adaptive control due to under or over parameterized model can be handled well.

7. The system can be designed such that the effects of the noise are minimal by controlling the bandwidth of the system.

8. When designing adaptive PID controller, the effect of each controller parameter is well understood. If adaptive PI controller is to be implemented, the effect of P or I gain variations on system is qualitatively known. This prior knowledge is useful and can be incorporated easily by putting some constraints over controller parameters. This is very useful at the time when process condition changes result in unreliable RLS estimates, which eventually result into impractical controller parameters.

2.3 MRAS Based on Frequency Domain Performance Specifications - Simulation Results

The MRAS based on frequency domain performance specifications is simulated here. The block diagram describing the MRAS is shown in Figure 2.3.
The simulated process consists of a continuous time process transfer function given in Equation (2.1).

$$G(s) = K \frac{e^{-s\tau_d}}{1 + s\tau} \tag{2.1}$$

16
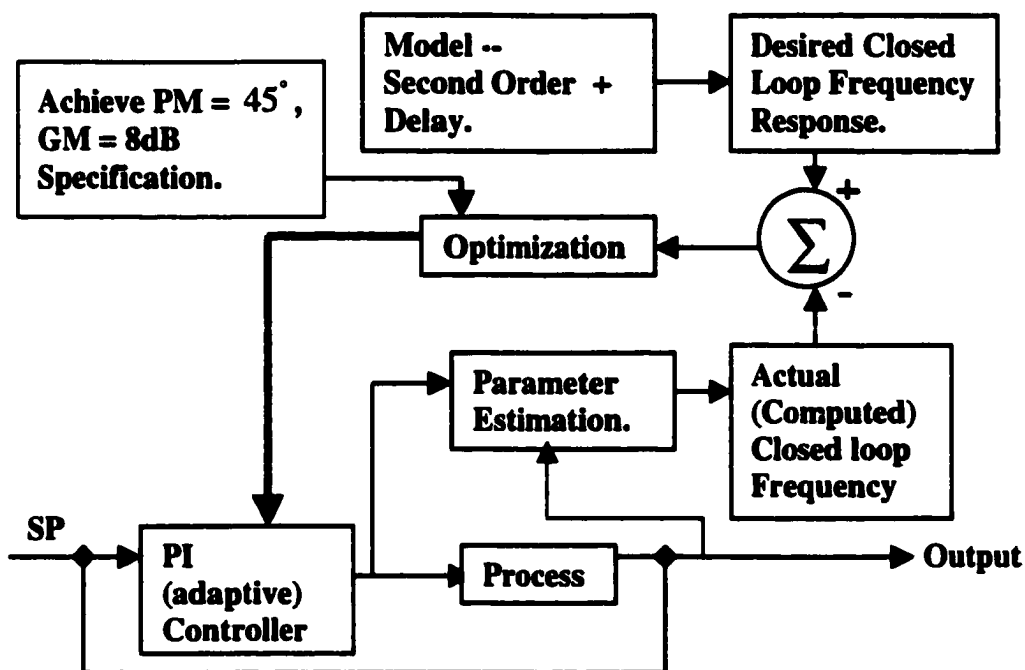
Figure 2.3: MRAS based on frequency domain design specifications.

The process parameters and their changes during the simulation are detailed as follows:

For time 0 to 40 s – Process gain K = 2, Time constant = 0.5 s, Delay = 0.8 s.
For time 40 to 120 s – Process gain K = 0.5, Time constant = 0.25 s, Delay = 0.4 s.
For time 120 to 200 s – Process gain K = 2, Time constant = 0.5 s, Delay = 0.8 s.

The adaptive controller (PI) transfer function in the z-domain is given in Equation (2.2), where T denotes the sampling period and K_P and K_I are the P gain and I gain respectively as estimated on each sample when adaptive control is implemented.

$$C(z) = K_P + \frac{K_I T}{1 - z^{-1}} \tag{2.2}$$

The PI controller updates manipulated variable every 50 ms. The manipulated variable is held at its last value until the next controller update (zero-order hold). The load disturbances are assumed to act on the process output additively and have dynamics given by Equation (2.3).

$$d(t) = A_{dis} e^{-t/\tau_{dis}} \cos(\omega_{dis} t) \tag{2.3}$$

A_{dis}, τ_{dis}, and ω_{dis} are the amplitude of the disturbance, the decay rate of the disturbance and the frequency of the disturbance in rad/s respectively. Time t in Equation (2.3) is measured from the start of the disturbance, not from the start of the simulation. A cosine

17

form is used so that by setting ω_{dis} to zero and by setting large value for τ_{dis} relative to total simulation time, it is possible to generate step disturbances.

The closed loop reference model assumed is a second order model as given in Equation (2.4).

$$T_{(Closed\ loop)} = \frac{e^{-s\tau_d}\ \omega_n^2}{s^2 + 2\xi\omega_n s + \omega_n^2} \tag{2.4}$$

Where ω_n is natural frequency, ξ is damping factor and τ_d is time delay. The time delay in Equation (2.4) is considered as zero for this simulation. This model is transformed into a discrete time model given in Equation (2.5) [10].

$$T(z) = \frac{k}{z^2 - 2e^{-\xi\omega_\delta}\cos(\sqrt{1 - \xi^2}\omega_\delta)z + e^{-2\xi\omega_\delta}} \tag{2.5}$$

Where ω_δ is normalized natural frequency $(\omega_d = \omega_n T)$. The value of k in Equation (2.5) guarantees the steady state DC gain of 1 and is given by Equation (2.6).

$$k = 1 - 2e^{-\xi\omega_\delta}\cos(\sqrt{1 - \xi^2}\omega_\delta) + e^{-2\xi\omega_\delta} \tag{2.6}$$

In the simulation the value of ω_δ used is 0.95 rad and ξ is 0.8 in the simulation. The frequency response of the reference model and resulting closed loop system model were compared at 13 frequency points, starting at normalized frequency 0.001 rad and then incrementing with step size of 0.05 rad. Thus the normalized frequency range of 0.001 rad to 0.601 rad is used. The frequency range selected is below ω_δ, where noise effects on system identification are low. With setpoint excitation period of 20 s (i.e. normalized frequency of $2\pi/20 \times T(T = 0.05) = 0.0157$ rad), the normalized frequency range (0.001 to 0.601 rad) covers the required odd harmonics (upto 19th odd harmonic) of the setpoint excitation frequency. The specifications for the stability margin requirements were specified in terms of phase margin and gain margin. The system is designed so that phase margin of at least 45° and gain margin of at least 8 dB are maintained in obtaining the controller parameters at each sampling instant.

For purpose of system identification, standard RLS using open loop identification is used. The delay assumed is 0.4 s for nominal process condition. The delay of 0.4 s with controller sampled at 50 ms results into delay of 8 samples, which is incorporated in discrete model. The discrete model assumed is an over parameterized model with delay of 8 samples as given by Equation (2.7). The forgetting factor of 0.99 is used. Initially, all elements of co-variance matrix and all coefficients of the model are set to 0.

$$G(z_{assumed}) = \frac{z^{-8}(b_0 + b_1 z^{-1} + \cdots + b_8 z^{-8})}{1 + a_1 z^{-1} + \cdots + a_8 z^{-8}} \tag{2.7}$$

To obtain PI controller, which minimize the difference between frequency response of closed loop reference model and resulting closed loop system, the simplex method [3, 7, 12] for

18

function minimization is used. The maximum iterations allowed in the optimization procedure in obtaining P and I gains at each sampling instant is set to 20. This is required to guarantee computations finish within a sampling period. The best value of P and I gains are those which give global minimum difference between frequency responses (i.e. frequency response of closed loop reference model and frequency response of resulting closed loop system with current estimated value of P and I gains) without violating stability margin requirements. The optimization is stopped at any instant when the simplex size is reduced to 0.1 [7] (i.e. less than ±0.1 changes in gains) or when 'error' (measure of difference between closed loop frequency responses) is less than predetermined value or 20 (maximum) iterations are reached. The 'error' which is minimized by optimization procedure is sum of 'error' at each frequency point considered. The 'error' at each frequency point is obtained as an absolute value of complex error, divided by the corresponding normalized frequency. The division by frequency ensures higher weighting of errors at lower frequencies. This weighting is implemented because of greater confidence in lower frequency response data than higher frequency response data due to higher noise levels in high frequency regions and the effects of sampling affecting identification [8, 2]. The complex error is the difference between the frequency response (complex) of the reference model and the current closed loop response computed using the identified process frequency response (process model identified through RLS) and estimated current P and I gains. The constraints on stability margins are applied as discussed in [3].

The process is simulated in a digital computer with a fine time step of 0.001 ms and all time constants and time delay have a minimum resolution of the same .001 ms. The setpoint is excited by a square waveform with amplitude ± 1 and a period of 20 s. The setpoint waveforms have no noise added. The setpoint period so selected ensures that the closed loop system tracks the setpoint before the next bump is applied i.e. steady state is achieved. Process output measurements are assumed to be corrupted by Gaussian random noise with variance of 1. The process input constrained to ±10. A disturbance of amplitude 0.3, period 5.5 s and decay time constant of 15 s is introduced at a time of 120 s in the simulation. The process is simulated initially up to 40 s with constant P gain and I gain of 0.2 and 0.5 respectively, for RLS to converge and estimate the process model. There after an adaptive PI controller is designed at each sampling instant. The P and I gains are evaluated at each sampling instant and are applied without constraints. The results of the simulation showing process variables - setpoint, process output and process input are shown in Figure 2.4. The value of P and I gains computed and applied by the adaptive method being considered (after time of 40 s) are shown in Figure 2.5. In Figure 2.5, the solid line is P gain and dashed line is I gain. The 'error' used in optimization and the number of iterations of the optimization routine to obtain P and I gains on each sample by adaptive method (after time of 40 s) is shown in Figure 2.6. The phase margin and gain margin of the system on each sample is shown in Figure 2.7.

The results of this simulation can be summarized as:

1. The specified performance of the system is regained as per reference model whenever

19
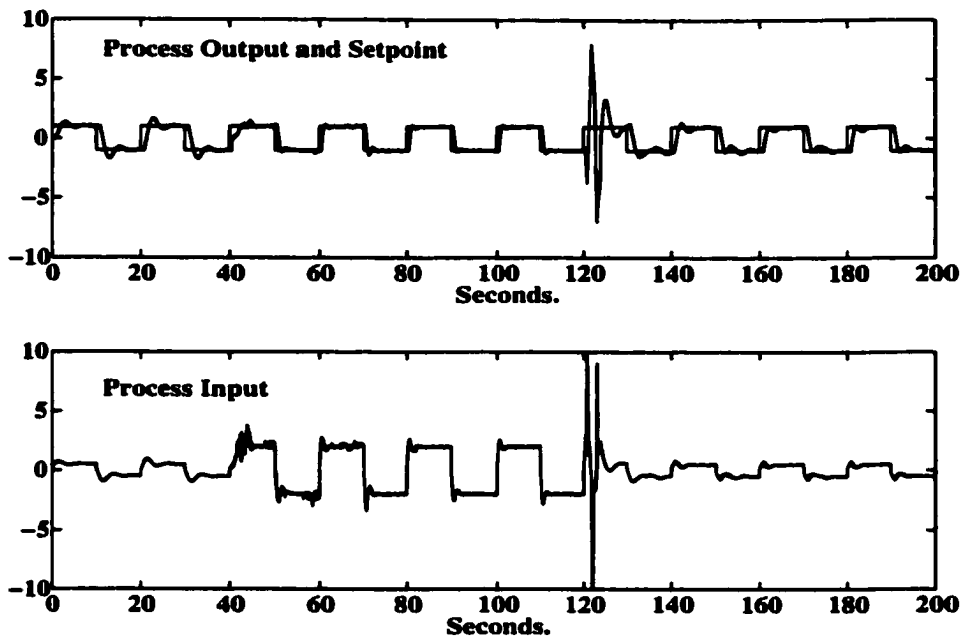
Figure 2.4: Process variables - setpoint, output and input.
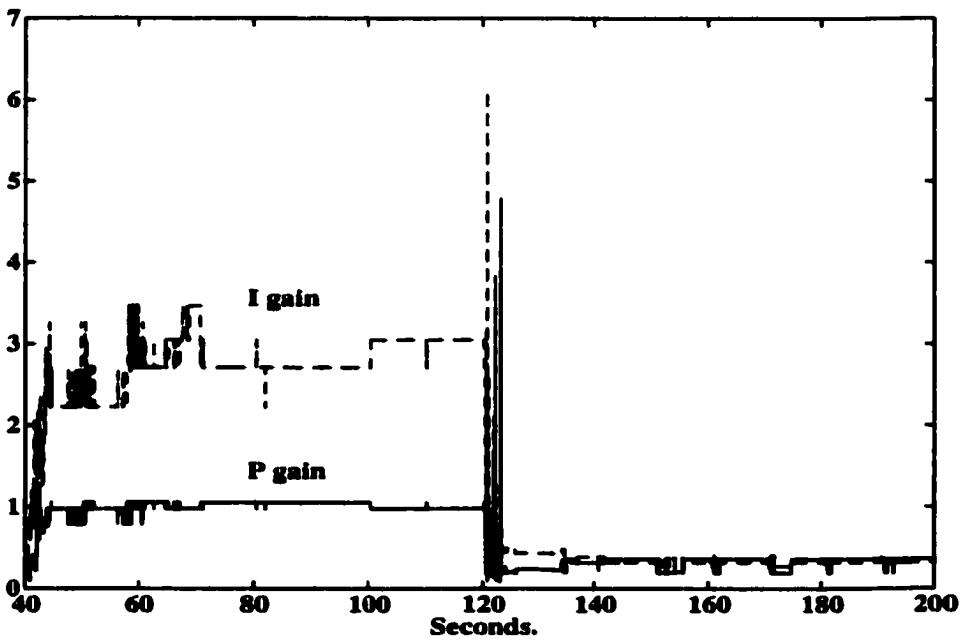
Figure 2.5: P gain (solid) and I gain (dashed) applied by adaptive controller.

20
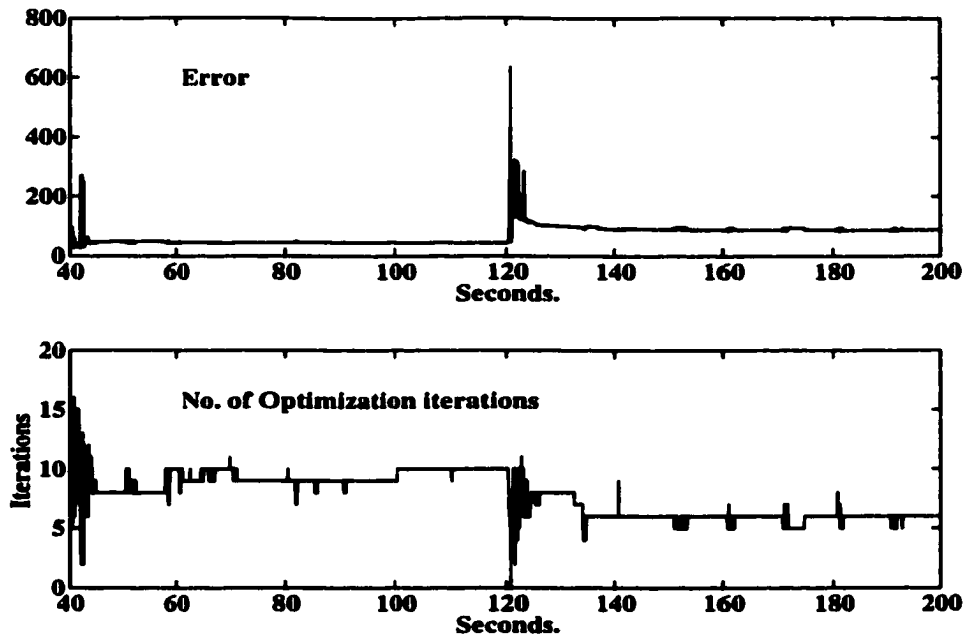
Figure 2.6: The 'error' as correlated to difference between frequency response of reference model and resulting closed loop system and number of iterations of optimization routine performed to obtain P and I gains on each sample.

    process conditions were changed, as can be seen in Figure 2.4. The system took around 1 period of excitation to regain performance after the disturbance and process changes were simultaneously applied at 120 s and onwards.

2. The P and I gains as shown in Figure 2.5 have some variations even when process is in same condition. These variations are caused due to the optimization procedure. This is not a limitation for practical application, because this can be overcome very easily if P and I gains update is done with constraints.

3. As shown in Figure 2.4, the process input went into saturation after process changes and disturbance activated at 120 s, but the system regains control. The saturation is due to the aggressive PI gains prior to 120 s where process has a low gain and immediately after 120 s the process has a high gain.

4. Figure 2.7 shows that the gain and phase margin of system according to identified process model were maintained. When process changes at 120 s (or immediately after the adaptive control is switched on at 40 s), stability requirements were violated. But the specifications were regained due to fast convergence of process identification in terms of frequency response.

5. Figure 2.8 shows the system performance with conventional fixed parameter PI con-

21
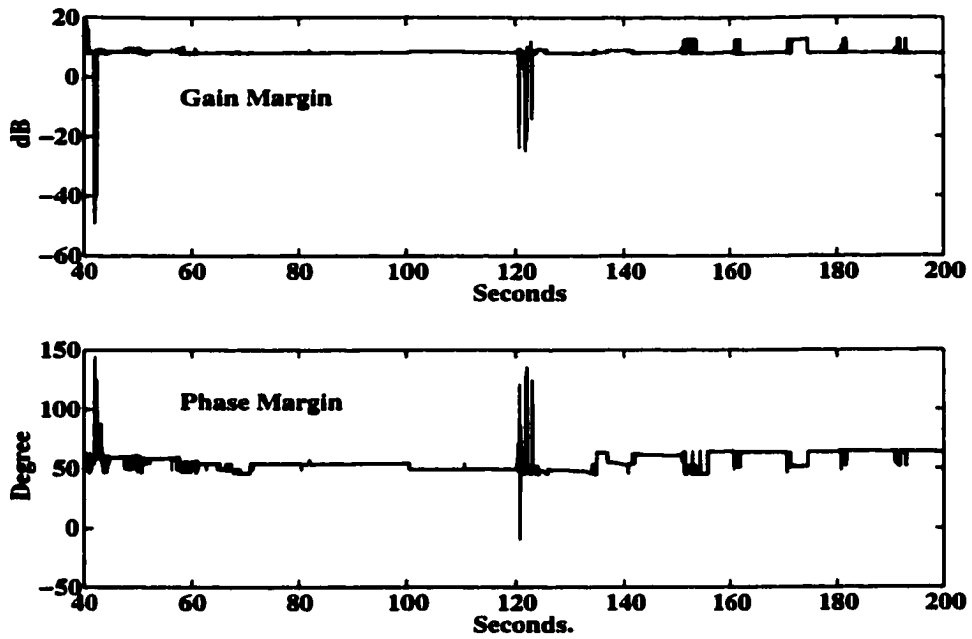
Figure 2.7: Gain margin and phase margin of system on each sample.
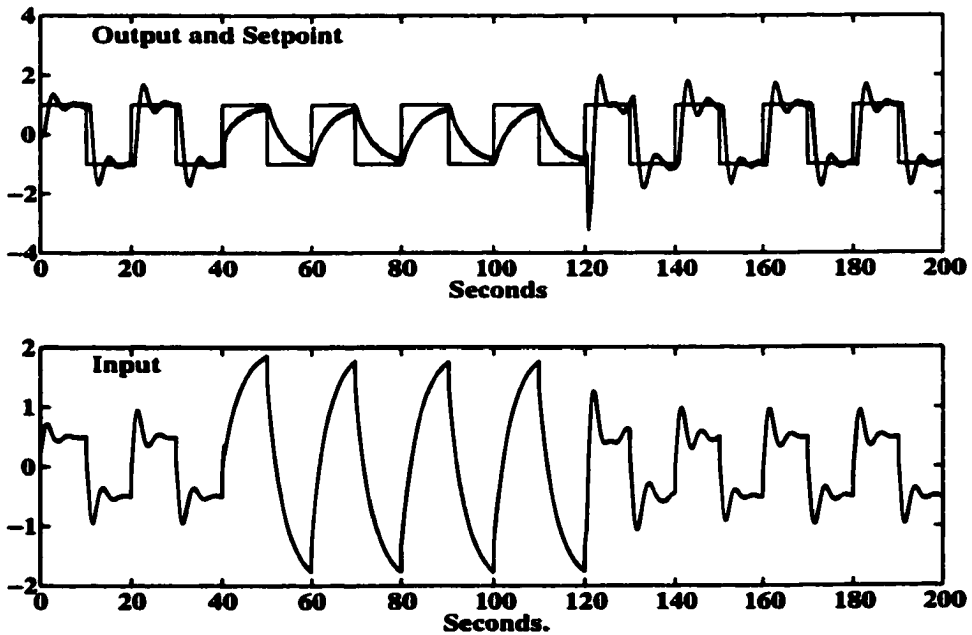
Figure 2.8: Process variables - setpoint, output and input with conventional fixed gain controller with P gain of 0.2 and I gain of 0.5.

22

troller with P gain of 0.2 and I gain of 0.5. When process gain increases, the system gave under damped response and when process gain decreases it gives over damped response. The need for an adaptive controller to maintain required performance of the system in all process conditions is evident.

The results obtained in these simulation is experimentally evaluated in the Section 2.4.

2.4 Preliminary Application of MRAS.

The application of MRAS based on frequency domain design needs some preliminary information. They are:

1. As the identification of system is to be carried out in terms of the frequency response, an adequate (high) sampling rate is required. The sampling rate should be at least 20 times faster than frequency (continuous) range of interest [8, 2, 3]. This may be a limitation in many older DCS systems. The requirement of sampling rate also enforce limitations on process model parameterization, maximum number of optimization iterations, number of frequency points considered etc. This is because the required computation has to be performed in the given sampling period.

2. It is required for MRAS implementation to specify suitable reference model. The MRAS based on frequency domain second order model design requires natural frequency, damping factor and time delay. A preliminary knowledge of these parameters for the system under consideration is required. This may require an experiment on the actual system. If natural frequency is specified much higher, then the controller gains will be aggressive driving the control effort into saturation, which will affect further identification. If natural frequency is lower, then the system response will be very sluggish with low gains for controller. The information about time delay of the plant can be obtained by bumping setpoint and monitoring output response of the plant. The value of time delay together with sampling rate of the controller fixes the order (numerator) of discrete model. The damping factor should be specified adequately. If damping factor is specified much lower, then the gains (especially I gain) will be of high values driving the control effort into saturation. If damping factor is higher then the system response will be very sluggish. These are not limitations for practical implementation as the required parameters are easy to obtain for a given system.

3. The setpoint should be excited with sufficient magnitude and also with required period. The setpoint is normally excited with square wave. It is required that the excitation frequency should be such that it provides rich excitation in the frequency range of interest. The frequency of excitation normally should be around the first frequency point of identification. Also the magnitude of excitation affects the signal to noise ratio and limits the frequency range for true identification. At higher frequencies,

23

the effective magnitude in frequency spectrum of the signal drops and noise starts corrupting the identification [2, 8, 17].

To evaluate the need for additional information if any, the MRAS is applied to the temperature control system as described in Appendix A in a preliminary experiment. The reference model assumed is closed loop second order model as given in Equation (2.4) and its discrete model in Equation (2.5). The value of ω_δ used is 0.012 rad (normalized) and ξ used is 0.8. A sampling period of 50 ms is used. The τ_d is zero for closed loop reference model. The stability margin requirements of 45° and 8 dB for phase and gain margins were imposed. The reference model and stability margin requirements are kept constant throughout all experiments performed hereafter in this thesis. The frequency responses were compared at 11 frequency points, starting at normalized frequency 0.0025 rad and then incrementing with step size of 0.0009 up to 0.0115 rad. The step size so selected is to have sufficient number of frequency data (upto 11 points) in the required frequency range. Standard RLS is used for process identification. The discrete plant model assumed is second order model as given in Equation (1.1). The model is reasonably parameterized with two unknowns in numerator and two unknowns in denominator using the open loop system identification method. A forgetting factor of 0.999 is used. Initially, all unknown coefficients of model are set to 0. The 'error' is computed as described in Section 2.3. The smooth switchover from conventional controller to adaptive PI controller and also between each sample as adaptive controller gain changes is obtained by adjusting integrator state to provide bumpless transfer [15]. Negative P and I gains are not applied to the process, as they are gross errors made by the optimization routine. No other constraint on P and I gains or on process input are considered. The DC bias from process input and process output is computed every 2000 samples. The maximum number of optimization iterations for determining P and I gains on each sample is set to 25. The optimization is stopped at any instant when the simplex size is reduced to 0.01 (i.e. less than ±0.01 changes in gains) or when 'error' is less than predetermined value or 25 iterations are reached. The setpoint excitation frequency is 0.01 Hz (period of 100 s). The conventional PI controller with P gain of 2 and I gain of 1 is used initially in the experiment. The adaptive controller is started at sample number 10001. The process is initially in low fan speed. No changes in process conditions were introduced in this preliminary experiment, as its goal is to evaluate the need for information for implementation of this MRAS scheme. The results of implementation of MRAS are shown in Figure 2.9. The process variables - setpoint, process input before bias removal, process output before bias removal, bias removed from input (dashed) and bias removed from output (dotted) are shown in Figure 2.9. The results of Figure 2.9 show a stable system. The process input is noisy. Also the exact specifications of reference model are not satisfied as can be seen in Figure 2.9. The experiment reveals some more requirements for implementation of the MRAS, which are summarized below:

1. The P and I gains computed by adaptive controller along with setpoint excitation are shown in Figure 2.10. The P and I gains up to 10000 samples are computed gains by

24
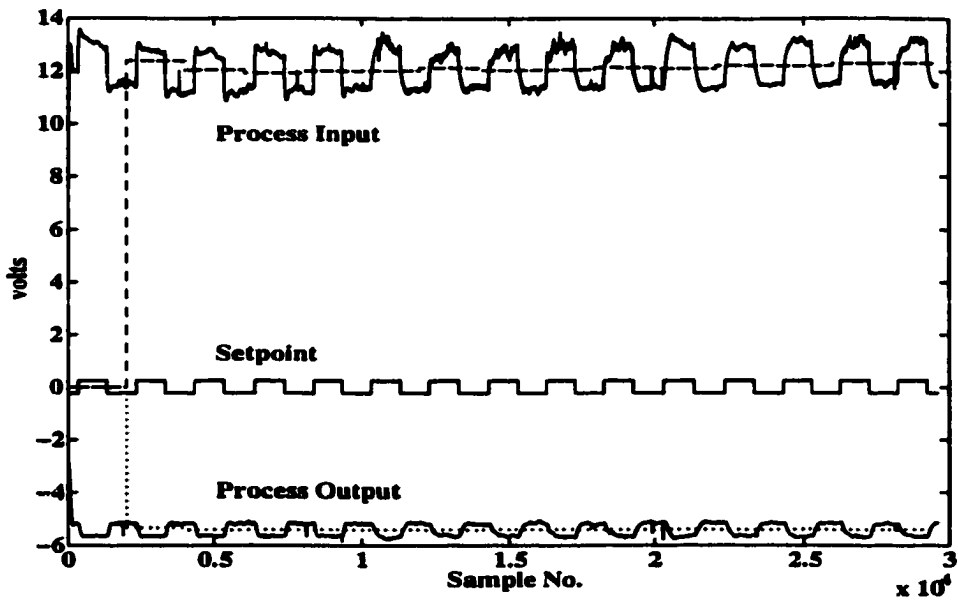
Figure 2.9: Process variables - setpoint, process input and process output, and DC bias in process input (dashed line) and in process output (dotted line).
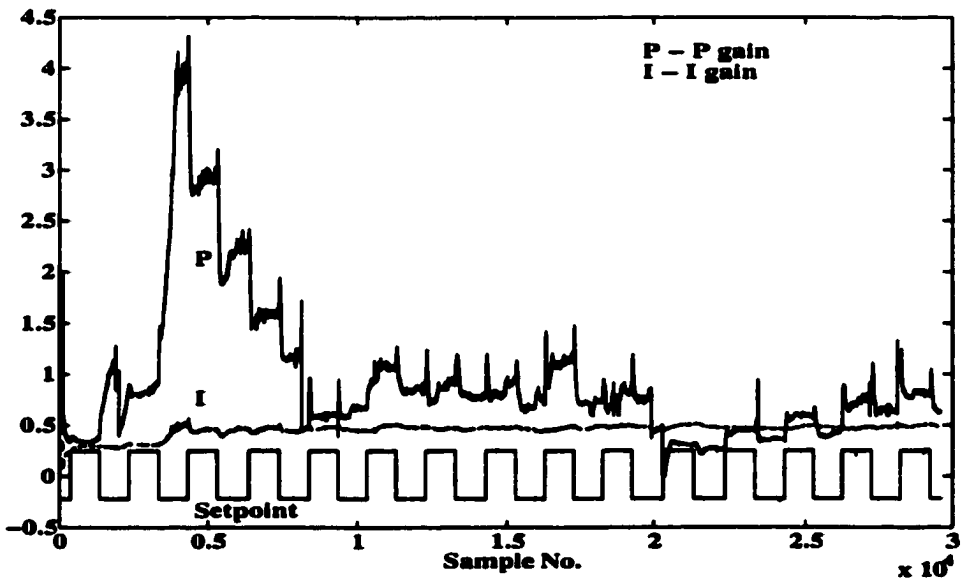
Figure 2.10: P and I gains as computed up to sample number 10000 and applied thereafter by adaptive controller to system.

25
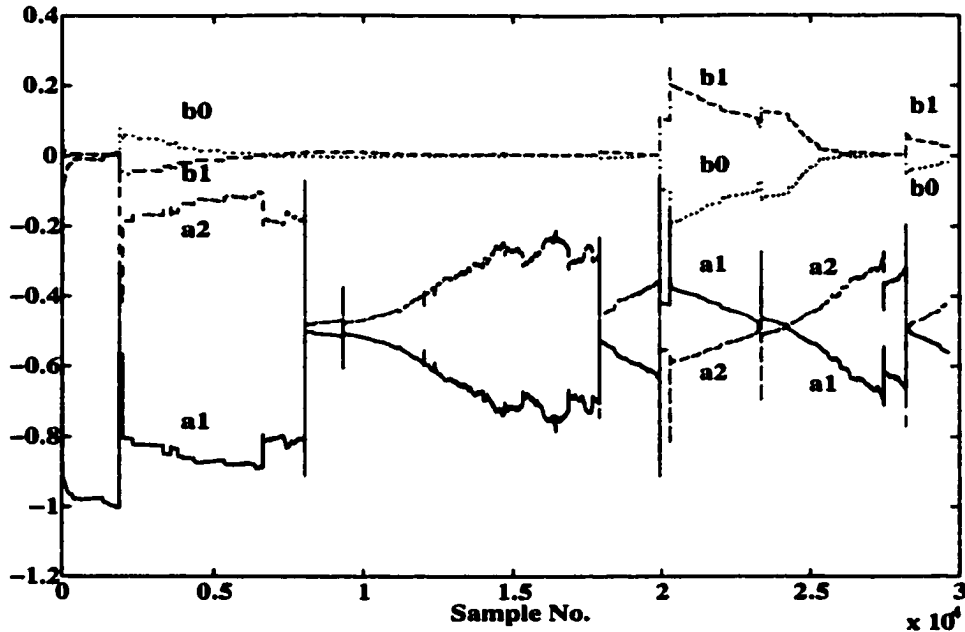
Figure 2.11: Variations in coefficients of estimated process model at each sample.

adaptive controller but are not applied, as the system was on conventional fixed gain controller. Only after switchover at sample number 10001 to adaptive control, are the gains actually applied. The solid line in Figure 2.10 is the P gain, while the dashed line is the I gain. The results show the tremendous impact of setpoint change on the controller gains, particularly P gain. We know that the 'frequency domain design' is based on steady state concepts. The concepts are however applied here to control and identify transients and fast dynamics of process. With adequately parameterized RLS model, it is logical to expect the effects of setpoint changes on the frequency response, which eventually affects the controller gains. This effect can be overcome by implementing a smoothing filter as given in Equation (2.8), on the coefficients of the estimated process model.

$$\hat{y}_k = (1 - \alpha)y_{k-1}^{\hat{}} + \alpha y_k \tag{2.8}$$

In Equation (2.8), y_k is actual value of coefficient calculated by RLS and $y_{k-1}^{\hat{}}$ and $\hat{y}_k$ are smoothed value of the coefficient used in estimating frequency response.

2. There is the presence of high frequency noise in form of 'spikes' in process variables (e.g. spikes in process input and process output around sample number 20000) as can be seen in Figure 2.9. This is due to the A/D Card or other electronic components used in the system. It can be seen that spikes in process output at sample number 20294, drives the P gain of controller to very low value. The gain is recovered later, but the spikes affect the system. The effect of the spikes can also be seen in Figure 2.11,

26
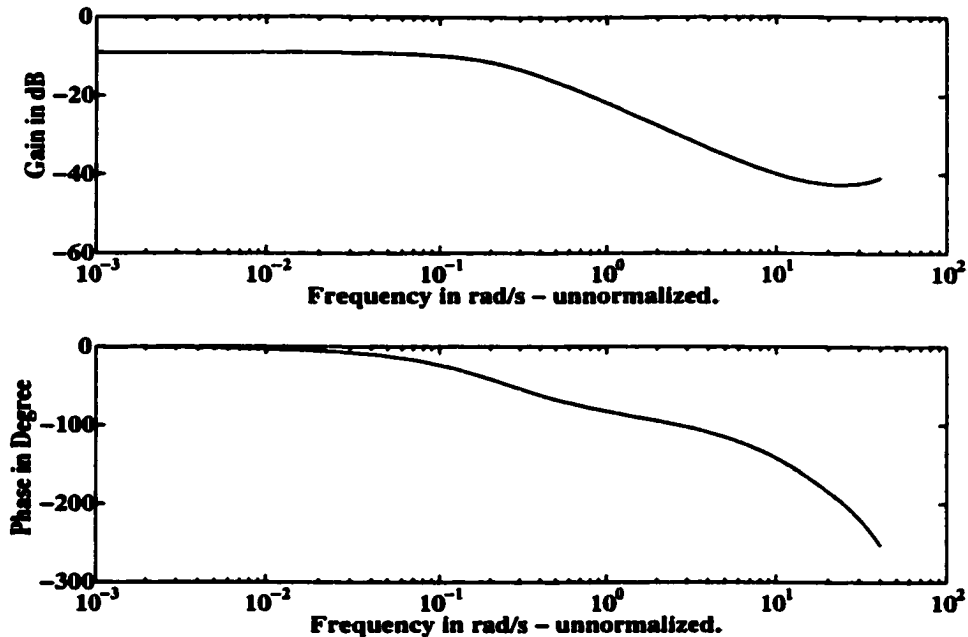
Figure 2.12: Open loop frequency response of identified process at sample number 10000 in low fan speed.

which shows the values of the coefficients of process model computed by RLS on each sample. The spikes in the process variables, particularly in input and output as shown in Figure 2.9, and sudden changes in value of coefficients of RLS as shown in Figure 2.11 are well correlated. The spikes can be removed from measured variables using a low pass filter, as spikes are normally high frequency noise. The low pass filter has to be implemented on all measured variables considered for system identification. This is because the filter causes phase lag, and this has to be equal on all variables to correctly identify the system. Thus it is required to filter process input and process output to remove 'spikes' and then use this filtered input and output for process identification.

3. In other preliminary experiments it was observed that sudden changes in bias also affects the gains of the controller. This bias change is caused not due to the process change, but due to number of samples considered in calculating bias. Due to this, use of bias removal based on the number of samples equal to number of samples in one period of setpoint excitation is required. This method is already implemented in the experiment performed here (DC bias is computed every 2000 samples which is equal to number of samples in one period of setpoint excitation (0.01 Hz $\equiv$ 100 s period $\equiv$ 2000 samples in one period at a sampling period of 50 ms), so the effect of sudden changes in bias via changes on RLS inputs and consequent changes in estimation are not seen in this experiment.

27

4. The open loop frequency response of process model at sample number 10000 is shown in Figure 2.12. The phase cross over frequency is about 10 rad/s (unnormalized, 0.5 rad normalized), which is much higher and not in the range of identification (0.0025 to 0.0115 rad normalized). A different frequency range is required for determining phase margin and may be even for gain margin. This can be implemented by increasing frequency step size for finding approximate phase margin and gain margin.

2.5 Application of MRAS Using Open Loop System Identification

The MRAS based on frequency domain design specifications using open loop system identification is now considered. The experimental conditions and model specifications were same as that of in Section 2.4. The requirements as identified in preliminary experiment performed on system in Section 2.4 are now implemented as follows:

1. The smoothing filter as given by Equation (2.8) with $\alpha = 0.2$ is implemented on the RLS coefficients.

2. To overcome effect of 'spikes' on identification, a low pass second order Butterworth filter with cut off at frequency (normalized) 0.63 rad (i.e. unnormalized frequency of 12.6 rad/s.) is used [13]. The low pass filter is implemented on process input and process output. Bias is first removed from process input and process output, then they are low pass filtered and finally used in RLS for process model identification.

3. If the phase margin or gain margin is not determined in the frequency range of identification (0.0025 rad to 0.0115 rad normalized) then a further frequency step size of 0.3 rad with 10 frequency points is used to determine phase and gain margins. In that case the frequency range to determine phase and gain margins is upto 3.0115 rad (0.0115 rad (maximum range considered for obtaining 'error') $+0.3*10 = 3.0115$ rad).

Initially, the process with low fan speed and with the conventional PI controller with P gain of 2 and I gain of 1 is used up to sample number 10000. There after the adaptive controller is applied. The variation in process variables - setpoint, input and output for different process conditions are shown in Figure 2.13. The PI gains are computed by adaptive controller up to sample number 10000 but not applied while thereafter they are applied to the system are shown in Figure 2.14. The solid line is P gain and dashed line is I gain.

The results can be summarized as:

1. When adaptive controller is implemented at sample number 10001 onwards, the system specifications were achieved as can be seen in Figure 2.13 and also in Figure 2.15 (comparing closed loop frequency responses). With conventional fixed gain controller, the system response is under damped in the low fan speed case, but with adaptive controller the specification of $\xi = 0.8$ is achieved and maintained.

28
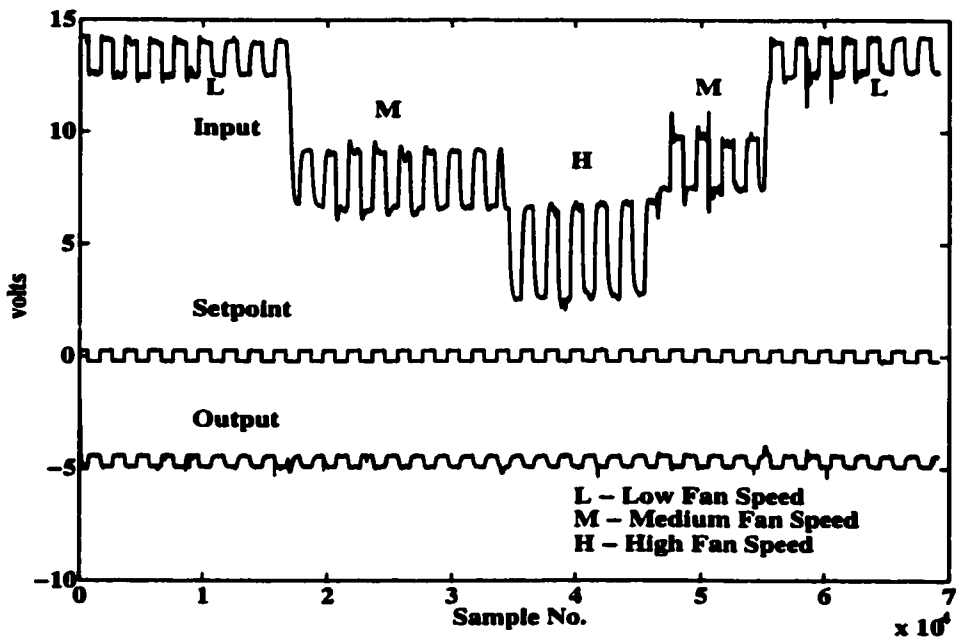
Figure 2.13: Process variables - setpoint, input and output.
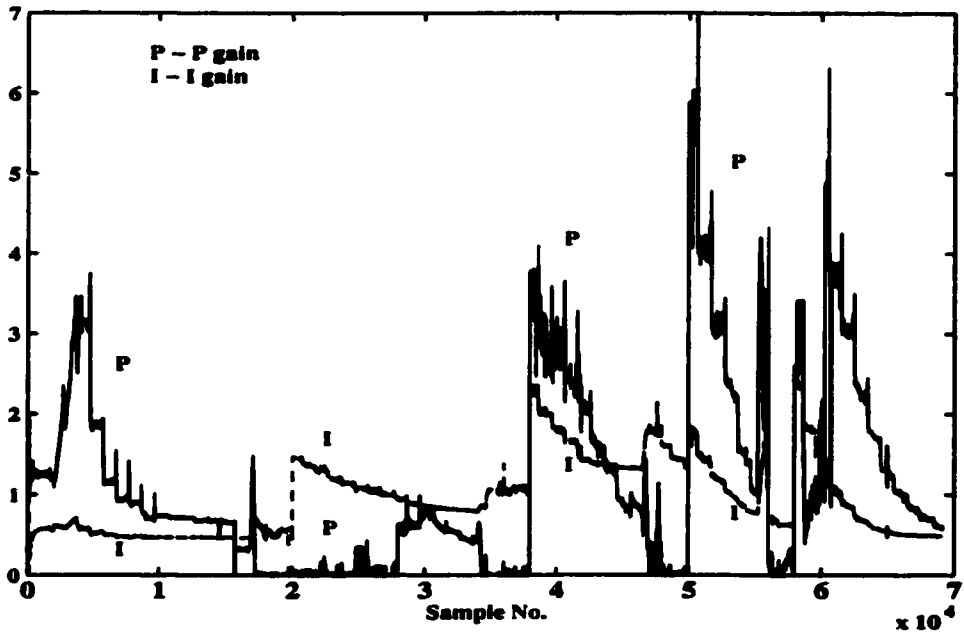
Figure 2.14: P gain (solid) and I gain (dashed) computed upto sample number 10000 and applied thereafter by adaptive controller.

29

Figure 2.15: Frequency of responses of reference model (solid) and resulting closed loop system (dashed) at sample number 11000.

2. The closed loop frequency response of system for that process condition and that of reference model are shown in Figure 2.15 at sample number 11000. The match in closed loop responses is good. While the main goal in evaluating P and I gains is to make system response achieve specifications, exact match at all frequencies is not possible. This is due to the limited frequency range for comparison and a limited number of controller variables, namely the P and I gains of the controller.

3. The effect of setpoint excitation on P and I gains as seen in Figure 2.10 is now overcome in Figure 2.14 by providing the smoothing filter of Equation (2.8) on RLS coefficients. The P and I gains are shown in Figure 2.14, have low correlation to setpoint changes. Another advantage of filtering RLS coefficients is that it also helps in reducing the effects of any spikes which are not fully filtered out by the low pass filter. The most significant disadvantage of the filter is that it slows fast updates in RLS coefficients and therefore slows down identification.

4. With the implementation of a low pass filter, the effects of spikes in process variables, is reduced as can be seen in Figure 2.16. The figure shows the variations in coefficient a_1, a_2, b_0 and b_1 in the estimated process model at each sample. The spike on the input/output still affects RLS coefficients, as can be seen for sample number 15708 (spike on input), which causes sudden drop in P gain. But the system regains performance fast by recovering the P gain. The disadvantage of filter on input and output

30
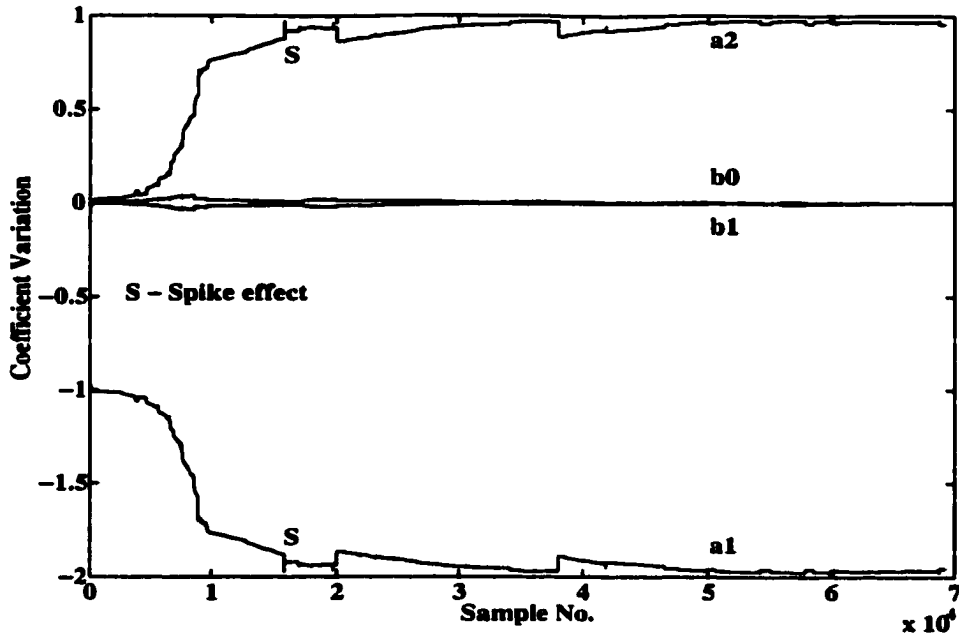
Figure 2.16: Variations in coefficients of estimated process model at each sample.

is that it slows down identification and adds computational overhead. Low pass filter may or may not be needed for general implementation of this scheme depending on presence of spikes in general.

5. The process changes were introduced by changing fan speed from low to medium speed at sample number 16800. The change in bias in process input can be seen in Figure 2.13. The DC bias in low pass filtered input and output, and input and output as fed to RLS after removal of DC bias are shown in Figure 2.17. The convergence of DC bias in input can be seen at about sample number 22000. It took about 3 cycles of setpoint excitation for correct estimation of DC bias after the process changes were introduced. It is important to note that there is hardly any DC bias change in process output. This is because it is maintained to setpoint by the PI controller. The DC bias in output only changes when there is setpoint 'DC bias' changes. Also the change in DC bias level in output is avoided because the controller is aggressive enough to bring the error to zero after every setpoint excitation. If the controller is non-aggressive as in the self-tuning experiment in Chapter 1, the DC bias may change on the output as the controller fails to brings down error to zero within setpoint changes.

6. After the DC bias convergence to true value at medium fan speed at about sample number 22000, it took up to sample number 27000 for the system to follow specifications as can be seen from Figure 2.13 and also in Figure 2.20 (comparing closed loop frequency responses).

31
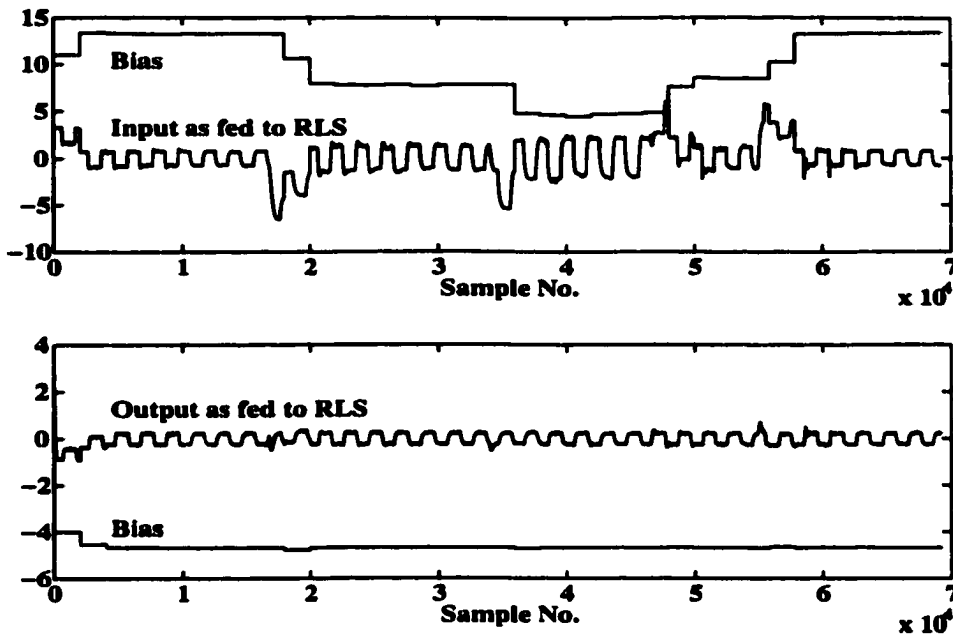
Figure 2.17: Estimated DC bias in low pass filtered input and input as fed to RLS, and DC bias in low pass filtered output and output as fed to RLS.
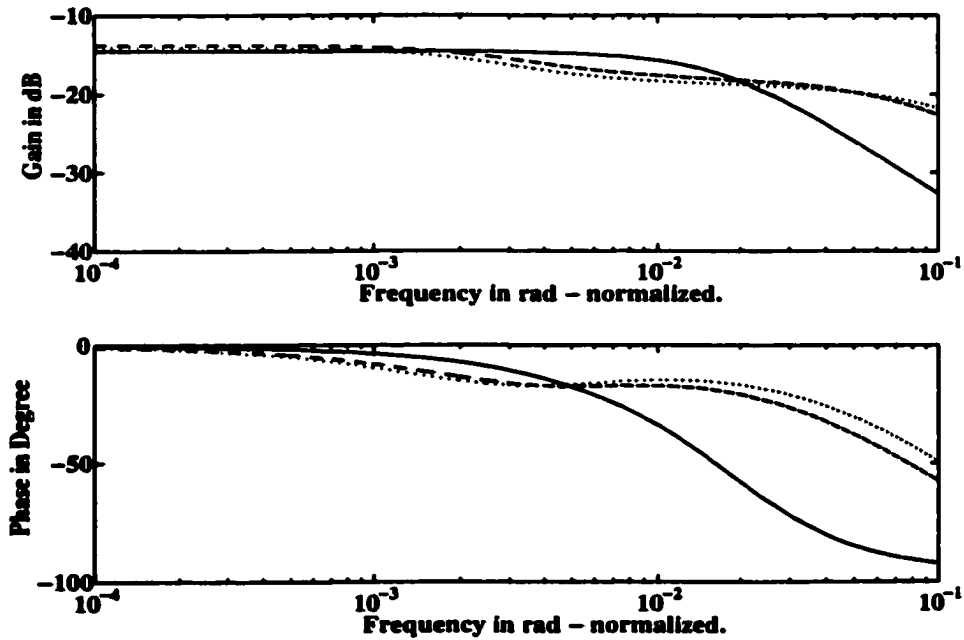
Figure 2.18: Open loop frequency responses at sample numbers 25000 (dotted), 27000 (dashed) and 33000 (solid).

32
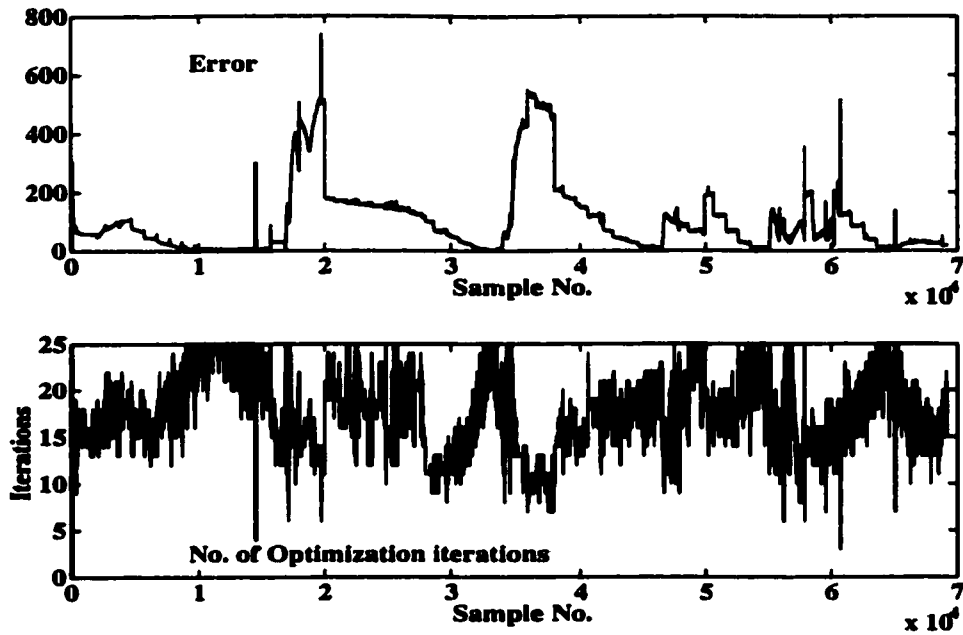
Figure 2.19: The absolute error computed and number of iterations of optimization routine performed on each sample.
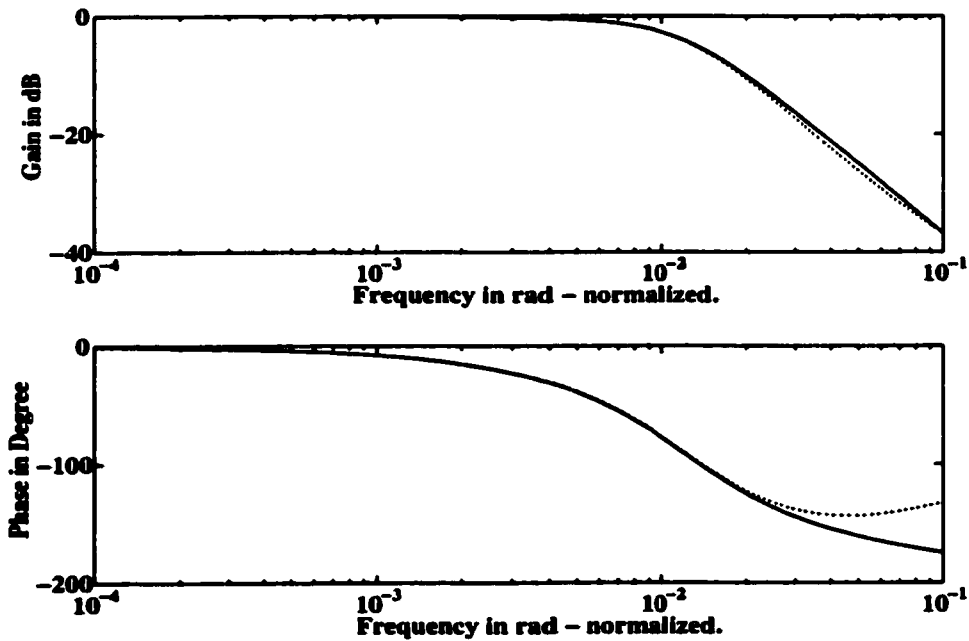
Figure 2.20: Frequency responses of reference model (solid) and resulting closed loop system (dotted) at sample number 33000 in medium fan speed condition.
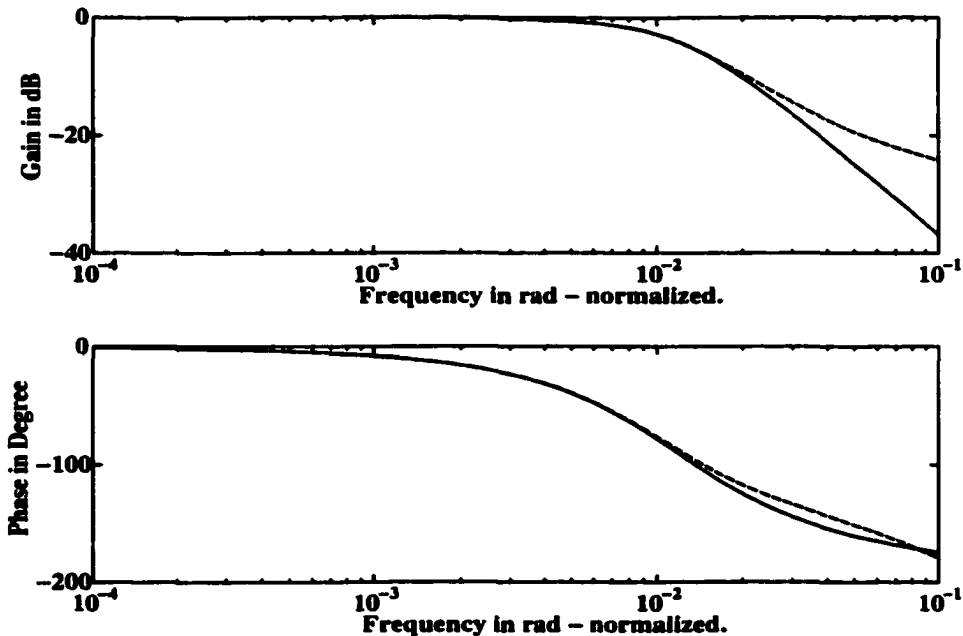
33
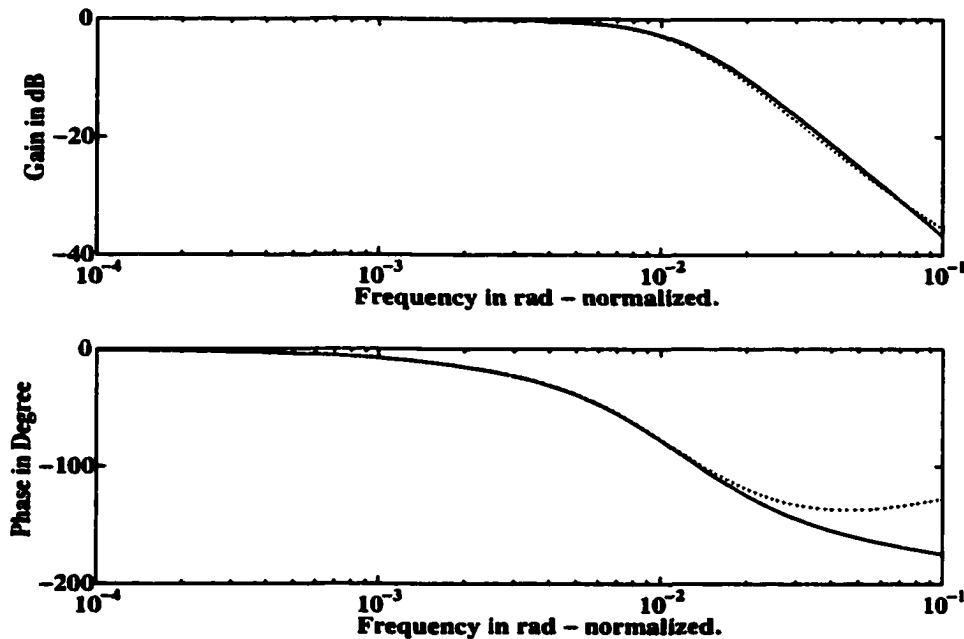
Figure 2.21: Frequency responses of reference model (solid) and resulting closed loop system (dotted) at sample number 46000 in high fan speed condition.

7. The open loop frequency response plots at sample number 25000 (dotted line), 27000 (dashed line) and 33000(solid line) in medium fan speed condition of the identified process model are shown in Figure 2.18, to show the convergence of the RLS in terms of frequency response. The convergence of RLS in terms of 'frequency response' takes about 10000 samples (from sample number 16800 to sample number 27000 approximately), i.e. 5 periods of excitation. The convergence is severely affected due to the DC bias change in process input due to process change. After sample number 27000 and onward the system specifications were achieved for medium speed fan condition as seen in Figure 2.13 and Figure 2.20.

8. Figure 2.19 shows the error computed at each sample and number of optimization iterations performed by optimization routine to calculate the P and I gains on each sample. The error settles down after system specifications were achieved. Also error increases whenever there is a change in process conditions. This behavior of error is of importance for practical consideration. The system identification by RLS requires persistent excitation. The excitation in setpoint is only required when system identification needs to be carried out i.e. only when plant parameters change. The continuous excitation of the system is not acceptable in industrial controls as it may affects the quality of the product. Instead a scheme can be hypothesized using the error and identified model to start and stop the excitation. For a given plant condition and with excitation in setpoint, the identification of system can be carried out continuously

34
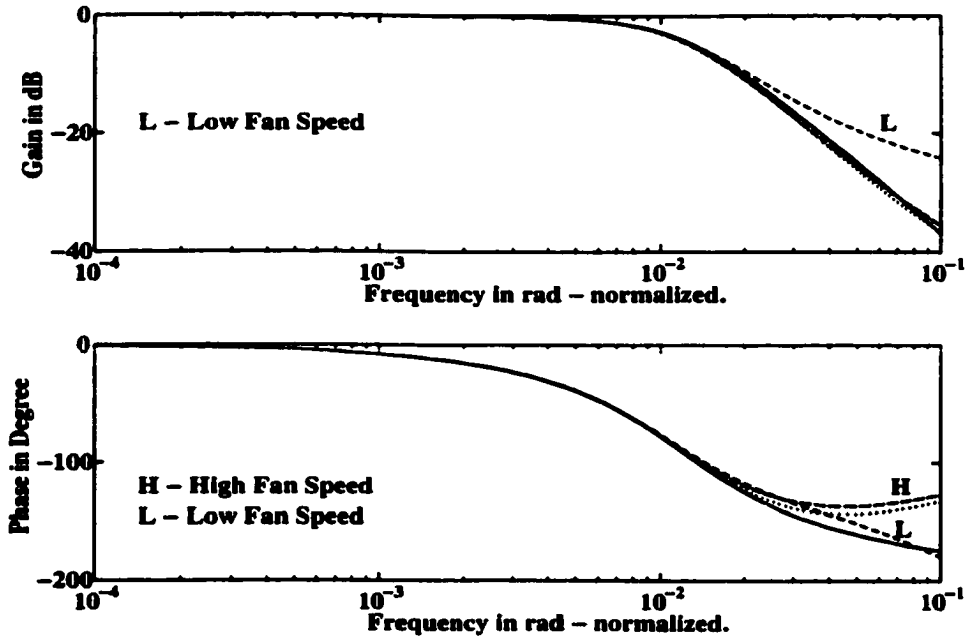
Figure 2.22: Frequency responses of reference model (solid) and resulting closed loop system at sample numbers - 11000 (low fan speed - dashdot), 33000 (medium fan speed - dotted) and 46000 (high fan speed - dashed).

until the error converges or reduces to the predefined value. Then the identification is not required and excitation can be stopped. The controller gains and identified model should be held constant for that condition of plant. A scheme has to be implemented to identify process change. This can be done using last identified model of the plant on each sample. For given input sequence, the estimated output of the plant can be computed using the last identified model. This estimated output could then be compared with actual plant output. The difference between them beyond a threshold can be used to identify a situation where the process has changed and once again to start the excitation and identification until error convergence is achieved. Care has to be taken that disturbances affecting the process do not falsely trigger adaptation.

9. Process change is again applied at sample number 33900 by changing the fan speed from medium to high speed. The specifications were achieved after about 4 cycles of excitation as can be seen from Figure 2.13 and also in Figure 2.21 (comparing closed loop frequency responses).

10. A further process change is applied at sample number 46500 by changing the fan speed to medium speed from high speed. As can be seen in Figure 2.13, the system once again converges to the required specifications.

35

11. Finally, a process change is again applied at sample number 55000 by changing the fan speed to low. Initially, the system response is under damped as expected due to change of process gain from low to high. The specifications however are achieved after about 5 cycles of excitation as can be seen in Figure 2.13.
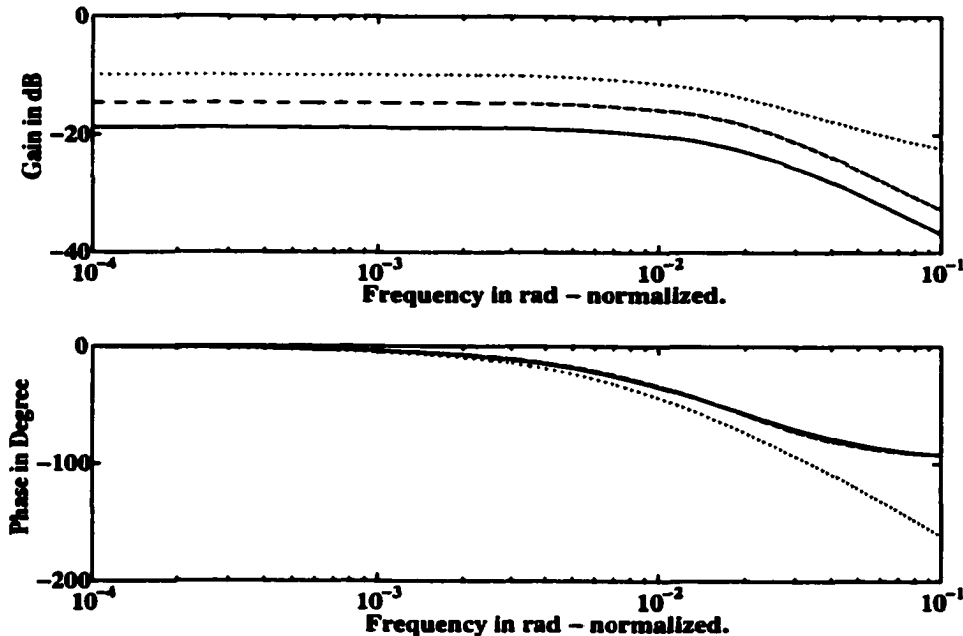
Figure 2.23: Open loop frequency responses of identified process model in low fan speed at sample number 11000 (dotted), medium fan speed at sample number 33000 (dashed) and high fan speed at sample number 46000 (solid).

12. The trend observed from Figures 2.13, 2.14 and 2.19 is that when system identification converges, the error and controller gains also converges meeting the specifications as required for all the process conditions.

13. The closed loop responses at different sample and in different process conditions are shown in Figure 2.22. The solid line is closed loop response of reference model. The dashdot line is closed loop response of system in low fan speed condition at sample number 11000. The dotted line is closed loop response of system in medium fan speed condition at sample number 33000. The dashed line is closed loop response of system in high fan speed condition at sample number 46000. Reasonable match between responses of reference model and the closed loop system is seen particularly upto -10 dB in magnitude and -150° in phase in all cases.

14. The trend in process input can be observed for different process conditions. With the process in low fan speed (high process gain), the control effort required is less to achieve same setpoint change, than that in high fan speed (low process gain). To

36

achieve the specifications the gains on controller has to be higher in low process gain than in the high process gain condition. This can be seen in Figure 2.14.

15. The open loop frequency plots of identified process model at different process conditions are shown in Figure 2.23. In this figure, the dotted line is frequency response in low fan speed condition (sample number 11000). The dashed line is frequency response is in medium fan speed condition (sample number 33000). The solid line is frequency response in high fan speed condition (sample number 46000). The plots were obtained from the frequency response of identified process model after the system identification converged and the specifications were achieved by the adaptive controller.

2.6 Conclusion

The MRAS implementation with frequency domain specifications based on frequency response and using open loop system identification has been studied and experimentally demonstrated. The scheme is able to perform as per the specifications in all process conditions. The practical implementation requires specific issues to be addressed as demonstrated in this chapter. The change in DC bias in process variables, when process changes, affects the identification severely unless the bias is appropriately factored out. An approach to DC bias estimation has been applied in this chapter.

Chapter 3

Model Reference Adaptive Control System Using Frequency Domain Performance Specifications And Closed Loop System Identification.

3.1 Introduction

The closed loop system identification uses the setpoint and process output for system identification. In this method of identification, first the closed loop system is identified from which the controller dynamics are removed to obtain open loop process information [8, 19, 20]. If $T(z)$ denotes the closed loop discrete time transfer function, then for unity feedback system, it is given by Equation (3.1).

$$T(z) = \frac{G(z)C(z)}{1 + G(z)C(z)} \tag{3.1}$$

Where $G(z)$ is open loop process transfer function and $C(z)$ is controller transfer function. Equation (3.1) can be rearranged to obtain open loop process transfer function using closed loop transfer function and controller transfer function as:

$$G(z) = \frac{T(z)}{(1 - T(z))C(z)} \tag{3.2}$$

There are two approaches possible for setting a parametric model of the closed loop system in closed loop system identification. In the first approach, assuming the parametric model of the open loop process transfer function, compute the structure of closed loop parametric transfer function using controller transfer function. It is possible to set up RLS in such a way to estimate directly parameters of the open loop transfer function. However in this approach the regression vector in RLS involves difference operation and usually therefore, has low

38

signal to noise ratio, causing unreliable estimation of coefficients [8]. This approach is therefore not very useful. A second approach to parameterization of the closed loop transfer function is to over parameterize it. In this approach the denominator is considerably over parameterized. It is now no longer possible to relate the estimated coefficients to the process transfer function parameters. However in this frequency domain approach of this thesis, the transfer function of the process is not needed, only its frequency response at some frequency points is required. Therefore this approach is suitable for MRAS in frequency domain and is used here.

3.2   Importance of Closed Loop System Identification

Importance of the closed loop system identification can be summarized as:

1. The primary advantage is that in all the feedback control systems the setpoint and process output are readily available in the digital control system for use in identification.

2. As observed in Chapter 2, using open loop system identification, the DC bias change in process input (when the process changes) delays the identification of the plant model. The closed loop system identification only uses setpoint and process output, not the process input and so it has a possible advantage, viz. the DC bias change in process input when the process changes will no longer affect identification and fast convergence of the RLS can be expected. The DC bias in output is not much affected by the changes in process conditions with reasonable PI controller as already observed. The anticipation of this major advantage is the motivation for investigating closed loop system identification over open loop system identification in adaptive control systems.

The over parameterization of closed loop model increases computational overhead. Also for practical implementation, issues arise due to fact that the open loop plant model is obtained using closed loop identified model and controller parameters. This means the change in controller parameters in adaptive controller could affect the change in open loop model, even if the open loop process condition is the same. This problem can be overcome by updating the controller after a certain number of samples when the open loop model converges instead of at every sample. After each update of controller parameter, the covariance matrix of the RLS is also reset to enable the new closed loop response to be identified. This approach delays fast update of the controller and will definitely affect the system performance when process changes and needs to update the controller as soon as possible. Also the controller gains will continue to be used up to the next update, even if the system does not meet required specifications.

39

3.3 Application of MRAS Using Closed Loop System Identification

The MRAS based on frequency domain performance specifications using closed loop identification is applied to the temperature control system (Appendix A). The reference model, stability requirements, frequency points considered and all other experimental details are the same as that described in Section 2.4. The closed loop over parameterized model assumed is second order numerator and fourth order denominator as given in Equation (3.3).

$$T(z) = \frac{b_0 z^{-1} + b_1 z^{-2}}{1 + a_1 z^{-1} + a_2 z^{-2} + +a_3 z^{-3} + a_4 z^{-4}} \tag{3.3}$$

The choice of two coefficients in the numerator is motivated by the PI controller and considering first order process. The denominator however is considerably over parameterized. The DC bias from setpoint and process output is removed every 2000 samples. The DC bias removal from setpoint is required because it was noticed that function generator used in experiment generates DC bias. This may not be needed for general implementation. The adaptive controller parameters were updated and covariance matrix of RLS is reset to value of 100 every 8000 samples after switch over to adaptive control. It is assumed that the identification convergence might take 8000 samples after the controller parameters are changed. The process frequency response (real and imaginary part of transfer function) is computed at required frequency points using the relation given by Equation (3.2), for use in the optimization routine to obtain P and I gains. The run time optimized c language code was generated using symbolic processing (Maple) software [14].

Initially, the process with low fan speed and with conventional PI controller with P gain of 2 and I gain of 1 is used up to sample number 10000. Thereafter the adaptive controller is designed (every 8000 samples) and applied. The variation in process variables - process input, process output and setpoint are shown in Figure 3.1 for different process conditions. The applied P and I gains are shown in Figure 3.2. The solid line in Figure 3.2 shows the P gain and dashed line is the I gain.

The results of the application can be summarized as:

1. After the adaptive controller is implemented at sample number 10001 with the system in low fan speed condition an under damped response is obtained, as can be seen in Figure 3.1.

2. The fan speed is changed to medium from low at sample number 20001. The system performance can be seen in Figure 3.1. Initially after the change in speed is applied, the system response is over damped. This is due to the gains of the controller are still that applied for low fan speed (high process gain). Finally, after the controller is updated with the gains obtained from system identification performed in medium speed the system response is under damped after sample number 32000. A process change is

40
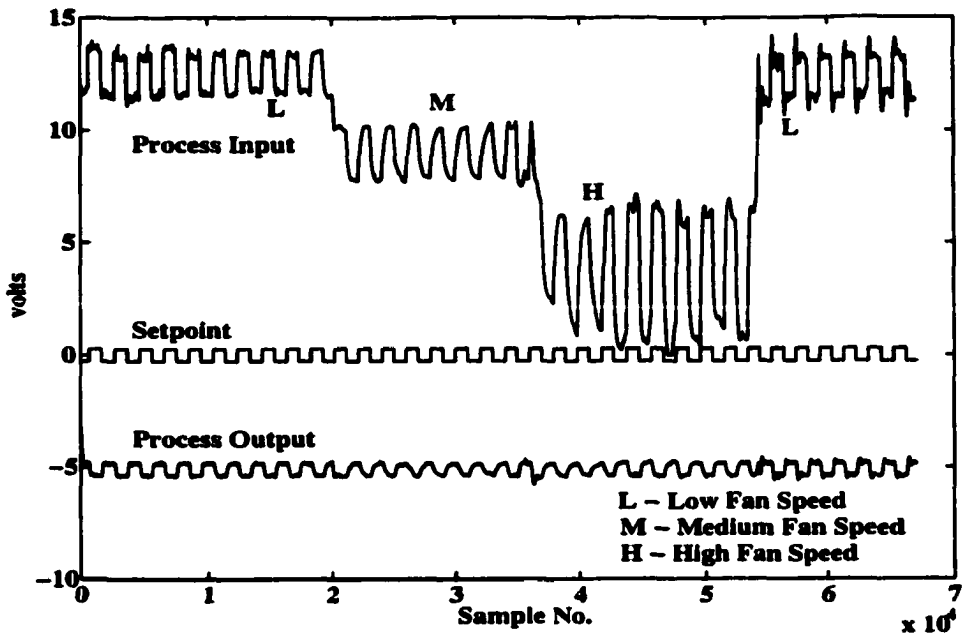
Figure 3.1: Process variables - setpoint, process output and process input.
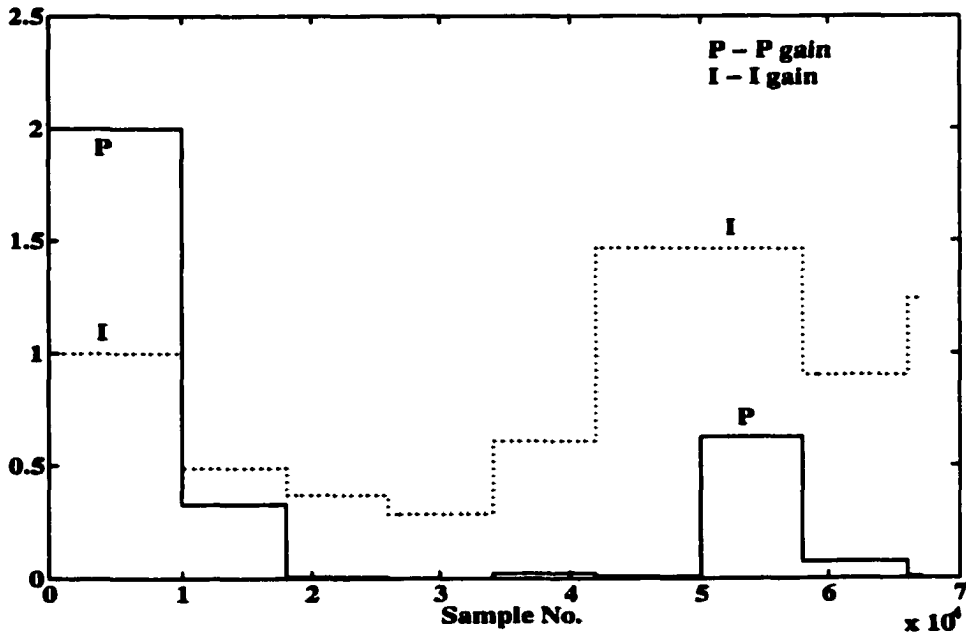
Figure 3.2: P gain (solid) and I gain (dotted) as applied by conventional controller upto sample number 10000 and applied thereafter by adaptive controller at every 8000 samples.

41
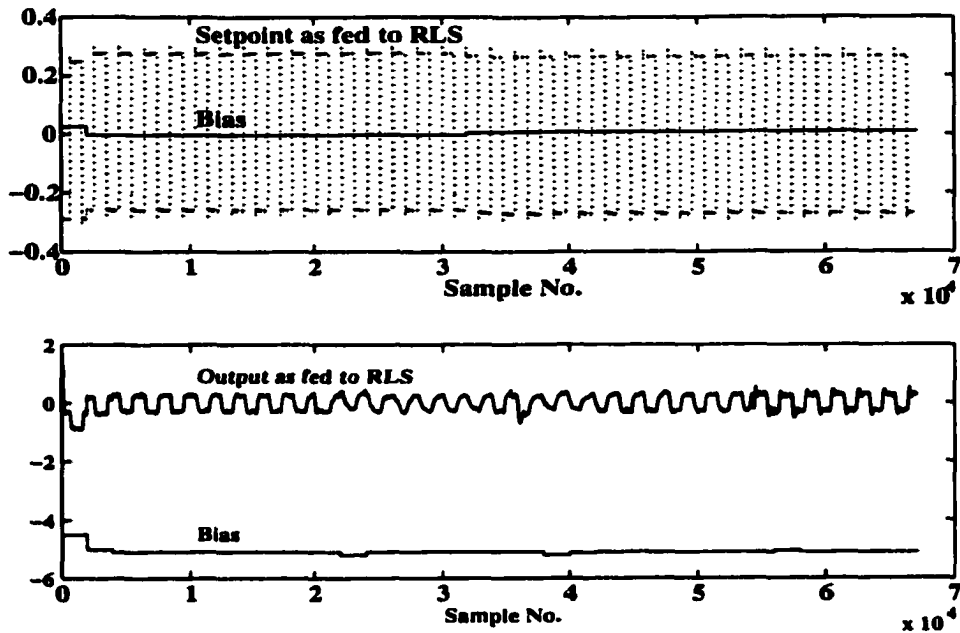
Figure 3.3: Estimated DC bias in filtered setpoint (solid) and setpoint as fed to RLS (dotted), and DC bias in filtered output (solid) and output as fed to RLS (solid).
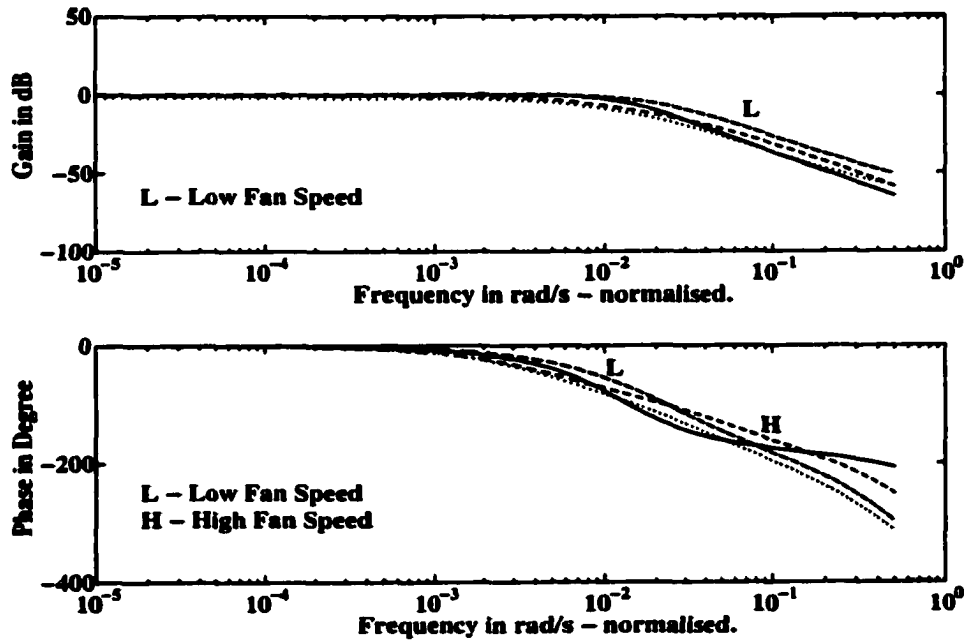
Figure 3.4: Frequency responses of reference model (solid) and identified closed loop system at sample numbers - 17000 (low fan speed - dashed), 34000 (medium fan speed - dotted) and 53000 (high fan speed - dashdot).

42

again applied by changing fan speed to high from medium at sample number 36000. The system response is under damped after the controller gains are updated at sample number 50000, as can be seen in Figure 3.1. To study the effect of severe changes in process conditions, the fan speed is changed to low from high at sample number 54000. The system response is immediately very under damped, because the controller gains are as identified in high speed (low process gain) condition. The sustained under damped response can be observed in Figure 3.1. The required specifications were not achieved.

3. The DC bias removed from process output and setpoint are shown in Figure 3.3. As expected, there is hardly any change in DC bias in process output in different process conditions. The severe effect of DC bias on identification as experienced in open loop identification is overcome in closed loop identification.

4. The closed loop frequency responses at different process conditions are shown in Figure 3.4. The solid line is closed loop response of reference model. The dashed, dotted, and dashdot lines are closed loop responses of identified model in low (sample number 17000), medium (sample number 34000) and high (sample number 53000) fan speed respectively. A reasonable match between frequency responses of identified closed loop and reference model is seen in Figure 3.4. The match in closed loop plots is however not as good as obtained with open loop identification in Figure 2.22.

5. The open loop frequency responses at different process conditions are shown in Figure 3.5. The dashed, dotted, and dashdot lines are open loop responses of process obtained from identified closed loop model in low (sample number 17000), medium (sample number 34000) and high (sample number 53000) fan speed respectively. The plots show that in low frequencies the magnitude identified is very low. This is due to the fact that the PI controller has very large magnitude in low frequencies, and as per Equation 3.2, the controller magnitude is in the denominator when obtaining the open loop response. Then small errors in $T(z)$ at low frequencies severely affect the response calculations [1].

6. The disadvantage of using closed loop identification is that controller updates are slow. The severely under damped system may result for a long time as can be seen in Figure 3.1, for change in fan speed from high (low process gain) to low (high process gain) speed at sample number 54000. This situation is not acceptable in industrial systems. The sustained under damped behavior will result whenever the process condition changes from low gain to high gain conditions, until convergence is achieved and controller parameters are updated.

7. It can be observed in Figure 3.1 that the resulting system response is under damped even with the controller gains implemented (as shown in Figure 3.2) after carrying out identification without changing process conditions. After implementing controller gains at sample number 10001, the system response is under damped for low speed
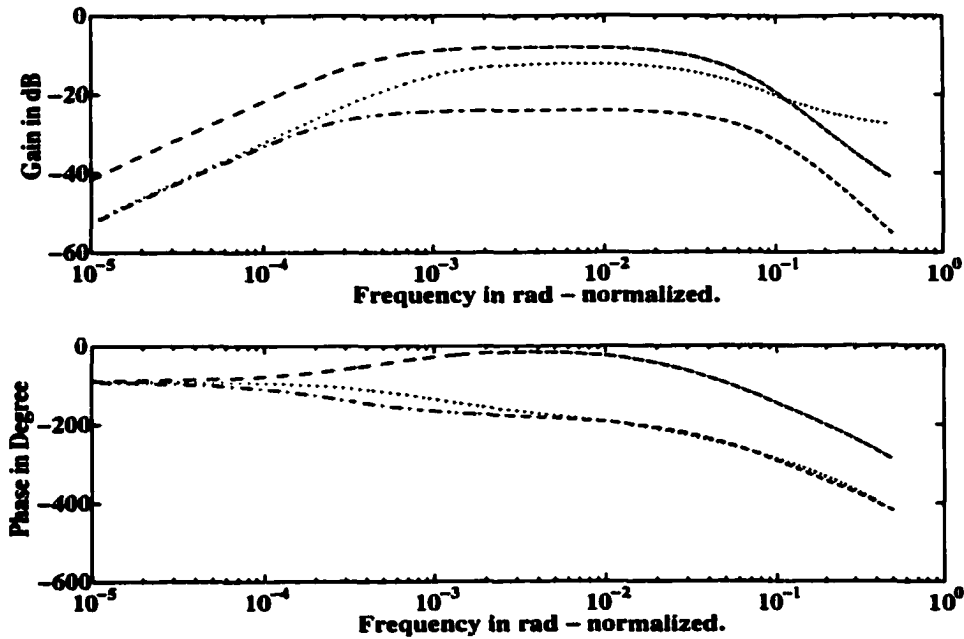
Figure 3.5: Open loop frequency responses of process at sample numbers - 17000 (low fan speed - dashed), 34000 (medium fan speed - dotted) and 53000 (high fan speed - dashdot).

condition. After the fan speed is changed to medium from low at sample number 20000 and carrying out the identification in the same process condition up to sample number 34000, the applied controller gains at 34001 makes the system response under damped for that process condition. Similarly in high fan speed condition too, the applied gains at sample number 50001 after carrying out the identification from sample number 36000 to sample number 50000, makes the system response under damped. The required specifications as given in reference model were not achieved. The under damped behavior of the system must be due to higher effort resulting due to higher gains on controller. The higher gains result due to the low gain of the open loop process (as observed in Figure 3.5) calculated in opening the loop using Equation (3.2) at frequency range considered in optimization routine to obtain controller gains. Since the open loop identification in Chapter 2 and PI gains computed from it led to better match in performance than from that in this chapter, it is obvious that open loop identification in Chapter 2 better reflects reality than the computed open loop response from closed loop identification in this chapter.

The under damped behavior of system in closed loop identification is now further investigated.

44

3.4 Comparison of Identified Models Using Open and Closed Loop System Identification

The cause for under damped adaptive control performance obtained when using closed loop identification needs to be determined. The main reason could be under parameterized model or some other unknown phenomenon. An experiment is performed to identify the process using open loop and closed loop identification simultaneously to compare frequency responses obtained from both identifications. The setpoint excitation amplitude is kept high to rule out a possible cause that the bad estimation is due to low setpoint excitation. The open loop model and closed loop model assumed is as given in Equation (3.3). All other experimental conditions were kept same as in Section 3.3. The adaptive controller is not implemented as the experiment is performed only for process identification. The controller with a P gain of 2 and an I gain of 1 is used. The frequency responses of open loop process model as identified by open loop and closed loop identification methods at sample number 10000 are shown in Figure 3.6. The solid line shows the response of process model as identified by closed loop and dashed line shows the response of process model as identified by open loop identification method. It can be observed that the magnitude of process identified by closed loop method is about 2 dB lower than that of open loop method in the frequency (normalized) range 0.0025 to 0.0115 rad, which is used for obtaining controller gains when adaptation is performed. To rule out effect of noise at considered sample instant, the plots were compared at many samples but similar results were obtained. As discussed in [4], a linear feedback of sufficiently low order may introduce linear dependencies among the columns of the measurement matrix in RLS and then parameters can not be determined uniquely. The problem with lack of identifiability due to feedback can be overcome by over parameterization of the model [4]. To confirm that this phenomena (i.e. lower magnitude in closed loop identification) is not caused due to the under parameterized closed loop model, an offline RLS simulation on the same input/output data is performed assuming over parameterized model. The over parameterized model assumed for both identification methods is 5th order numerator and 15th order denominator as given in Equation (3.4).

$$T(z) = \frac{b_0 z^{-1} + \cdots + b_4 z^{-5}}{1 + a_1 z^{-1} + \cdots + a_{15} z^{-15}} \tag{3.4}$$

The open loop frequency responses of the identified process at sample number 10000 with both identification methods with over parameterization is shown in Figure 3.7. The solid line shows the response of process model as identified by closed loop and dashed line shows the response of process model as identified by open loop identification method. The same difference in magnitude plot is obtained. This rules out the possibility that model considered in Equation (3.3) was an under parameterized model.

It is observed that in closed loop identification, the process gain identified in low frequencies is low. This is due to high controller gain in low frequencies. This problem could be avoided by guaranteeing a DC gain of unity in identified closed loop model. Assuming

Figure 3.6: Open loop frequency responses of process as identified in open loop (dashed) and closed loop (solid) identification method at sample number 10000.

Figure 3.7: Open loop frequency responses of process as identified in open loop (dashed) and closed loop (solid) identification methods with over parameterized model at sample number 10000.

46

Figure 3.8: Open loop frequency responses of process as identified in open loop (dashed) and closed loop (solid) identification method with guaranteed DC gain of unity in closed loop identification at sample number 10000.

the closed loop model as given by Equation (3.3), the unity DC gain can be guaranteed if Equation (3.5) could be satisfied all the time.

$$\frac{b_0 + b_1}{1 + a_1 + a_2 + a_3 + a_4} = 1 \tag{3.5}$$

Using Equation (3.5) with model as given by Equation (3.3) and eliminating b_1 coefficient for setting up the regression vector, one can get relation as given by Equation (3.6).

$$y_k - u_{k-2} + a_1(y_{k-1} - u_{k-2}) + a_2(y_{k-2} - u_{k-2}) + a_3(y_{k-3} - u_{k-2})$$
$$+a_4(y_{k-4} - u_{k-2}) = b_0(u_{k-1} - u_{k-2}) \tag{3.6}$$

The RLS can be set up to estimate the required coefficients in Equation (3.6). The value of b_1 can always be obtained using Equation (3.5). The offline simulation on same set of data is performed again with guaranteed DC of unity in closed loop model. The open loop process model obtained in both methods by simulation is shown in Figure 3.8. The solid line shows the response of process model as identified by closed loop and dashed line shows the response of process model as identified by open loop identification method. As required the effect of controller gain in low frequencies is eliminated. But still the identification by closed loop method results in a lower gain. The phase matches exactly in
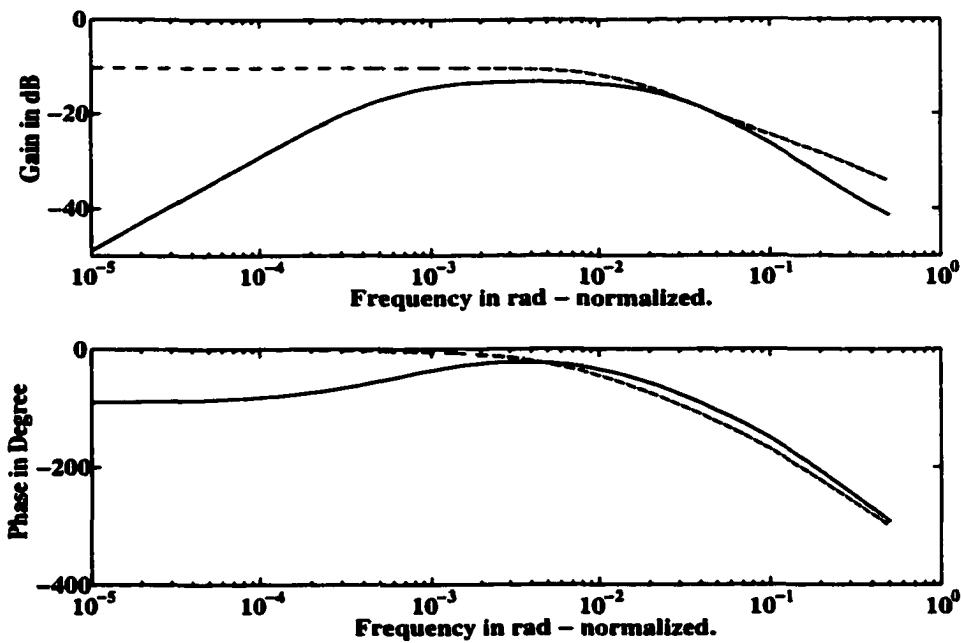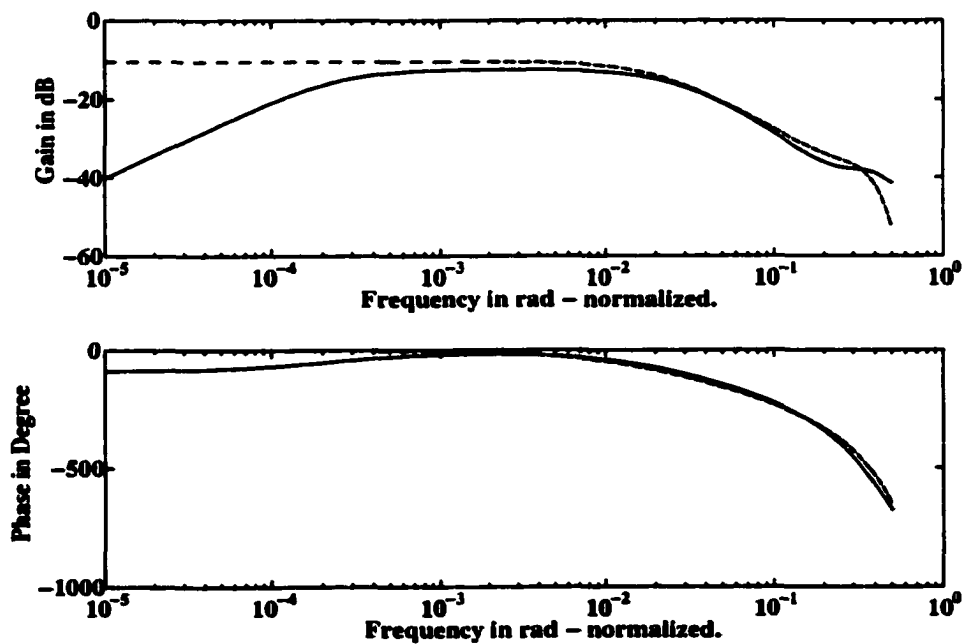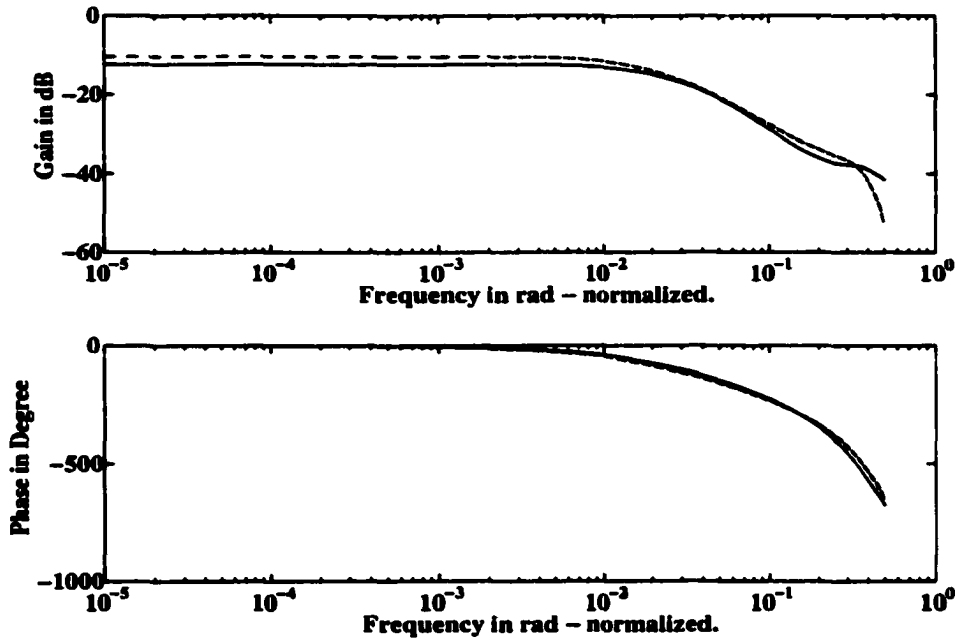
47

Figure 3.9: Open loop frequency responses of process as identified in open loop (dashed) and closed loop (solid) identification method with over parameterized model and with P gain of 0.8 and I gain of 0.3 at sample number 10000.

both identification methods. From these studies (Figure 3.6, 3.7 and 3.8), it is evident that the higher PI gains in adaptive control, which make the system response under damped (Figure 3.1), were caused by lower process gain obtained in closed loop identification in the frequency range used in optimization routine to obtain adaptive PI gains. It is important to note that there is perfect match in magnitude plots at certain frequency from both identification methods as shown in Figures 3.6, 3.7 and 3.8. This frequency (normalized) is the same in all and is about 0.05 rad. Also closed loop identification always produces lower gain for process then open loop identification.

To investigate the effects of controller dynamics in closed loop identification, an experiment is performed with different P and I gains. The P gain of 0.8 and I gain of 0.3 is implemented. The data from this experiment were used in an offline simulation for performing comparisons. The over parameterized model for open and closed loop identification is as given by Equation (3.4). The open loop frequency responses of the process obtained from both identifications at sample number 10000 is as shown in Figure 3.9. The solid line shows the response of the process model as identified by closed loop and dashed line shows the response of the process model as identified by open loop method. The offline simulation on same set of data is performed again with guaranteed DC gain of unity in closed loop model. The open loop frequency responses of the process obtained at sample number 10000 by simulation are shown in Figure 3.10. Again the magnitude plots at frequency 0.007 rad
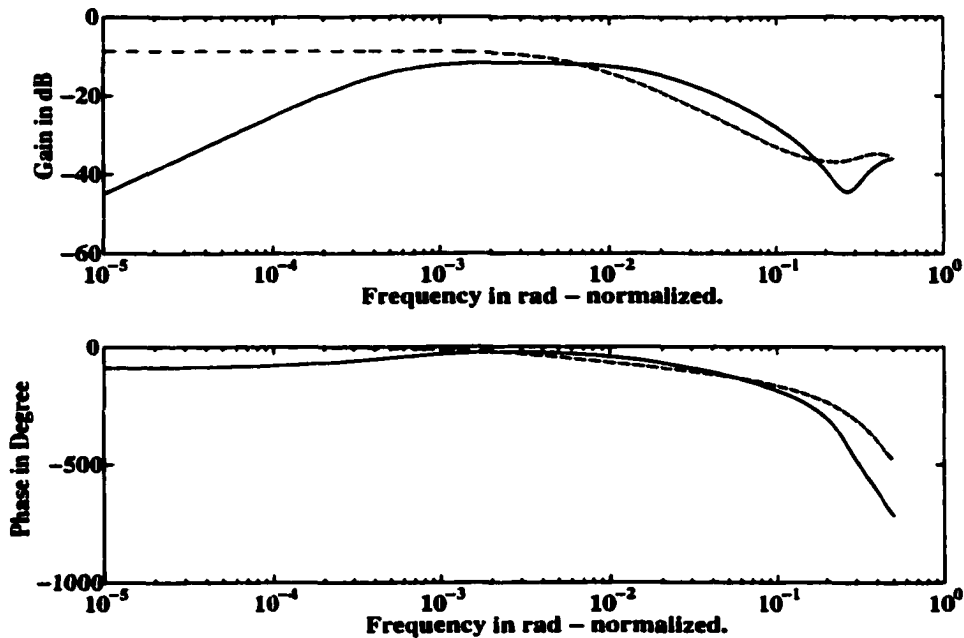
48

Figure 3.10: Open loop frequency responses of process as identified in open loop (dashed) and closed loop (solid) identification method with guaranteed DC gain of unity in closed loop identification and with P gain of 0.8 and I gain of 0.3 at sample number 10000.

matches from both identification as can be seen in Figures 3.9 and 3.10. The frequency responses at different samples were checked and same type of behavior was noticed. The frequency where magnitude plots in both identification matches is different with different controller parameters. To show the effects of controller gains on closed loop system identification, the magnitude plots of process obtained in both identification methods with different controller gains and the frequency responses of each controller are shown in Figure 3.11. The figure shows the process open loop magnitude plots as obtained from open loop identification, closed loop identification with guaranteed DC and magnitude plot of respective controller. The solid line is response from closed loop identification. The dashed line in figure is the response from open loop identification. The dotted line is controller magnitude response. It is important to note that the frequency around which identification matches in both methods is the frequency at which the controller gains negatively equals the process gain in dB. This is logically true because in closed loop system the unity gain can be achieved when controller gain equals negative of process gain in dB. Thus true identification of the process through closed loop identification is not possible. It could be possible to design adaptive controller based on identification around this frequency (where controller gain equals negative of process gain). But as seen, that the adaptive changes in controller parameters changes this frequency, making it practically impossible to implement the closed loop identification in adaptive control.
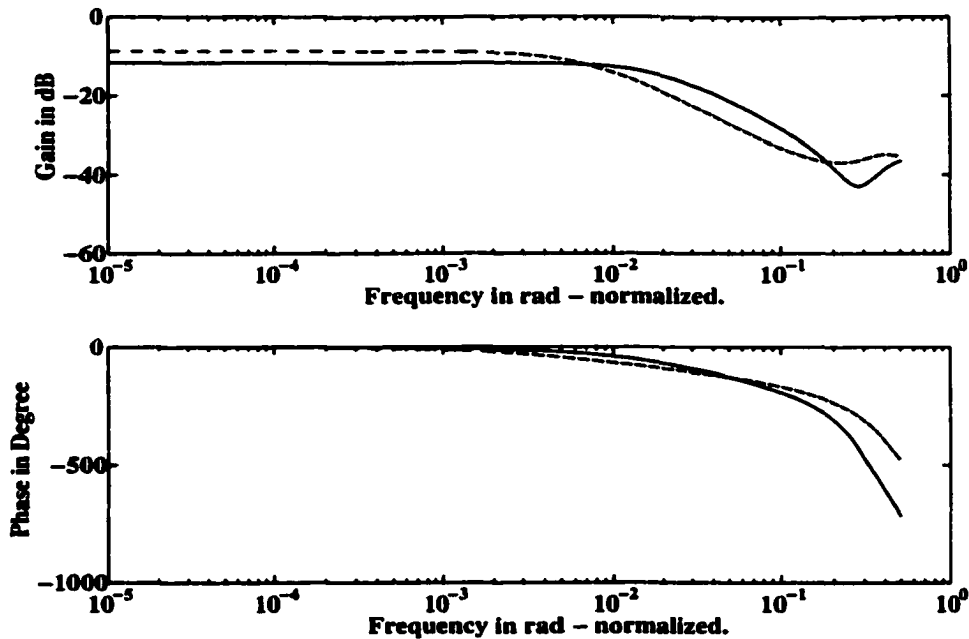
49
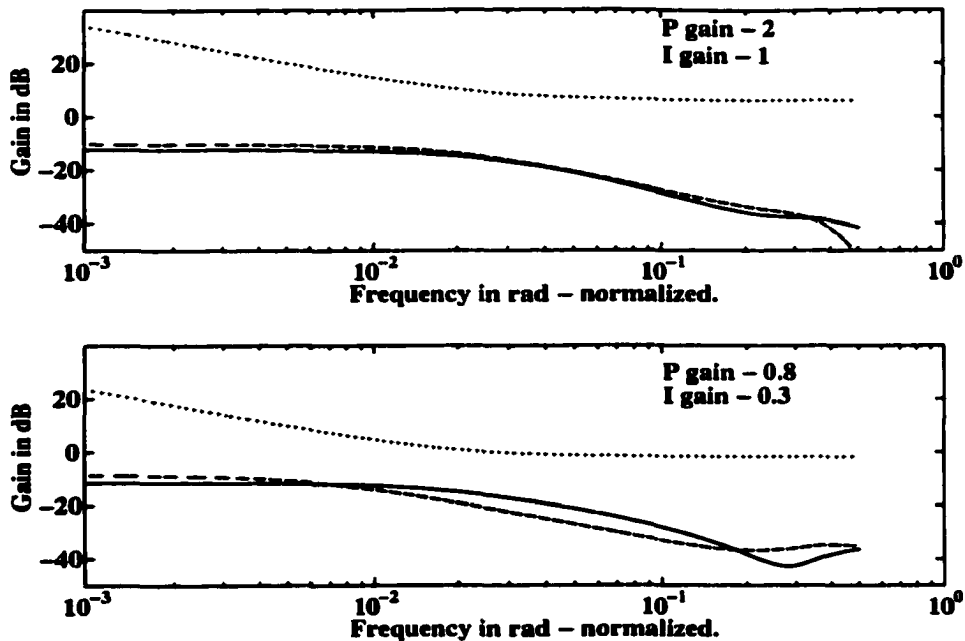
Figure 3.11: Open loop frequency responses of process as identified in open loop (dashed) and closed loop (solid) identification methods with guaranteed DC gain of unity in closed loop identification with P gain of 2 and I gain of 1, and P gain of 0.8 and I gain of 0.3 at sample number 10000 with respective controller magnitude responses (dotted).

3.5 Conclusion

Closed loop system identification can overcome the effect of DC bias on identification. For use of closed loop identification in adaptive control, the change in controller parameters has to be implemented after certain samples, which sometimes results in unacceptable system response in the interim period. From closed loop identification, low frequency estimation of open loop process is poor and this was explored. Based on these, it is concluded that the closed loop identification method cannot be used in MRAS implementation in the frequency domain.

50

Chapter 4

Model Reference Adaptive Control System Using Frequency Domain Performance Specifications And Bandpass Filters For System Identification.

4.1 Introduction

Recursive online system identification methods are usually based on discrete-time transfer function models of the process with unknown coefficients, which are then estimated as already seen in Chapters 1,2 and 3. Traditional adaptive control techniques [4] are based on the estimated coefficients and therefore a basic requirement is a clear knowledge about the order of transfer function. The actual order of transfer function can vary considerably with the change in dead time of process in different conditions. If there is an order mismatch, then the coefficients of the parameterized transfer function are no longer correct. There are different alternatives for simultaneous estimation of order and parameter estimation, but these techniques usually call for a large overhead of computation time, slowing down the identification process considerably and affecting the system performance when used in adaptive control. A different approach for system identification using bandpass filters which estimates directly the frequency response at a finite number of harmonics of setpoint excitation and studied in [2, 3, 8] can be used. The schematic of estimating the gain and phase shift at one harmonic frequency in the excitation and the corresponding frequency in the output is shown in Figure 4.1. The sampled process input and the sampled process output are fed in open loop identification using band pass filters and similarly sampled setpoint and the sampled output are fed in closed loop identification using bandpass filters. The required process variables are fed to a series of parallel channels, each performing
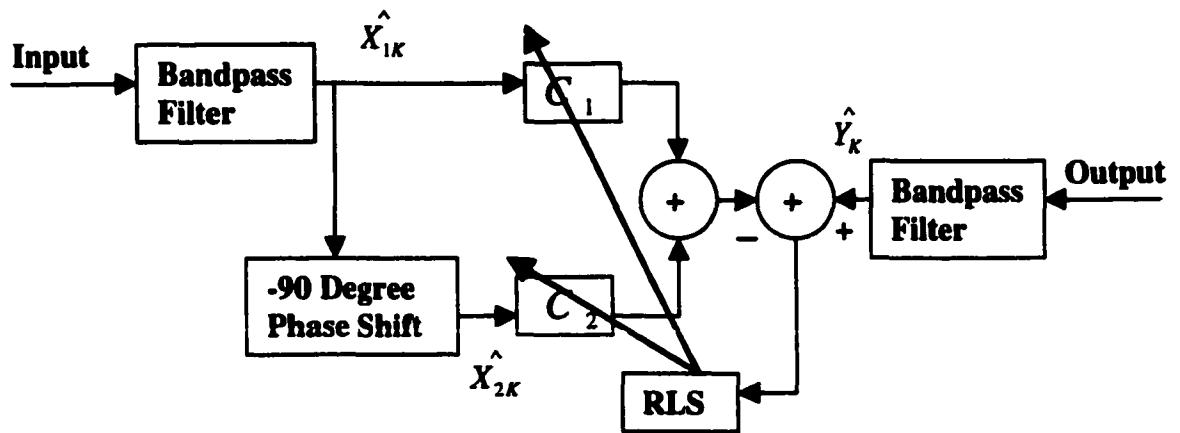
51

Figure 4.1: Identification scheme using Bandpass Filters.

frequency response estimation at one frequency point. The frequency points are normally, the odd harmonic frequencies of the excitation frequency as the Fourier series expansion for a square wave is made up of a sum of odd harmonics. The output of the input bandpass filter $(\hat{X}_{1k})$ is phase shifted by -90° through a quadrature filter $(\hat{X}_{2k})$. Considering the setpoint excitation signal is square wave of frequency w_c, the output of the bandpass filters with center frequency at odd harmonics of the setpoint signal will be sine waveforms. Let the output $(\hat{X}_{1k})$ of the input bandpass filter with center frequency w_c (1st harmonic) be $A_{in}\sin(w_c t)$. Then the -90° phase shifted component $(\hat{X}_{2k})$ will be $-A_{in}\cos(w_c t)$. Let the output of the output bandpass filter $(\hat{Y}_k)$ be $A_{out}\sin(w_c t - \phi)$, where ϕ is the phase lag equal to phase shift of the process. Figure 4.2 shows $\hat{X}_{1k}$, $\hat{X}_{2k}$ and $\hat{Y}_k$ vectors. The RLS algorithm adjusts the coefficients C_1 and C_2 until the sum of the weighted output of the input bandpass and quadrature filter matches the output of the output bandpass filter $(\hat{Y}_k)$ as shown in Figure 4.1 and given by Equation (4.1).

$$C_1 A_{in} \sin(w_c t) - C_2 A_{in} \cos(w_c t) = A_{out} \sin(w_c t - \phi) \tag{4.1}$$

The vectors C_1 and C_2 are shown in Figure 4.3. The relations given by Equations (4.2) and (4.3) are derived from the Figure 4.3.

$$\sin\theta = \frac{C_2}{\sqrt{C_1^2 + C_2^2}} \tag{4.2}$$

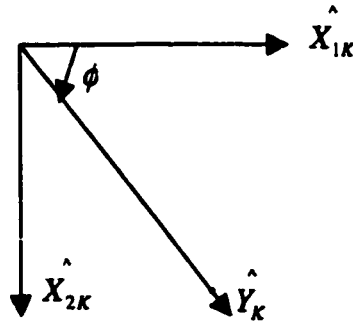$$\cos\theta = \frac{C_1}{\sqrt{C_1^2 + C_2^2}} \tag{4.3}$$

52

Figure 4.2: Vectors $\hat{X}_{1k}$, $\hat{X}_{2k}$, $\hat{Y}_k$ and phase shift ϕ.

The Equation (4.1) can be modified using relations given by Equations (4.2) and (4.3) and Equation (4.4) can be obtained.

$$A_{in}\sqrt{C_1^2 + C_2^2}(\cos\theta\sin(w_c t) - \sin\theta\cos(w_c t)) = A_{out}\sin(w_c t - \phi) \tag{4.4}$$

The Equation (4.4) can be reduced to Equation (4.5) using trigonometric relations.

$$A_{in}\sqrt{C_1^2 + C_2^2}\sin(w_c t - \theta) = A_{out}\sin(w_c t - \phi) \tag{4.5}$$

The required information for process gain and process phase shift at harmonic frequency w_c can be obtained from Equation (4.5) by comparing amplitude and phase on both sides of the equation. The process gain and process phase shift is then given by Equation (4.6) and Equation (4.7) respectively in terms of C_1 and C_2.

$$\text{Process gain} = \frac{A_{out}}{A_{in}} = \sqrt{C_1^2 + C_2^2} \tag{4.6}$$

$$\text{Process phase lag} = \phi = \theta = \tan^{-1}\left(\frac{C_2}{C_1}\right) \tag{4.7}$$

The Equation (4.6) and Equation (4.7), which conveys required process information can be represented in complex form as $C_1 + jC_2$. Thus the process gain and phase shift at required harmonic frequencies can be obtained directly in this approach.

The advantages of using bandpass filters for identification are:

1. It is non-parametric type of identification and thus overcomes the problems associated with parameterization and order of the transfer function model in RLS.

2. The method directly estimates the magnitude and phase of the system at a finite number of frequencies and is suitable for MRAS based on frequency domain performance specifications.

3. The sampling rate of the identification experiment and that of the control loop can now be different. The synchronization between the two loops is not required. That
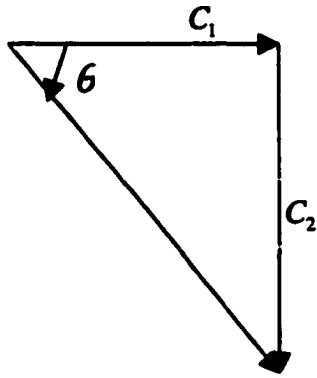
53

Figure 4.3: Vectors C_1 and C_2.

means one can implement the identification experiment on a separate computer system without disturbing the DCS (Distributed Control System) and update only the controller gains on the DCS [8].

4. In system identification using bandpass filters, the identification is performed only based on the information on the odd harmonics of the excitation frequency. Thus effect of noise on the identification can be reduced by controlling the bandwidth of the bandpass filters. A technique using guard filters for checking confidence in the identification experiment is available in [2, 8].

5. The bandpass filter system identification approach overcomes the effects of disturbance on identification. If a disturbance does not have a periodic component, it is well filtered by the bandpass filters and therefore does not affect estimates. If the disturbance is periodic, as long as its energy distribution lies outside the bandwidth of the bandpass filter, the disturbance does not affect the estimates. When a constant amplitude periodic disturbance affects the process and has energy distribution in the bandwidth of the bandpass filters, the resulting estimates are biased. In such an event, the knowledge about disturbance nature can be used to avoid its affect on identification by changing the setpoint excitation frequency [2].

The system identification using bandpass filters has limitation that the method can be used for identification only up to certain number of odd harmonics. The signal to noise ratio reduces with increase in harmonic number and at higher frequencies the noise starts affecting identification. The frequency range up to which reliable identification can be performed depends on magnitude and frequency of excitation. The excitation magnitude should be high enough, such that signal strength of its frequency spectrum should be higher than the noise in the system for true identification at that frequency. Any anticipated deviations in excitation frequency can be covered by increasing bandwidth of filters. But increase in bandwidth of filters will increase effects of noise on identification. Therefore it is preferred to maintain excitation frequency variations as small as possible.

54

4.2 MRAS Using Frequency Domain Performance Specifications and Bandpass Filters for Open Loop System Identification.

The MRAS based on frequency domain design using bandpass filters for open loop system identification is applied to the temperature control system (Appendix A). The reference model, stability requirements and all other experimental setup are the same as that described in Section 2.4. The sampling period is kept at 50 ms. The excitation frequency is chosen such that the identification is performed around the required bandwidth of the system. The excitation frequency chosen is 0.006 Hz. Five parallel channels of bandpass filters were designed, starting with center frequency at 1st harmonic frequency (0.0019 rad, normalized) up to 9th (0.0169 rad, normalized) harmonic frequency of excitation frequency. All bandpass filters are fourth order Butterworth bandpass filters [13, 17]. The -3 dB bandwidth of each filter is 0.4 of the excitation frequency on either side from the center frequency of the bandpass filter (i.e. total bandwidth is 0.8 of the excitation frequency). The RLS parameters for each channel are: initial diagonal covariance of 100, forgetting factor for each channel is computed from desired one cycle forgetting factor [2] of 0.999 in a period of the harmonic of the excitation passed by the particular channel's filter and initial parameters C_1 and C_2 for each filter are 0. The forgetting factor so implemented will ensure uniform forgetting in RLS for all frequencies as required. The higher frequency will be forgotten faster as they change faster as compared to lower frequency. The DC bias from process input and process output is removed every 3333 samples. The process gain and phase information at crossover frequencies cannot be obtained accurately as the crossover frequencies are much higher than the range of identification (9th harmonic frequency). Thus in obtaining P and I gains, the phase margin and gain margin are inferred based on the gain and phase information at harmonic frequencies considered in identification. The phase margin is inferred at the harmonic frequency with gain nearest to 0 db. The gain margin is inferred based on the phase angle nearest to -180°. The DC bias removed data are then fed to the bandpass filters. The conventional PI controller with P gain of 2 and I gain of 1 is used. Initially, the process with low fan speed and with the conventional PI controller is used up to sample number 10000. Thereafter the adaptive controller is designed and applied.

The results of the experiment are now discussed. The variations in the process variables - input, output and setpoint are shown in Figure 4.4. The P gain (solid) and I gain (dashed) as applied to the system are shown in Figure 4.5. The variations introduced in the process and the analysis of the results are summarized as:

1. After the adaptive controller is implemented at sample number 10001 the system in low fan speed condition seems sluggish as can be seen in Figure 4.4. The frequency response estimates for the open loop process for low fan speed at sample numbers - 10000(+), 20000(o) and 25000(*) are shown in Figure 4.6. It can be observed that system identification at 10000 sample has not converged. The system gain as identified at sample number 10000 is higher than that identified at sample number 25000. The

55
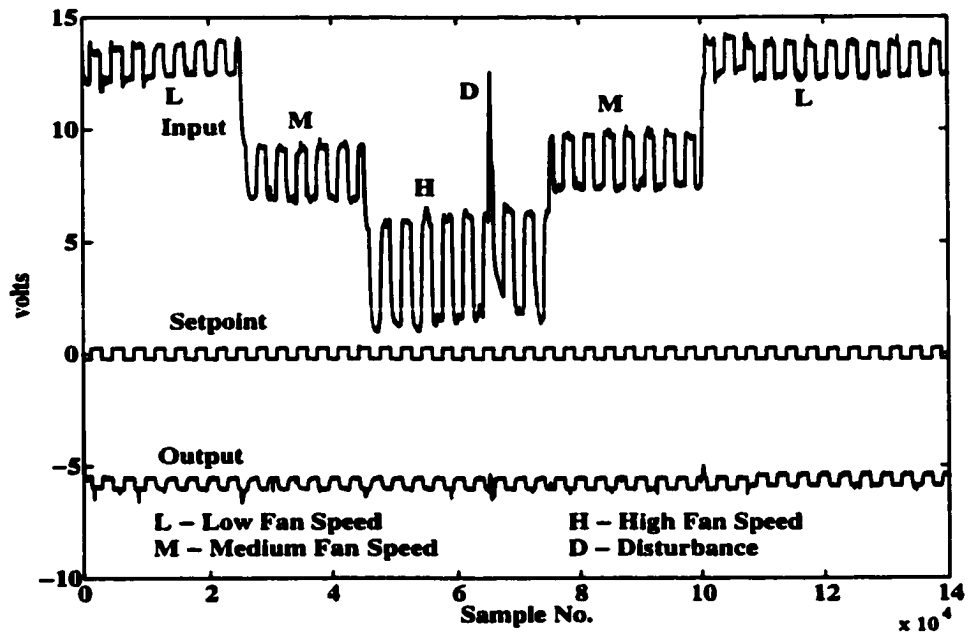
Figure 4.4: Process variables - setpoint, output and input.
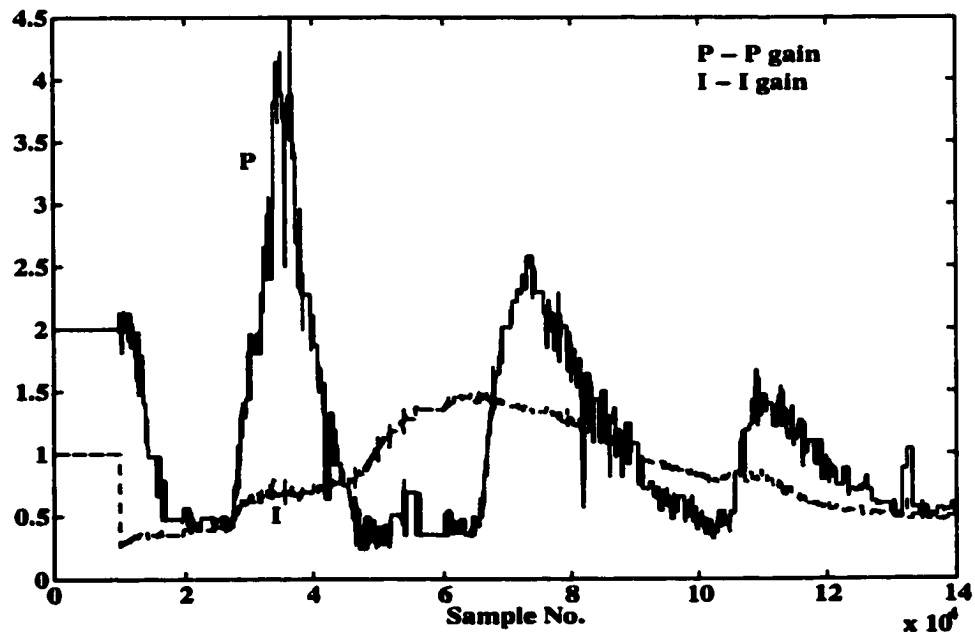
Figure 4.5: P gain (solid) and I gain (dashed) as applied by conventional controller upto sample number 10000 and applied thereafter by adaptive controller.

56
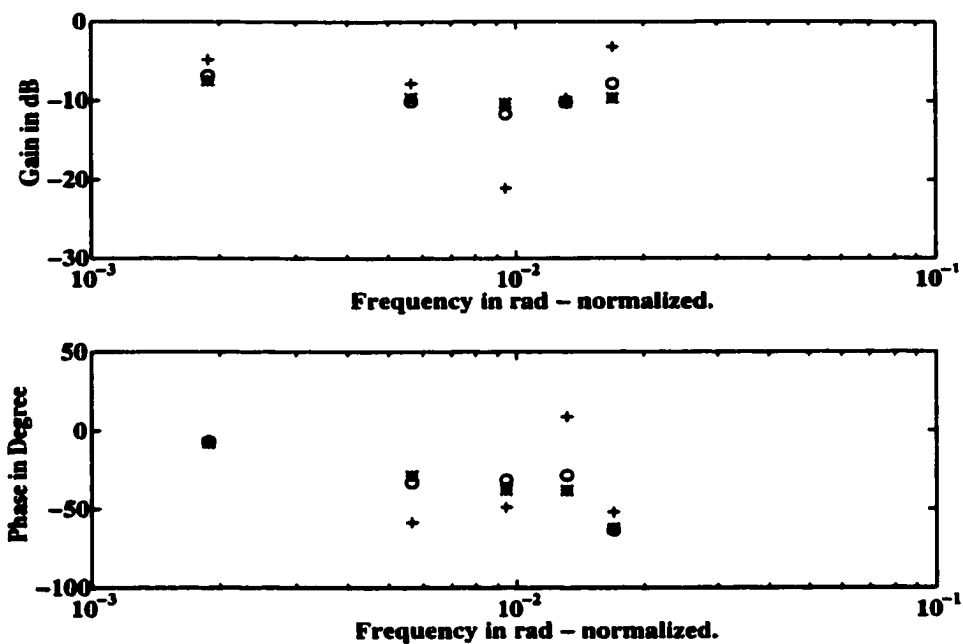
Figure 4.6: Open loop process frequency response estimates at 1st to 9th (odd) harmonic frequencies at sample numbers - 10000(+), 20000(o) and 25000(*) in low fan speed.
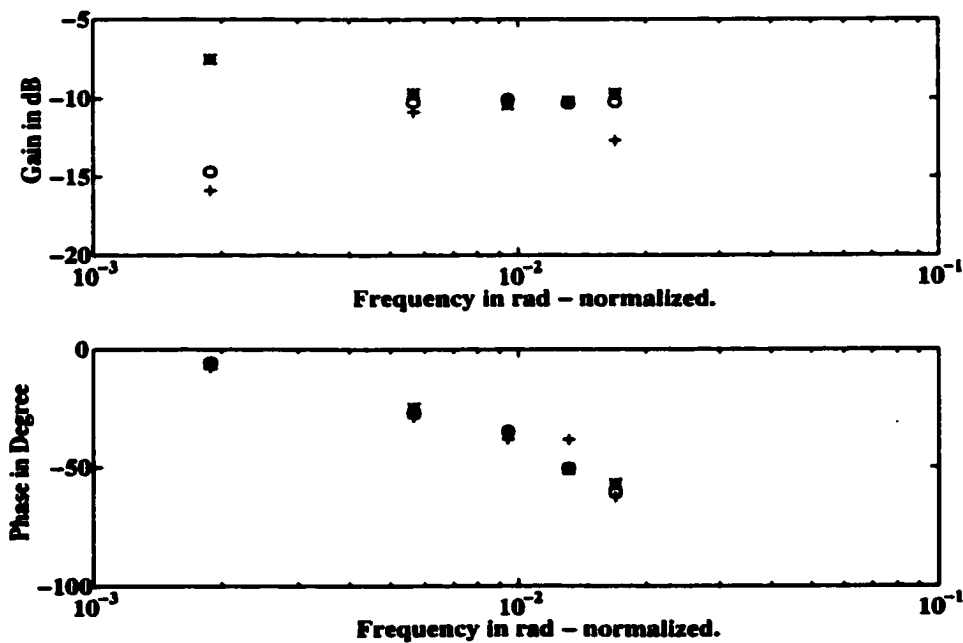
Figure 4.7: Open loop process frequency response estimates at 1st to 9th (odd) harmonic frequencies at sample numbers - 25000(*), 130000(+) and 139900(o) in low fan speed.

57

system response in such condition remains sluggish with lower gain on controller until the estimates converges.

2. The fan speed is changed to medium from low at sample number 25001. The system specifications seems to be achieved after about four cycles of excitation as can be seen in Figure 4.4.

3. The fan speed is again changed to high from medium at sample number 45000. The system seems to meet the required specifications. A disturbance is applied at sample number 65000 by blocking the air flowing through the system. The system immediately reacts to annul the effect of disturbance as can be seen by a sudden increase on controller gain values, to achieve performance. The disturbance applied is not periodic but affects the system.

4. The fan speed is changed to medium from high at sample number 75000. The system performance as can be seen in Figure 4.4 was not achieved and under damped results are obtained even after 7 cycles of excitation.

5. The fan speed is again changed to low from medium speed at sample number 100000. The system performance remains under damped even after a sufficient number of excitation cycles.

6. The P and I gains estimated and applied to the system are noisy and makes the system noisy. This is due to large bandwidth of the bandpass filters used in the identification.

7. The identification at higher frequencies especially the 7th and 9th harmonics is noisy as can be seen in Figures 4.6 and 4.7. This is because the excitation signal strength is low at these higher frequencies and noise starts affecting the identification. Also these frequency points are beyond the bandwidth of the system.

8. The identification in this method is performed only up to certain limited number of frequencies. It was difficult to exactly determine stability margins. The exact stability margin cannot be determined from the data and used for obtaining P and I gain in the optimization routine. One has to interpolate or extrapolate for the stability margins based on the gain and phase data obtained through identification.

9. The sustained under damped behavior of the system resulting after the changes in process applied from low gain (higher fan speed) to high gain (lower fan speed) conditions needs to be investigated. The frequency response estimates of open loop process as identified in low fan speed at sample numbers 25000(*), 130000(+) and 139900(o) are shown in Figure 4.7. At sample number 25000, it is assumed that the system identification must have converged as specifications were met as can be seen in Figure 4.4. It can be seen in Figure 4.7 that the system identification is not converging at all harmonic frequencies for sample numbers 130000 and 139000. The identification (process gain) at higher harmonics is converging but the identification at lower harmonics is

58

much lower in magnitude. In the optimization routine to determine PI gains, the lower frequency estimate is weighted higher and so the higher controller gains are obtained making the system under damped. The same behavior was observed for under damped system behavior in medium fan speed. The slower convergence in lower frequency can be due to inadequate forgetting factor or inadequate bandwidth of the bandpass filter. Faster convergence of identification using bandpass filters can be achieved by increasing the bandwidth of the bandpass filters. The bandpass filters with different bandwidths and different forgetting factors were experimentally tried but convergence of identification was not fast enough to improve the MRAS in frequency domain using bandpass filters for identification.
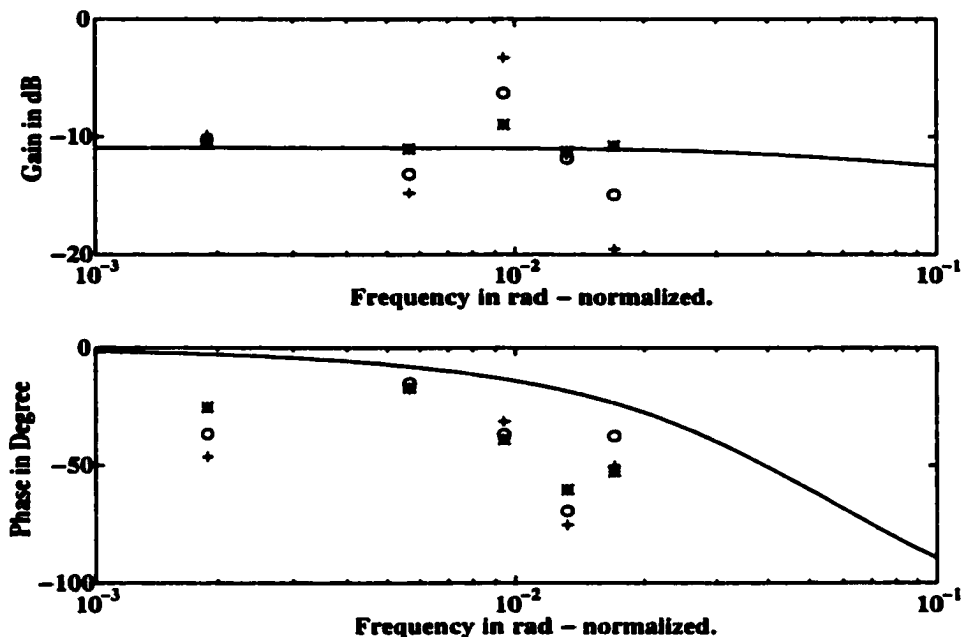
Figure 4.8: Open loop frequency response estimates at sample numbers - 20000(+), 30000(o) and 39000(*) in closed loop system identification using bandpass filters and open loop frequency response of process model as identified in open loop system identification (solid).

4.3 Closed Loop Identification With Bandpass Filters.

As observed in Chapter 3, closed loop identification leads to poor estimation of process frequency response at low frequencies. It is therefore important to evaluate bandpass filters for closed loop identification for adaptive control. The experimental conditions are the same as in Section 2.4 (Section 4.2). The setpoint and output are now fed to bandpass filters as required in closed loop identification. The system identification is performed up

59

to sample number 39000. The open loop process magnitude and phase is obtained using Equation (3.2). The open loop process frequency response estimates are shown in Figure 4.8. The figure shows the open loop frequency response estimates at 1st to 9th (odd) harmonic frequencies at sample numbers 20000(+), 30000(o) and 39000(*). The solid line is the frequency response of process model using Equation (1.1) as identified in offline open loop identification with RLS performed on same data upto sample number 39000. It is important to note that the system as identified (particularly process gain) on the lower frequencies viz. 1st and 3rd harmonic frequency is as identified using open loop offline identification. This is significant as closed loop identification and adaptive control is now possible using bandpass filters. The draw back of using bandpass filters is again the same viz. that it requires much more samples for convergence. The long convergence of system identification is not acceptable for adaptive control.

4.4 Conclusion

The bandpass filters approach can be used to perform both, open and closed loop system identification. Though it is flexible and useful for performing system identification, it has limitation for applying it in MRAS based on frequency domain due to slow convergence. Fast convergence can be achieved by increasing bandwidth of filters, but then it was observed that the noise affects system identification. Bandpass filters with different bandwidths were tried experimentally but convergence of system identification was not fast enough to improve adaptive control. The system identification method using bandpass filters is therefore not suitable for applying to MRAS in frequency domain.

Chapter 5

Model Reference Adaptive Control System Using Frequency Domain Performance Specifications And Kalman Filters For System Identification.

5.1 Introduction

An alternate approach to bandpass filters for system identification is to use Kalman filters [18, 2, 5]. The use of Kalman filter as a state estimator is described in many books such as [10]. The same approach can be used to estimate the states and their $90°$ phase shifted component at required center frequencies [18].

Given a noisy sinusoid with frequency f_c, sampled at intervals of T s and a measurement process as described in Equation (5.1).

$$\begin{bmatrix} x_1 \\ x_2 \end{bmatrix}_{k+1} = \begin{bmatrix} \cos(2\pi f_c T) & \sin(2\pi f_c T) \\ -\sin(2\pi f_c T) & \cos(2\pi f_c T) \end{bmatrix} \begin{bmatrix} x_1 \\ x_2 \end{bmatrix}_k + w_k = A\, X_k + w_k$$

$$Y_k = \begin{bmatrix} 1 & 0 \end{bmatrix} \begin{bmatrix} x_1 \\ x_2 \end{bmatrix}_k + v_k = C\, X_k + v_k \tag{5.1}$$

One can design a steady-state Kalman filter (observer) to provide estimates of the vector X_k as shown in Figure 5.1. As the covariance Q of the state noise vector w_k is reduced compared to the covariance R of the measurement noise v_k, the steady-state Kalman filter transfer function approaches a narrow bandpass filter with center frequency f_c [2, 18]. A signal $A\sin(2\pi f_c t - \phi)$ can be expressed as given in Equation (5.2).

$$A\sin(2\pi f_c t - \phi) = A\cos\phi \sin(2\pi f_c t) - A\sin\phi \cos(2\pi f_c t) \tag{5.2}$$
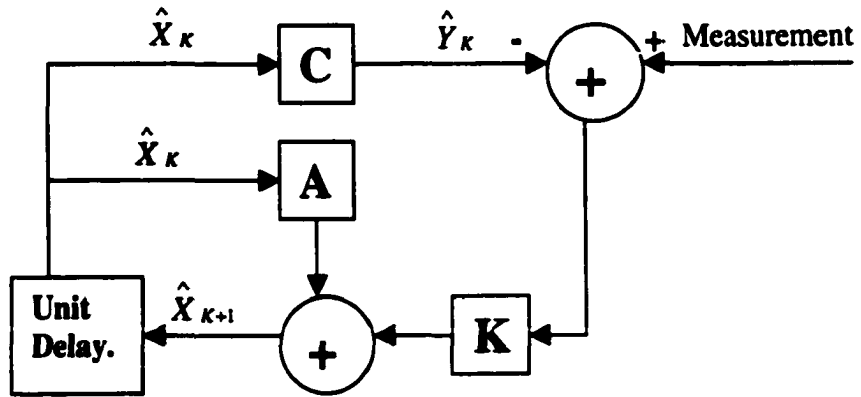
61

Figure 5.1: Estimation scheme using Kalman filter.

The Equation (5.2) can be represented in the discrete time state space as given by Equation (5.3), where $x_1 = -A \sin \phi$ and $x_2 = A \cos \phi$.

$$A \sin(2\pi f_c t - \phi) = x_1 \cos(2\pi f_c T) + x_2 \sin(2\pi f_c T) \tag{5.3}$$

The magnitude A and phase ϕ of the signal can be obtained from estimates x_1 and x_2. The Equation (5.4) expresses the relationship between magnitude A with x_1 and x_2. The Equation (5.5) expresses the relationship between phase ϕ with x_1 and x_2.

$$A = \sqrt{x_1^2 + x_2^2} \tag{5.4}$$

$$\phi = \tan^{-1}\left(\frac{-x_2}{x_1}\right) \tag{5.5}$$

The Equations (5.4) and (5.5) can be combined in complex form as given by Equation (5.6).

$$I_{(f_c)} = x_1 - jx_2 \tag{5.6}$$

The complex amplitude and phase information at each harmonic frequency can be obtained from process input and process output. The obtained information can then be used to obtain frequency response estimates at that frequency using Equation (5.7).

$$T_{(j)} = \frac{Y_{(j)}}{I_{(j)}} \tag{5.7}$$

Where $I_{(j)}$ and $Y_{(j)}$ are complex amplitude phase information from process input and process output obtained from estimator with j^{th} center frequency. The magnitude and phase can be computed from the complex amplitude phase information at each harmonic in the usual way. The gain matrix K is obtained as the optimal steady-state Kalman gain. The
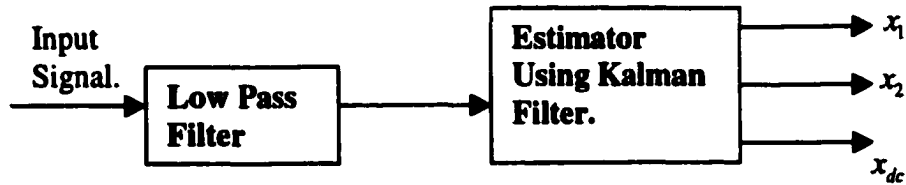
62

Figure 5.2: DC Bias estimation scheme using Kalman filter.

gain matrix K is a trade-off between fast response and high noise amplification, which is controlled by an appropriate choice of the weighting matrices (Q and R) associated with the quadratic performance measure. By using Q and R as design parameters for designing the (Kalman filter) observer, one can generate filters with varying bandwidth. The bandwidth of such filters is indirectly related to the values of Q and R and its specification in the design process is by trial and error [2]. This is a major disadvantage in comparison with filter designs such as Butterworth as seen in Chapter 4, where bandwidth is an explicit design parameter. An advantage of the Kalman filter technique is that it also provides 90° phase shifted signal in its second state.

In the Sections of this chapter, system identification based on Kalman filter is provided. In Section 5.2, the estimation of DC bias using Kalman filter is studied and compared with the batch method used so far in the thesis. In Section 5.3, the effect of noise on system identification using Kalman filter is studied. In Section 5.4, the system identification is performed using Kalman filter and compared with the results of identification obtained using bandpass filter.

5.2 DC Bias Estimation Using Kalman Filter

The drawback of the batch type DC bias method used in Chapters 2,3 and 4 was that DC bias was estimated only after a certain number of samples. The delay in DC bias estimation also delays convergence of system identification. The steady-state Kalman filter can be used to estimate DC bias on each sample. The input and output signals of the plant contains DC, harmonic components of the excitation signal and noise. It is thus required to remove the higher harmonics to achieve good DC estimation based on Kalman filter approach. To limit noise, a low pass filter is also used. The scheme as shown in Figure 5.2 can be used for DC bias estimation from the signal. A 2nd order Butterworth low pass filter with cutoff (bandwidth -3 dB) at 1st harmonic frequency of excitation signal is used to remove all higher harmonics. Then the output of low pass filter is used in estimator to estimate the DC bias. The state space internal model description of the estimator is given in Equation (5.8).

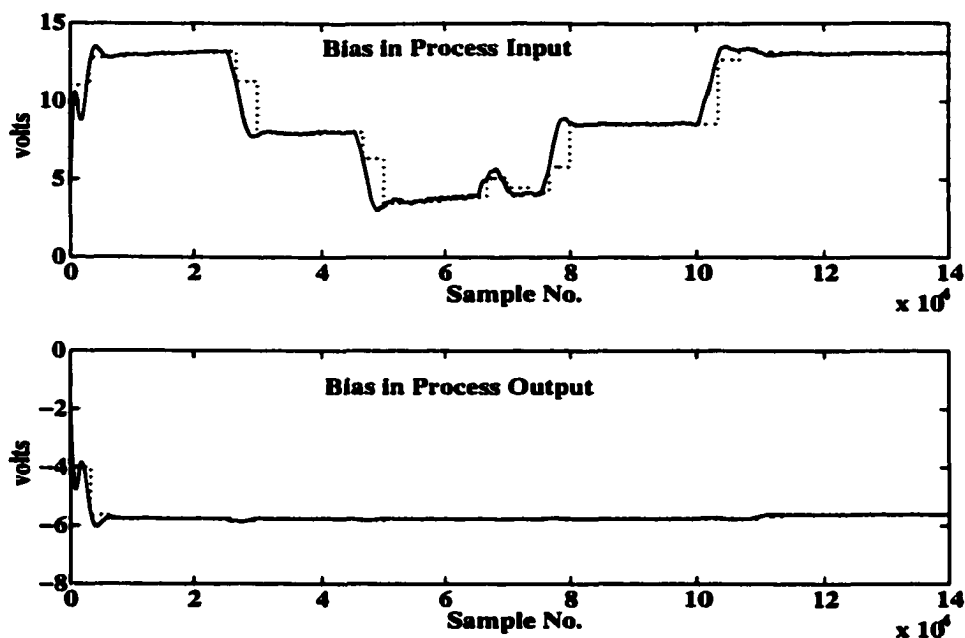$$X_{k+1} = A\ X_k\ ;$$
$$Y_k = C\ X_k\ ;$$

63

Figure 5.3: DC Bias estimation using Kalman filter method (solid line) and conventional batch method (dotted line).

$$A = \begin{bmatrix} \cos(2\pi f_c T) & \sin(2\pi f_c T) & 0 \\ -\sin(2\pi f_c T) & \cos(2\pi f_c T) & 0 \\ 0 & 0 & 1 \end{bmatrix} \tag{5.8}$$

$$C = \begin{bmatrix} 1 & 0 & 1 \end{bmatrix}$$

In Equation (5.8) f_c is the first harmonic frequency of excitation used. T is the sampling period of the system. The estimator can be implemented as shown in Figure 5.1. The noise statistics for the Kalman filter, used as a bandwidth adjusting mechanism are $Q = $ diag$[1, 1, 1]$ and $R = 0.1$. To study the performance of this method by simulation, the process data shown in Figure 4.4 are used. The DC bias estimated using Kalman filter and that obtained using batch method of Chapter 4 in process input and process output are shown in Figure 5.3 for comparison. The solid line in figure shows DC bias estimated using Kalman filter. The dotted line in the figure is the DC bias obtained using batch method estimating DC bias every 3333 samples as in Chapter 4.

The DC bias estimated using Kalman filter method converges faster as compared to batch method. Also the DC bias estimated using Kalman filter method is not constant over a number of samples and it starts responding immediately to the process change. The faster convergence of DC bias has the potential benefit of achieving faster convergence in system identification.
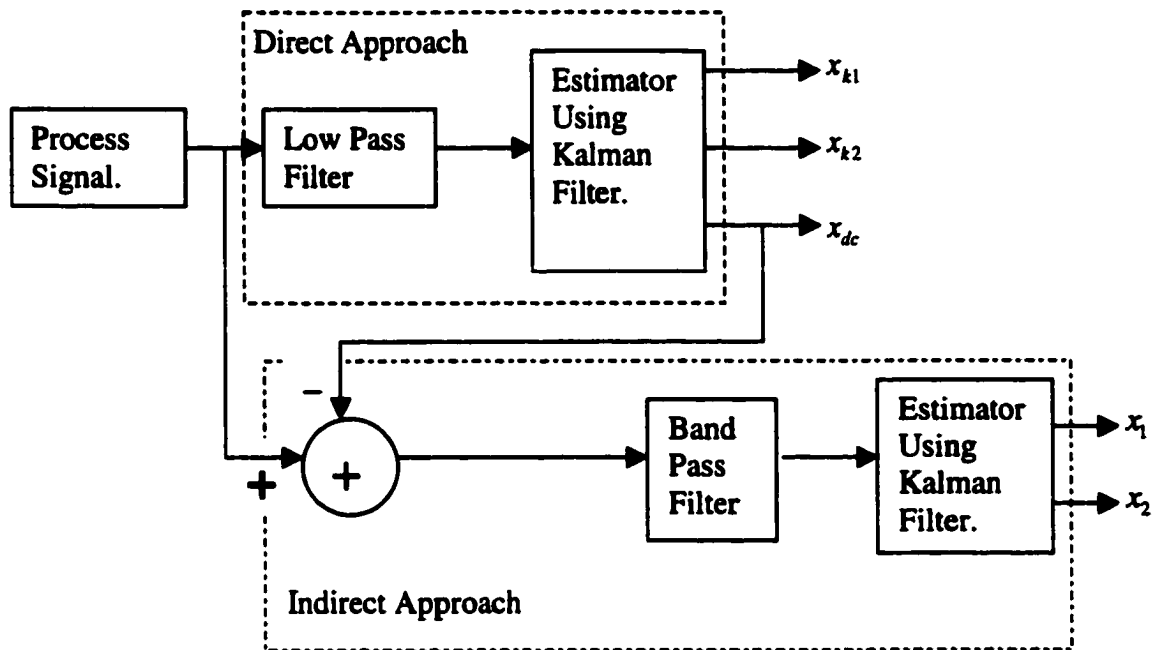
64

Figure 5.4: System identification scheme using Kalman filter alone (Direct Approach) and Kalman filter along with bandpass filter (Indirect Approach).

5.3 Effect of Noise on System Identification Using Kalman Filter Method

The effect of noise on system identification using Kalman filter and bandpass filter is compared in this Section. The disadvantage of using Kalman filter for identification is that one has no explicit control over noise rejection properties of the designed filter. While effect of noise on system identification using bandpass filter can be controlled by bandwidth of the bandpass filter [2]. To investigate the effect of noise on system identification based on Kalman filter method, a simulation is performed as shown in Figure 5.4. Two different approaches are used here using Kalman filters for system identification. The low pass filter has a cut off frequency equal to 1st harmonic frequency of excitation (at 0.006 Hz). Thus the output of low pass filter is a signal with DC, some 1st harmonic content and low frequency system noise. Then the filtered signal is fed to estimator using Kalman filter set up with model as per Equation 5.8 and with $f_c = 0.006$ Hz. The estimator separates directly the 1st harmonic frequency state and it's 90° phase shifted state and DC state of the signal (Direct Approach in Figure 5.4). This approach directly uses Kalman filter to

65

estimate the state, which are then used for identification. In the other approach (Indirect Approach in Figure 5.4) the estimated DC state is used to remove DC bias from the input signal. The DC bias removed signal is then fed to a bandpass filter with center frequency f_c (1st harmonic) and of bandwidth equals to 0.006 Hz (i.e. combine bandwidth of both sides of filter is 0.006 Hz). The output of bandpass filter contains less noise as noise outside upper and lower cut off frequency is filtered out. The filtered signal is then used for system identification using the Kalman filter as shown in Figure 5.4. The estimates x_1 and x_2 should be clean as compared to x_{k1} and x_{k2} and should provide better identification. Such estimators are implemented for process input and process output signal. The estimates are then used to obtain magnitude and phase of the transfer function as described in Section 5.1. The process data used are that shown in Figure 4.4. The results of both approaches are shown in Figure 5.5. The figure shows the magnitude and phase of the process transfer function at 1st harmonic frequency on each sample. The solid line in figure is magnitude and phase from direct approach using only Kalman filter. The dotted line is the results obtained by using bandpass and Kalman filter (Indirect Approach). The convergence of the
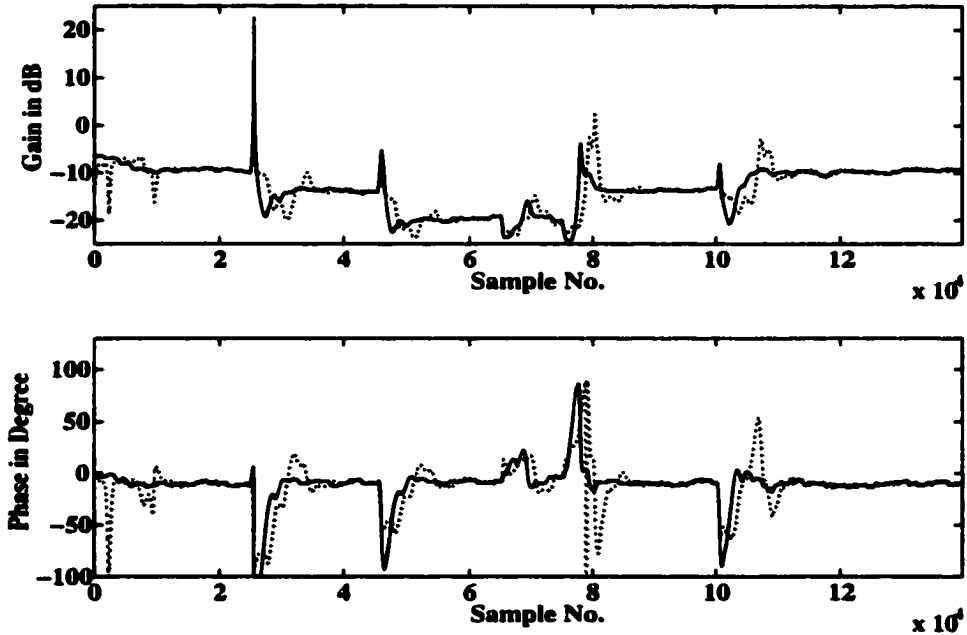

Figure 5.5: Magnitude and phase estimated using Kalman filter alone (solid line) and Kalman filter with bandpass filter (dotted line).

system identification using the direct approach is faster than using bandpass filtered signal for estimation. The delay in convergence is due to use of bandpass filter. The magnitude and phase estimated directly are not much more noisy when compared with the indirect approach using bandpass filter. The disturbance effect at sample number 65000 in both method is comparable. The system identification using only Kalman filter takes about 8000

66

samples for convergence when the process condition changes. This rapidity of convergence is a great improvement over the bandpass system identification of Chapter 4. The system identification using estimator based on Kalman filter at required harmonic frequencies is discussed in the following Section.

5.4   System Identification Using Kalman Filter Method

The steady-state Kalman filter method for system identification is used here to estimate magnitude and phase at each odd harmonic up to 9th harmonic frequency of excitation frequency. The data of Figure 4.4 are used for this purpose. The setpoint excitation frequency is 0.006 Hz. The process output and process input are fed to the low pass filter with cutoff at 9th (odd) harmonic frequency. This removes all unwanted higher harmonics and high frequency noise. The filtered signals now containing 1st to 9th (odd) harmonics, DC and system noise are fed to the estimator. The scheme is implemented as shown in Figure 5.1. The state matrix 'A' of Equation (5.8) is augmented for estimating states up to the 9th harmonic which is given by Equation 5.9. The gain matrix K and matrix C are given in Equation 5.10.

$$A = \begin{bmatrix} A_1 & 0 & 0 & 0 & 0 & 0 \\ 0 & A_3 & 0 & 0 & 0 & 0 \\ 0 & 0 & A_5 & 0 & 0 & 0 \\ 0 & 0 & 0 & A_7 & 0 & 0 \\ 0 & 0 & 0 & 0 & A_9 & 0 \\ 0 & 0 & 0 & 0 & 0 & 1 \end{bmatrix}$$

(5.9)

Where A_i is given as: $A_i = \begin{bmatrix} \cos(2\pi * i * f_c T) & \sin(2\pi * i * f_c T) \\ -\sin(2\pi * i * f_c T) & \cos(2\pi * i * f_c T) \end{bmatrix}$

Where i = 1,3,5,7 and 9 as per the harmonic.

$$C = \begin{bmatrix} 1 & 0 & 1 & 0 & 1 & 0 & 1 & 0 & 1 & 0 & 1 \end{bmatrix}$$

$$K = \begin{bmatrix} K_1 \\ \vdots \\ K_{10} \\ K_{dc} \end{bmatrix}$$

(5.10)

The noise statistics for designing the Kalman filter are $Q = \text{diag}[1,1,1,1,1,1,1,1,1,1,1]$ and $R = 0.1$. The estimated states are then used to obtain complex transfer function as described in Section 5.1, at each harmonic frequency on each sample. The magnitude and phase are obtained from complex transfer function at each harmonic at every sample. The

67

magnitude and phase of open loop process at 1st, 3rd, 5th, 7th, and 9th (odd) harmonic frequencies are shown in Figures 5.6, 5.8, 5.10, 5.12 and 5.14 respectively.

To compare the convergence and effect of noise on identification using the Kalman filter approach to that of the bandpass filter approach, a simulation for process identification using bandpass filter approach is performed on same set of data. The magnitude and phase of open loop process at 1st, 3rd, 5th, 7th and 9th (odd) harmonic frequencies obtained at each sample using bandpass filter approach are shown in Figures 5.7, 5.9, 5.11, 5.13 and 5.15 respectively. It can be observed that for all the process changes the Kalman filter approach takes only about 8000 samples to converge, as can be seen in Figure 5.6 (also in Figures 5.8, 5.10, 5.12 and 5.14.). The slow convergence in system identification using bandpass filter approach can be seen in Figures 5.7, 5.9, 5.11, 5.13 and 5.15. The effect of noise on system identification is severe in identification using the Kalman filter as compared to that of using bandpass filters. The effect of noise on system identification can be compared by comparing magnitude and phase at each odd harmonic frequency obtained using Kalman filter approach to that of bandpass filter approach. The effect of noise on system identification using Kalman filter is due to characteristic of filter generated by the Kalman filter model. The magnitude frequency response of the Kalman filter model used for system identification and that of a bandpass filters for 1st, 3rd, 5th and 9th harmonic frequencies are shown in Figures 5.16, 5.17, 5.18 and 5.19 respectively. The solid line in these figures is the magnitude frequency response of Kalman filter model and dotted line is magnitude frequency response of bandpass filters. The filters generated using Kalman filter model have gradual upper and lower cutoff. The bandwidth (in logical sense) of filters generated using Kalman filter is much higher as compared to bandwidth of bandpass filters. The effect of noise on identification increases with increase in bandwidth of filter. The filters provide only about 10 dB of attenuation in the higher frequencies as compared to much higher and increased attenuation with frequencies in bandpass filters. The sharp notches at 3rd, 5th, 7th and 9th harmonic frequencies in Figure 5.16 (considering 1st harmonic frequency) are due to the model of the Kalman filter used. Similar notches can be observed in Figures 5.17, 5.18 and 5.19. The higher frequencies above 9th harmonic frequency are removed by low pass filter used in system identification but the noise between the harmonic frequencies corrupts the identification due to lower attenuation. The noise effect on identification increases with frequency as can be seen in Figures 5.6, 5.8, 5.10, 5.12 and 5.14.

An offline simulation is performed to determine P and I gains of controller using the magnitude and phase obtained by system identification using Kalman filter. The reference model and stability margins are the same as that described in Section 2.4. The P gain and I gain thus obtained on each sample are shown in Figure 5.20 and Figure 5.21 respectively. The gains obtained are noisy due to the effect of noise on system identification.
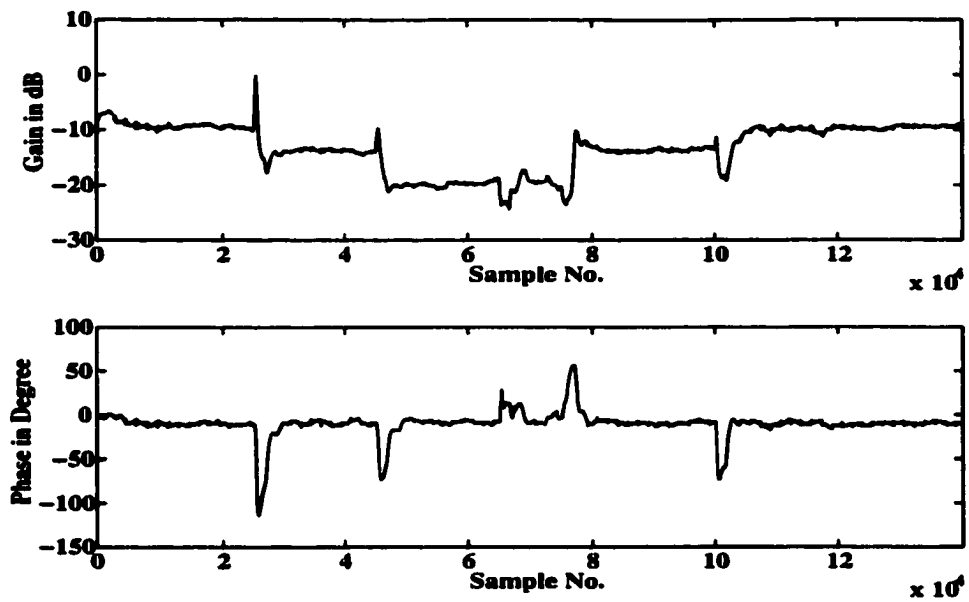
68

Figure 5.6: Magnitude and phase of open loop process as identified by Kalman filter approach at 1st harmonic frequency at each sample.
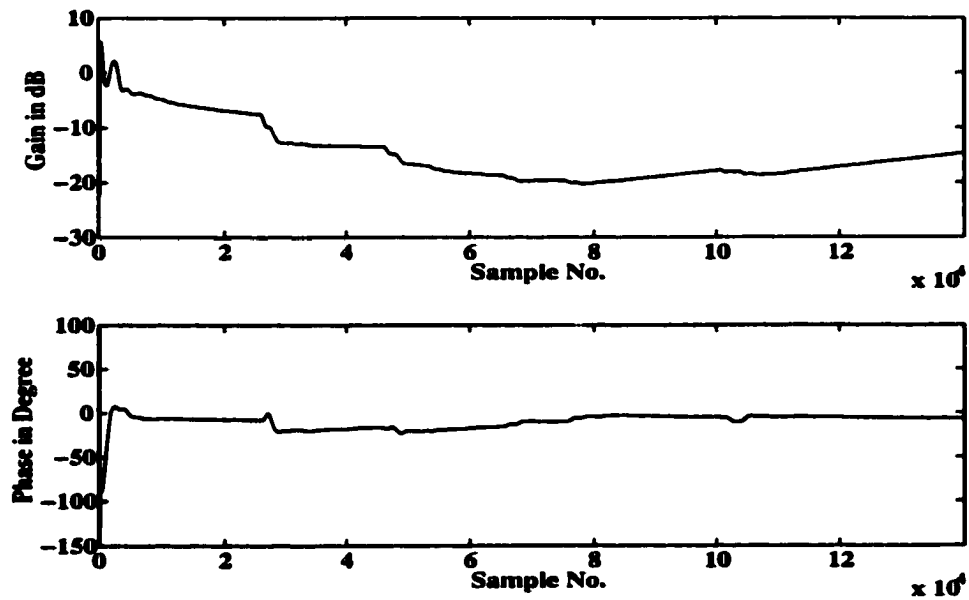

Figure 5.7: Magnitude and phase of open loop process as identified by bandpass filter approach at 1st harmonic frequency at each sample.
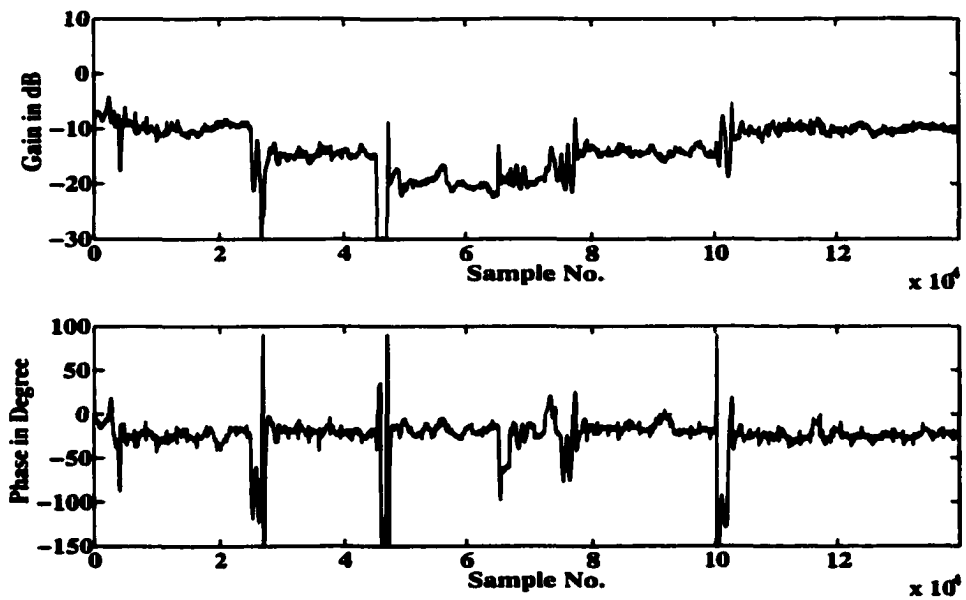
69

Figure 5.8: Magnitude and phase of open loop process as identified by Kalman filter approach at 3rd harmonic frequency at each sample.
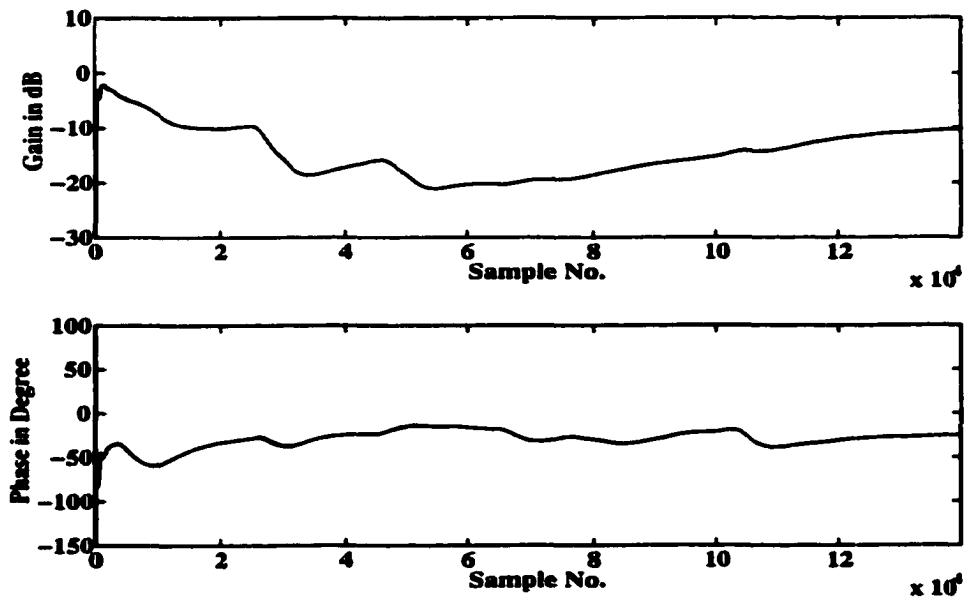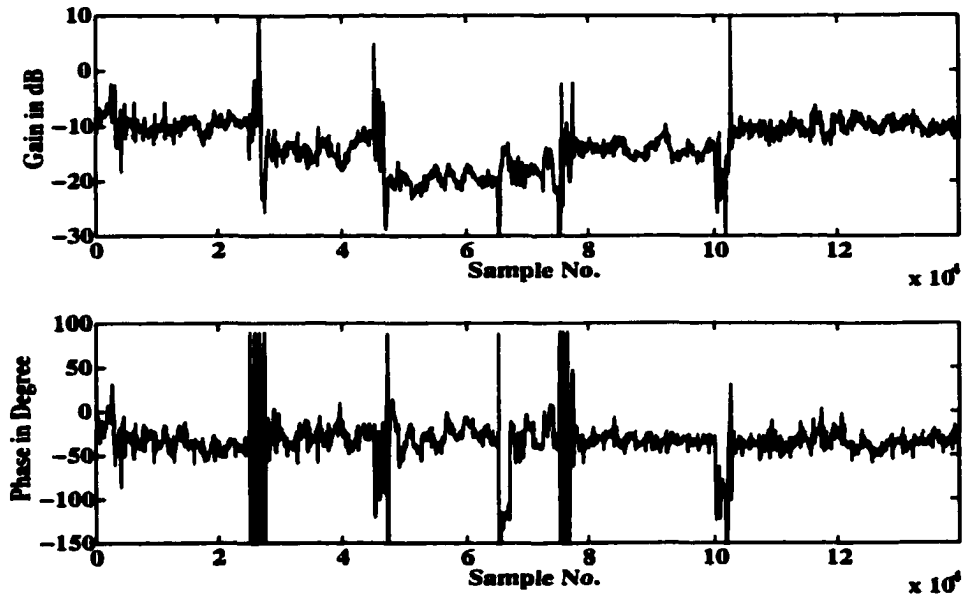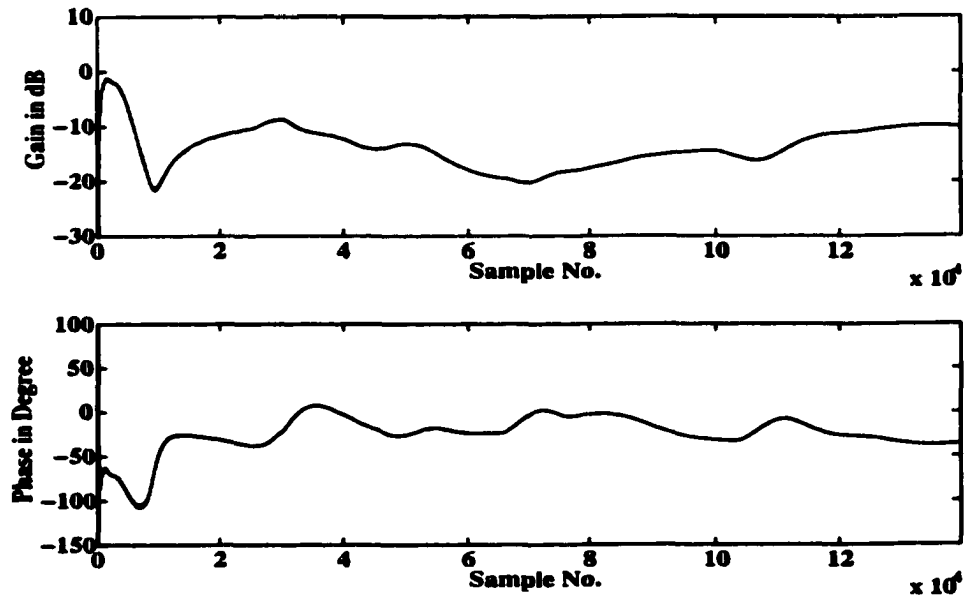

Figure 5.9: Magnitude and phase of open loop process as identified by bandpass filter approach at 3rd harmonic frequency at each sample.

70

Figure 5.10: Magnitude and phase of open loop process as identified by Kalman filter approach at 5th harmonic frequency at each sample.

Figure 5.11: Magnitude and phase of open loop process as identified by bandpass filter approach at 5th harmonic frequency at each sample.
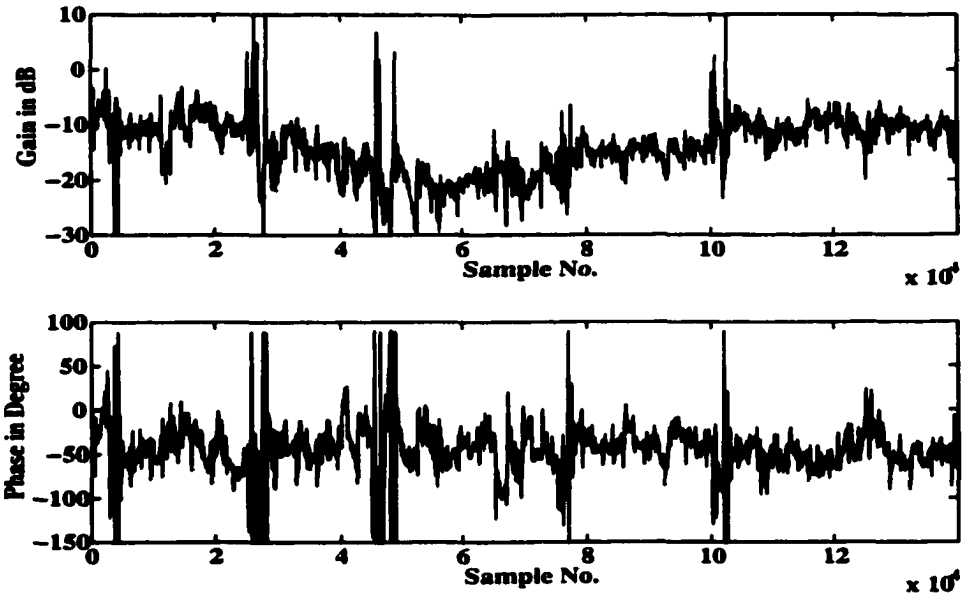
71

Figure 5.12: Magnitude and phase of open loop process as identified by Kalman filter approach at 7th harmonic frequency at each sample.
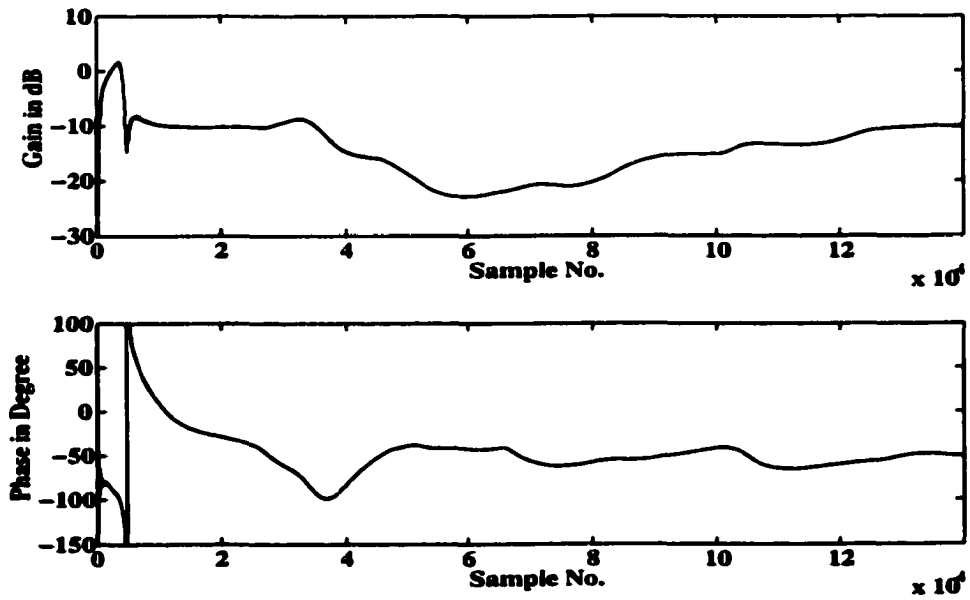

Figure 5.13: Magnitude and phase of open loop process as identified by bandpass filter approach at 7th harmonic frequency at each sample.
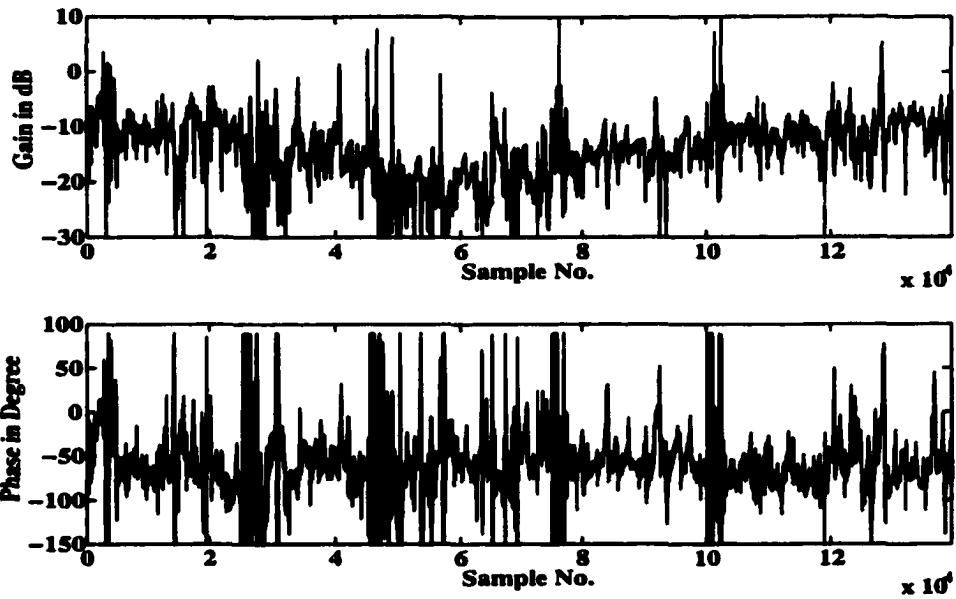
72

Figure 5.14: Magnitude and phase of open loop process as identified by Kalman filter approach at 9th harmonic frequency at each sample.
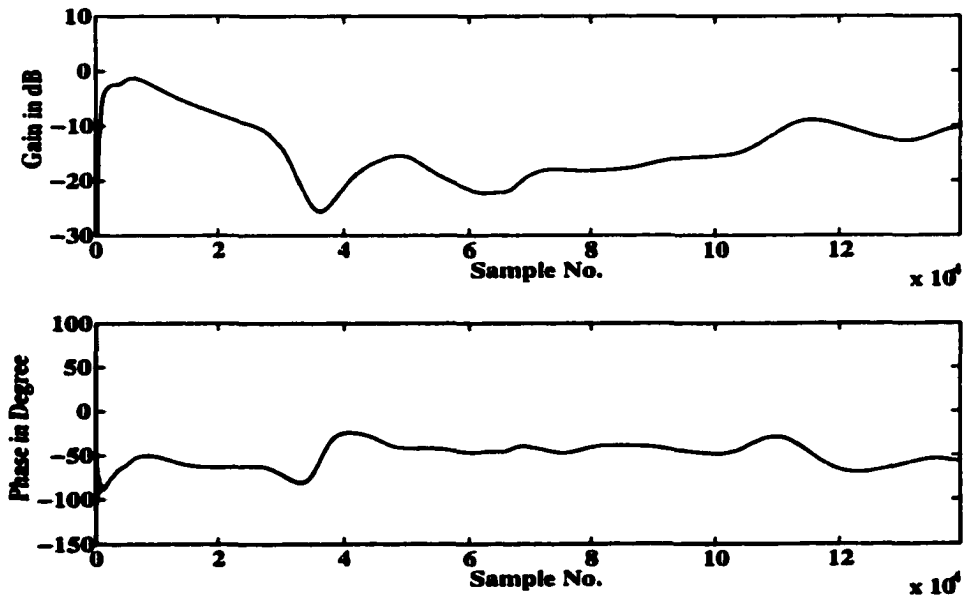

Figure 5.15: Magnitude and phase of open loop process as identified by bandpass filter approach at 9th harmonic frequency at each sample.
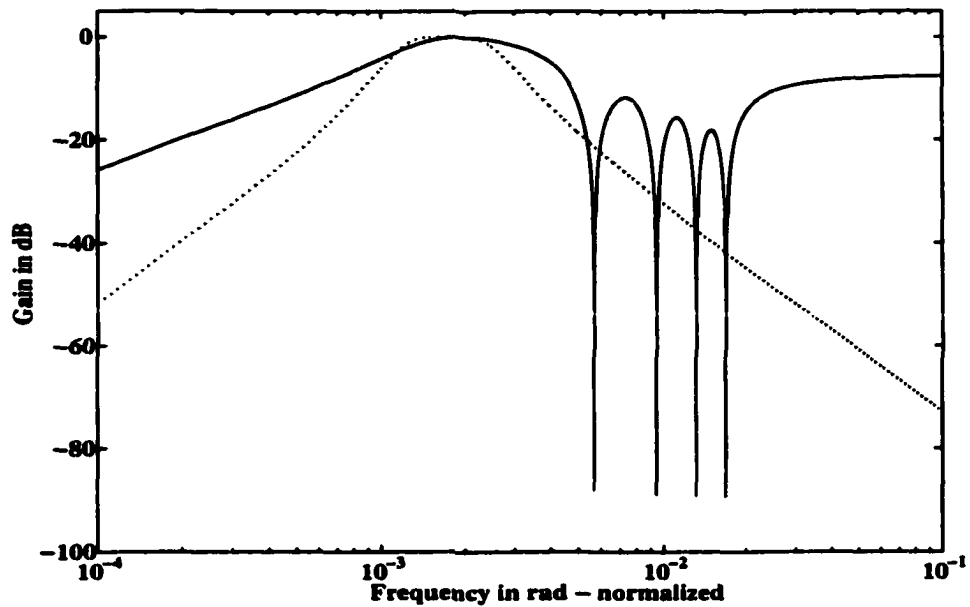
73

Figure 5.16: Magnitude frequency responses of Kalman filter model (solid line) and bandpass filter (dotted line) at 1st harmonic frequency.

Figure 5.17: Magnitude frequency responses of Kalman filter model (solid line) and bandpass filter (dotted line) at 3rd harmonic frequency.

74

Figure 5.18: Magnitude frequency responses of Kalman filter model (solid line) and bandpass filter (dotted line) at 5th harmonic frequency.

Figure 5.19: Magnitude frequency responses of Kalman filter model (solid line) and bandpass filter (dotted line) at 9th harmonic frequency.
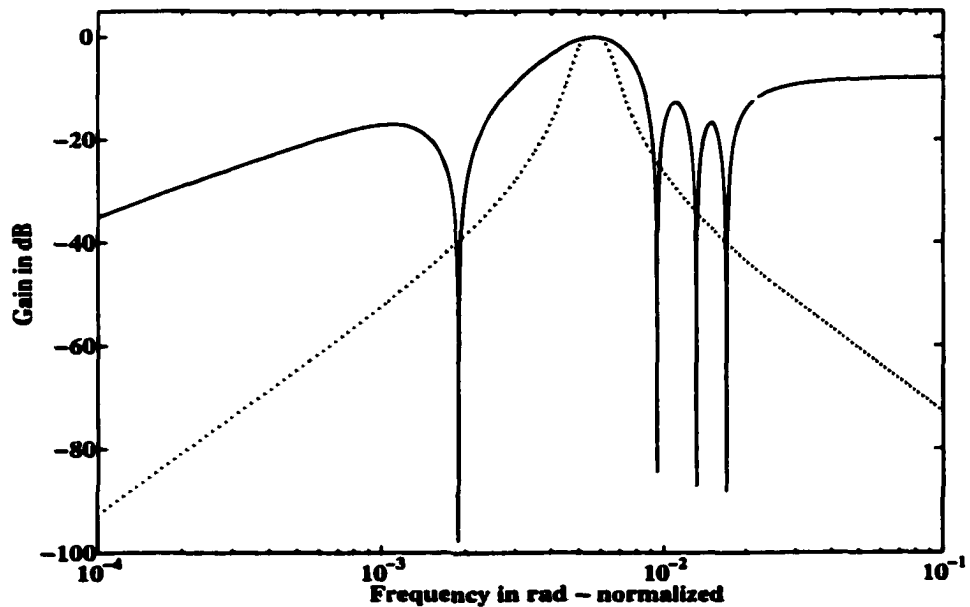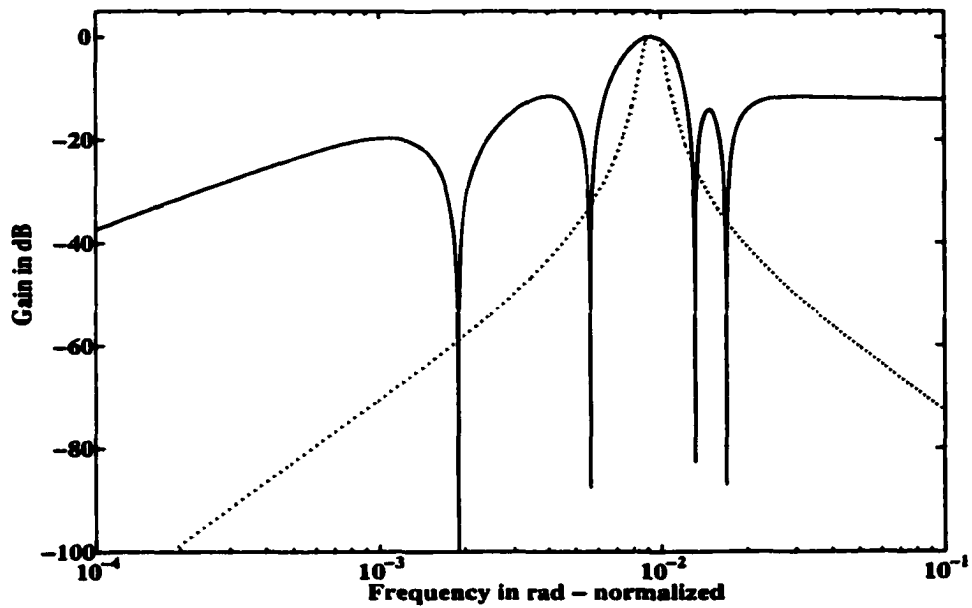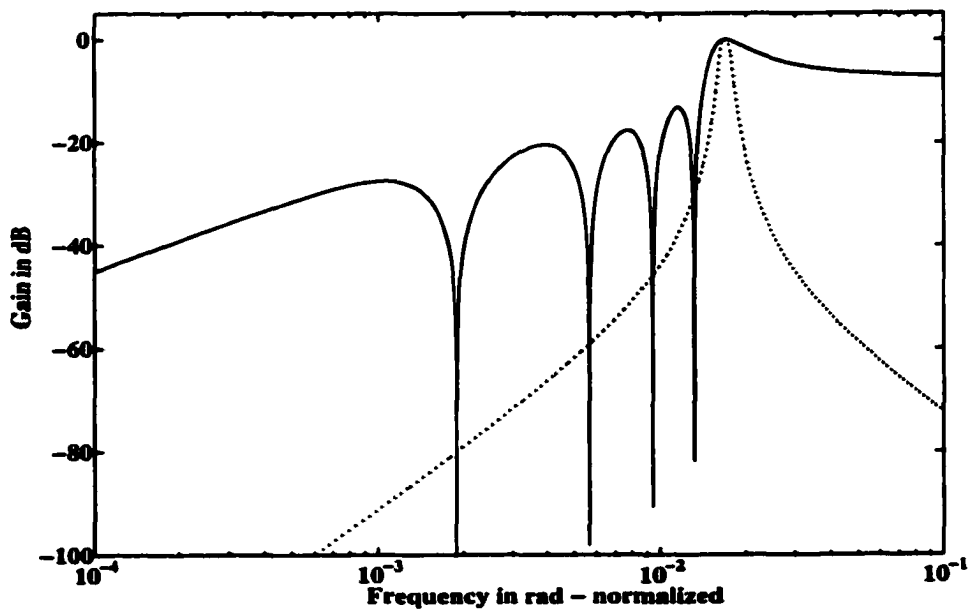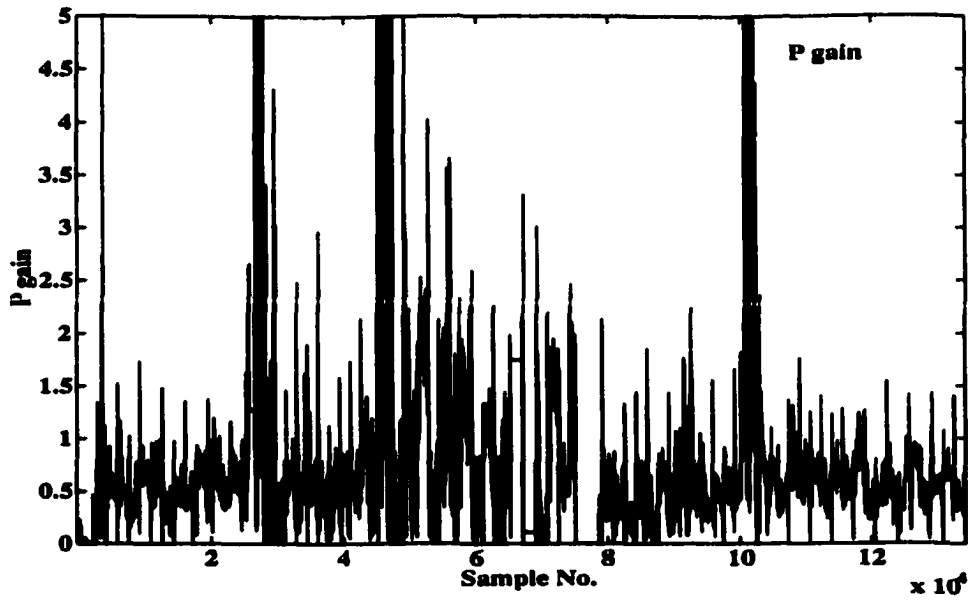
75

Figure 5.20: P gain on each sample based on system identification using Kalman filter.
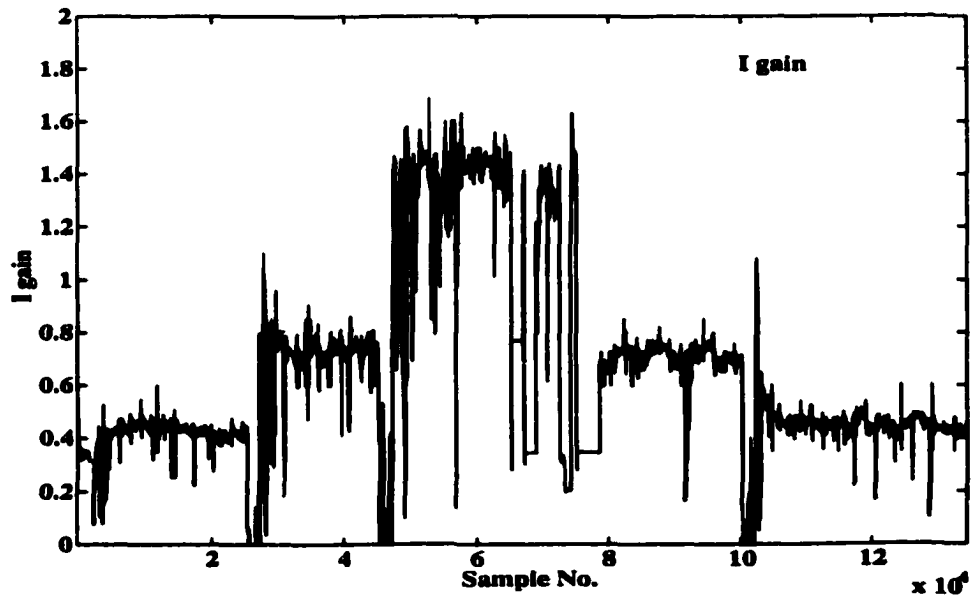

Figure 5.21: I gain on each sample based on system identification using Kalman filter.

76

5.5 Conclusion

The Kalman filter approach for system identification has advantage of fast convergence over the bandpass approach. The disadvantage associated with the use of Kalman filter approach is that the effect of noise on system identification is severe. The effect of noise is due to larger bandwidth and lower attenuation of higher and lower frequencies from the harmonic frequency considered for identification. The effect of noise can be overcome by using bandpass filtered signal for estimation as in Section 3. But as observed, this scheme delays convergence in system identification. A disadvantage of the Kalman filter is that the computational over head on the under lying digital system increases with number of frequency points in identification, even for identification up to 9th harmonic, the state matrix is a 11 by 11 matrix. The P and I gains obtained were also found to be noisy.

77

Chapter 6

Future Work

The thesis has studied MRAS to achieve frequency domain performance specifications. It has been shown that over parameterized transfer function based open loop RLS identification and frequency response computations enable MRAS to deliver good performance. To use MRAS in industry, it is required that the continuous excitation in setpoint needs to be eliminated. More experimental work needs to be done to control the start and stop of the excitation using error computed as discussed in Section 2.5. Also correlation can be developed for required minimum excitation magnitude by measuring signal to noise ratio in the frequency range of interest [2].

The DC bias estimation using Kalman filter method converges faster as compared to batch method. The MRAS using open loop system identification and Kalman filter for DC bias estimation needs to be tried.

The closed loop system identification can be tried using bandpass filters approach or Kalman filters approach. The same can be tried based on estimation of sensitivity function as described in [1].

The MRAS is applied to SISO (Single Input Single Output) system in this work. The same work needs to be extended to MIMO (Multiple Input Multiple Output) system along the lines of [8].

Appendix A

Temperature Control System.

The process considered is an experimental laboratory temperature control system. The temperature control system process schematic and its control system is shown in Figure A.1. The process consists of a heater, fan, circuit for supplying heater power, thermistor and bridge amplifier. The heater power is controlled by the DC voltage applied to the circuit using a controlled rectifier circuit. The details of the circuit are not included here. The process input is a voltage to the circuit supplying power to the heater. The process output is the output of the bridge amplifier, which amplifies the thermistor output. It is important to note the location from which process variables were taken into the computer as shown in schematic diagram. In this setup, the setpoint and process output will be apart by a measure equal to output bias. The error will be zero when 'setpoint + output bias' equals negative of process output. The experimental plots attached for process variables in the report are variables measured at the points shown in schematic diagram A.1.

Assuming that the electronic circuit time constants are very fast compared to the thermal time constant of the heater, the time constant of the process will be equivalent to the time constant of the heater. As the process input voltage increases, the heater temperature decreases, and so the process output also decreases. Thus the process is a negative gain process. As the thermistor is located physically at a distance away from the heater, there is a delay associated between temperature measured and temperature of heater.

The process can be modeled as first order process with delay in continuous time or s domain [15]. The variations in the process dynamics are introduced by varying the fan speed. Different fan speeds give different process gains, time constants and time delays. Increases in fan speed decreases gain of the process as the amount of air flowing through the system increases which takes away more heat out of the heater, resulting in a low temperature in the system. It also decreases the time constant and time delay. The heater dynamics can be different for heating up when power is supplied (active) and while cooling when lower of no power is supplied (active or passive). The process is noisy and varies considerably at different fan speed depending on inherent variabilities and ambient conditions. For e.g. if the process is continuously running for considerable time the temperature of the aluminum

79
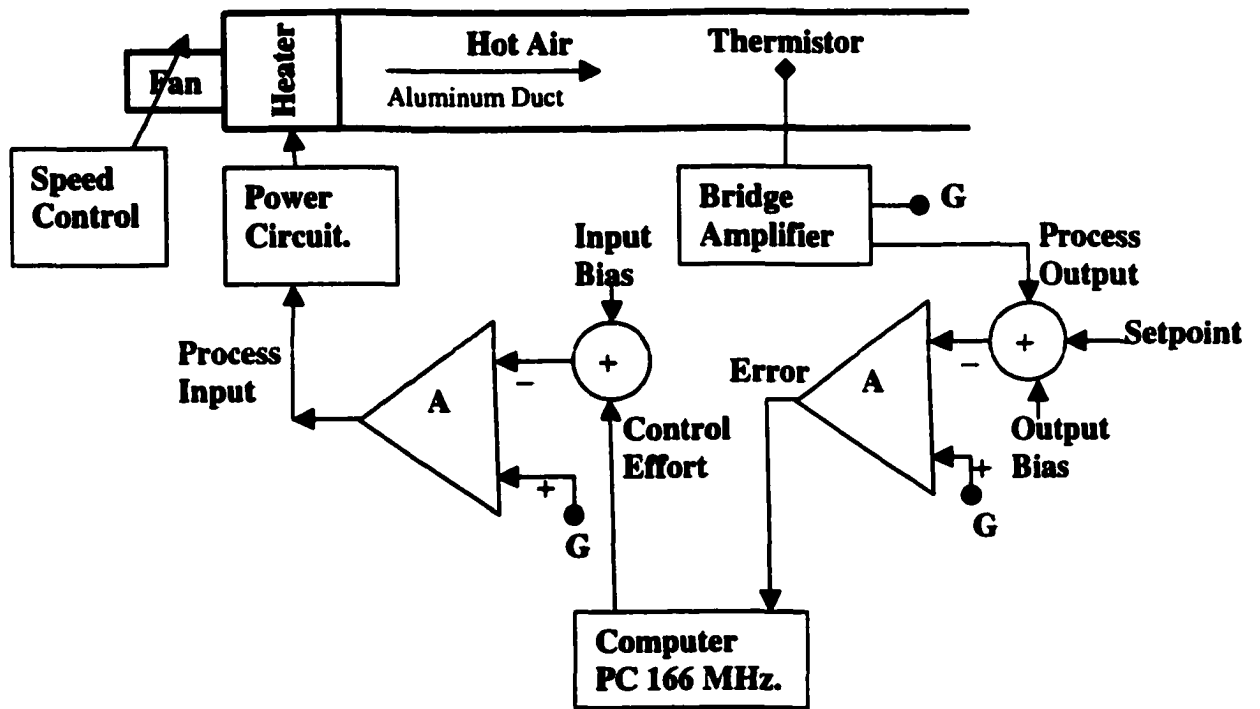
A – Amplifier with unity gain.
G - Ground of the system.

Figure A.1: Temperature control system.

duct also affects the process gain.

Bibliography

[1] Huang Biao and Shah, Sirish L.,"Closed-loop Identification: a Two Step Approach.", Int. Jou. of Process Control, Vol. 7, pp. 425-438,1997.

[2] Natarajan, K. and Gilbert, A.F.,"System Identification and PID Controller Tuning Using Band Pass Filters.", The Canadian Jou. of Chem. Engg., Vol. 75, pp. 765-777, August 1997.

[3] Natarajan, K. and Gilbert, A.F.,"On direct PID Controller Tuning Based on Finite Number Of Frequency Response Data.", ISA Transactions, Vol. 36, pp. 139-149, 1997.

[4] Astrom, K.J. and Wittenmark, B. *"Adaptive Control"*, second edition, Addison Wesley Publishing,1995. ISBN 0-201-55866-1.

[5] Natarajan, K. and Sivakumar, S.,"Design Of a Fixed-Point Digital Filter for State Estimation for UPS Applications", Submitted to Can. Jou. of Electrical Engg.

[6] Wellstead, P.E. and Zarrop, M.B., *"Self-tuning Systems"*, John Wiley and Sons, Inc., 1991. ISBN 0-471-92883-6.

[7] Press, W.H., Teukolsky, S.A., Vetterling, W.T. and Flannery, B.P., *"Numerical Recipes in C"*, Cambridge University Press, 1994. ISBN 0-521-35465-X.

[8] Yousef, A.,"Frequency Response Based System Identification and Controller Tuning", Masters Thesis 1997, Lakehead University.

[9] Ogata, K., *"Modern Control Engineering"*, Prentice Hall, Inc. ISBN 13-590232-0.

[10] Franklin G.F., Powell, J.D. and Workman, M.L., *"Digital Control of Dynamic Systems"*, Addison-Wesley Inc.,third edition, 1998. ISBN 0-201-82054-4.

[11] Sternby, J.,"Adaptive Control of Ultrafiltration", IEEE Transactions on Control Systems Technology, Vol. 4, pp. 11-17, January 1996.

[12] Nelder, J.A. and Mead, R., "A Simplex Method for Function Minimization", Computer Jou., Vol. 7, pp. 308-313, 1965.

[13] Ingle, V.K. and Proakis, J.G., *"Digital Signal Processing"*, PWS Publishing Company, 1997. ISBN 0-534-93805-1.

[14] Char, B.W., Geddas K.O., Gonnet G.H., Leong B.L., Monagan M.B. and Watt M.S., *"An Introduction to Maple V"*, Springer - Verlag, ISBN 0-387-97621-3.

[15] Shinskey, F.G., *"Process Control Systems Application, Design, and Adjustment"*, McGraw-Hill Inc. Third Edition, 1988. ISBN 0-07-056903-7.

[16] Van de Vegte, J., *"Feedback Control Systems"*, Third Edition, Prentice Hall, 1993. ISBN 0-13-016379-1.

[17] Oppenheim, A.V. and Schaeffer, R.W., *"Digital Signal Processing"*, Prentice-Hall, 1974. ISBN 0-13-214635-5.

[18] Bitmead, R.R. and Parker, P.J., "Adaptive Frequency Response Identification", Proc. Conf. IEEE Control and Decision, Los Angeles, CA, Dec. 9-11, 1987, IEEE Service Center, Piscataway, NJ (1987), pp. 348-353.

[19] Box, G.E.P. and MacGregor, J.F., "Parameter Estimation with Closed Loop Operating Data.", Technometrics, 18, pp. 371-380, 1976.

[20] Defalque, B., Gevers, M. and Installe, M., "Combined Identification of the Input-output and Noise Dynamics of a Closed Loop Controlled Linear System.", Int. Jou. of Control, 24, pp. 345-360, 1976.

[21] Rosenbrock, H.H., *"Computer-Aided Control System Design"*, Academic Press, 1974. ISBN 0-12-597450-7.

[22] Ljung, L. and Söderström T., *"Theory and Practice of Recursive Identification."*, MIT Press, 1983. ISBN 0-262-12095-X.

[23] Wellstead, P.E. and Edmunds, J.M., "Least-squares Indentification of Closed Loop Systems.", Int. Jou. of Control, 21, pp 689-699, 1975.

[24] Wellstead, P.E., Edmunds, J.M., Prager, D. and Zanker, P., "Self-Tuning Pole-zero Assignment Regulators.", Int. Jou. of Control, 30, pp. 1-26, 1979.

[25] Clarke, D.W. and Gawthrop, P.J., "A Self-Tuning Controller.", IEEE Proc. 122, pp. 929-934, 1975.

[26] Kwon, W.H. and Pearson, A.E., "A Modified Quadratic Cost Problem and Feedback Stabilization of a Linear System.", IEEE Trans. AC-22, PP. 38-42, 1977.

[27] Parks, P.C., "Lyapunov Redesign of Model Reference Adaptive Control Systems.", IEEE Trans., AC-11, PP. 362-365, 1966.

[28] Middleton, R.H., "Frequency Domain Adaptive Control.", IFAC workshop on Robust Adaptive Control, Australia, pp. 200-205, 1988.